

Aus dem Institut für Laboratoriumsmedizin
der Ludwig-Maximilians-Universität München

Direktor: Univ. Prof. Dr. med. Daniel Teupser

**An LC-MS/MS-based approach for analysis of site-specific
core-fucosylation of low-concentrated glycoproteins in
human serum using the biomarker prostate-specific
antigen (PSA) as example**

Dissertation

zum Erwerb des Doktorgrades der Humanbiologie

an der Medizinischen Fakultät der

Ludwig-Maximilians-Universität zu München

vorgelegt von

Robert Lang

aus

Leipzig

2018

Mit Genehmigung der Medizinischen Fakultät der Universität München

Berichterstatter: Prof. Dr. med. Michael Vogeser

Mitberichterstatter: Prof. Dr. rer. nat. Thomas Carell
Prof. Dr. med. Raphaela Waidelich
Prof. Dr. med. Jürgen Ruland

Dekan: Prof. Dr. med. dent. Reinhard Hickel

Tag der mündlichen Prüfung: 19.12.2018

Eidesstattliche Versicherung

Robert Lang

Ich erkläre hiermit an Eides statt,
dass ich die vorliegende Dissertation mit dem Thema

„An LC-MS/MS-based approach for analysis of site-specific core-fucosylation of low-concentrated glycoproteins in human serum using the biomarker prostate-specific antigen (PSA) as example“

selbstständig verfasst, mich außer der angegebenen keiner weiteren Hilfsmittel bedient und alle Erkenntnisse, die aus dem Schrifttum ganz oder annähernd übernommen sind, als solche kenntlich gemacht und nach ihrer Herkunft unter Bezeichnung der Fundstelle einzeln nachgewiesen habe.

Ich erkläre des Weiteren, dass die hier vorgelegte Dissertation nicht in gleicher oder in ähnlicher Form bei einer anderen Stelle zur Erlangung eines akademischen Grades eingereicht wurde.

Robert Lang

München, den 08.06.2018

Acknowledgements

First of all, I would like to thank Prof. Dr. Michael Vogeser from the University Hospital at the Ludwig-Maximilians-Universität in Munich for the external supervision. I am very grateful for his academic guidance and support. Equally, I would like to thank Dr. Andreas Leinenbach for giving me the opportunity to perform my PhD in his working group and for the great technical support during the last three years. I also want to thank Dr. Uwe Kobold for offering the PhD position in the “Instrumental analytics” division. I kindly thank Dr. Johann Karl and Dr. Magdalena Swiatek-de Lange for the financial support and their input in many lively discussions in the late afternoons.

I am very grateful to my colleagues Andreas Huber and Thomas Duelffer for introducing me into the LC-MS instrumentation in our group and for extremely valuable advices in the daily laboratory routine. Special thanks also go to Dr. Eirini Frylingou for her assistance in LTQ-FTICR measurements as well as to Michael Kampe and Marie Steger for their guidance in several MALDI-TOF tasks. My sincere thanks go to Monika Briechle und Gertrud Freisl. Without their, the everyday life in the laboratory would not be so comfortable. I also thank Ekkehard Rudy and Jo Anne Wright for their support in the procurement of laboratory equipment and reagents. Of course, I warmly thank Lisanne Grund, Robert Gossmann, Stefanie Schedlbauer, Manuela Collins, Katrin Gradl, Milou van Rooij, Sandra Fleischer, Angela Puhlmann, Ulrike Schauer, Pia Eberhardt, Korbinian Huber, Thomas Hausler, Christine Wintterle-Roehm, Tahira Abubaker, Matthias Metz, Ingrid Munk, Rupert Schmid, Dr. Martin Rempt, Dr. Christian Geletneky, Dr. Judith Taibon, Dr. Holger Busskamp, Stephan Pongratz, Dr. Frank Wedekind, and Dr. Julian Hofmann for the very friendly working atmosphere in our division.

My sincere thanks go to Dominic Knoblauch from the group of Dr. Glòria Tabarés for his MS support in intact protein measurements. I also thank Dr. Tobias Oelschlaegel for providing the lectin-separated PSA material and Dr. Markus Habberger for the LC-MS-based N-glycan analysis of PSA. I thank Leopold von Proff for surface plasmon resonance measurements. Many thanks go to Dr. Heike Wegmeyer for providing clinical and pathological information of patient samples. I thank Peter Stegmüller and Dagmar Knodel for the Elecsys® measurement of total and free PSA levels in PSA spiked-in serum samples and human specimens. Thanks to Dr. Sandra Rutz for her good advices during the method optimization phase. I also thank Dr. Lars Hillringhaus for the synthesis of several peptide standards.

Last, my hearty thanks go to my mother, Kerstin, and my friends for their joyful and constant support.

Table of contents

Table of contents.....	5
Table of abbreviations	9
Abstract.....	13
Zusammenfassung.....	15
 Chapter I: Aim of the thesis.....	 17
 Chapter II: Theoretical part.....	 19
1. Biological samples – Focus on blood and its fractions.....	20
2. Structure of proteins.....	22
2.1. Amino acids – Building blocks of proteins.....	22
2.2. The peptide bond	23
2.3. Levels of protein structures	24
3. N-linked glycosylation of proteins.....	25
3.1. Biosynthesis of N-glycans and their major structural types	25
3.2. Strategies for analysis of protein N-glycosylation	26
3.2.1. Analysis of intact glycoproteins	26
3.2.2. Analysis of glycopeptides.....	28
3.2.3. Analysis of glycans.....	29
4. Hybrid immunoaffinity mass spectrometry (IA-MS).....	32
4.1. Immunoassays (IA)	32
4.2. Triple quadrupole mass spectrometry (TQMS).....	33
4.3. Opportunities of hybrid IA-MS-based assays.....	35
 Chapter III: Development of an LC-MS/MS-based strategy for analysis of site-specific core-fucosylation of prostate-specific antigen (PSA) in the low ng/mL range in human serum.....	 37
1. Introduction	38
1.1. The role of human protein glycosylation	38
1.2. Prostate-specific antigen (PSA)	38
1.3. Approaches for the analysis of core-fucosylated proteins	39
2. Experimental section	41
2.1. Reagents and materials	41
2.2. Instruments and equipment.....	41
2.3. PSA spiked-in serum samples and human specimen	42

2.4.	Endoglycosidase selection	43
2.5.	Protease and surrogate peptide selection	44
2.6.	Analyte-specific MS parameter tuning	47
2.6.1.	Tuning of surrogate peptides generated by protease Arg-C digestion	47
2.6.2.	Tuning of surrogate peptides generated by tryptic digestion	49
2.7.	Immunoaffinity enrichment	50
2.7.1.	MSIA tip-based approach.....	50
2.7.2.	Magnet bead-based approach	50
2.8.	Partial deglycosylation and digestion	50
2.8.1.	Protease Arg-C-assisted approach using MSIA tips (in solution protocol)	50
2.8.2.	Trypsin-assisted approach using MSIA tips (on tip protocol).....	51
2.8.3.	Trypsin-assisted approach using magnet beads (on bead protocol).....	51
2.9.	LC-MS/MS analysis.....	51
2.9.1.	RPLC-MS/MS analysis of protease Arg-C derived PSA peptides	51
2.9.2.	HILIC-MS/MS analysis of tryptic PSA peptides	52
2.9.3.	Multiple reaction monitoring cubed (MRM ³)	53
2.10.	Data acquisition and analysis.....	53
3.	Results and discussion	54
3.1.	Endoglycosidase selection	54
3.2.	Protease and surrogate peptide selection	57
3.2.1.	<i>In silico</i> digestion of PSA.....	57
3.2.2.	<i>In vitro</i> digestion of PSA.....	58
3.3.	Protease Arg-C-based approaches	60
3.3.1.	Surrogate peptide selection and MRM parameter optimization.....	60
3.3.2.	Overview of the experimental workflow using MSIA tips	63
3.3.3.	Determination of core-fucosylated and total PSA in serum samples.....	64
3.3.4.	Optimization approaches	65
3.3.4.1.	Antibody type.....	65
3.3.4.2.	Antibody and enzyme amount.....	66
3.3.4.3.	Order of digestion and elution steps	67
3.3.4.4.	Multiple reaction monitoring (MRM) compared to selected ion monitoring (SIM).....	68
3.4.	From reversed phase to hydrophilic interaction liquid chromatography	70
3.5.	Trypsin-based approaches.....	75
3.5.1.	Surrogate peptide selection and analyte-specific MS parameter optimization	75
3.5.2.	Overview of the experimental workflow using MSIA tips	76
3.5.3.	Determination of partially deglycosylated and total PSA in spiked serum samples	76
3.5.4.	Feasibility of the method in native serum samples	79
3.5.5.	Optimization approaches	80
3.5.5.1.	Transitions.....	80
3.5.5.2.	Differential ion mobility mass spectrometry (DMS)	82

3.5.5.3. Multiple reaction monitoring cubed (MRM ³)	83
3.5.5.4. Derivatization using tandem mass tags (TMT)	84
3.5.6. Overview of the experimental workflow using magnet beads	87
3.5.7. Development of the magnet bead-based workflow	87
3.5.7.1. Optimization of immunoaffinity enrichment	87
3.5.7.2. Optimization of partial deglycosylation and tryptic digestion	89
3.5.8. Comparison of streptavidin-coated solid support materials for immunoaffinity enrichment	91
3.5.9. Characterization of the final workflow using magnet beads	92
3.5.9.1. Linearity, LLOD, LLOQ and imprecision of the magnet bead-based workflow	92
3.5.9.2. Analysis of serum samples containing different amounts of fucosylated PSA	94
3.5.9.3. Analysis of human specimens	95
4. Conclusions	96
 Chapter IV: A case study: Is core-fucosylated prostate-specific antigen (PSA) a refined biomarker for differentiation of benign prostate hyperplasia (BPH) and prostate cancer of different aggressiveness?	
1. Introduction	98
2. Experimental section	101
2.1. Reagents and materials	101
2.2. Preparation of calibrators and control samples	101
2.3. Patient samples	101
2.4. Quantification of total and free PSA by ECLIA	102
2.5. LC-MS/MS-based analysis of total PSA and core-fucosylated PSA	102
2.6. Study design	104
2.7. Data analysis and statistics	104
3. Results	105
4. Discussion	110
5. Conclusions	113
 Chapter V: References	115
 Appendix	127

Table of abbreviations

ABC	Ammonium bicarbonate buffer
ACN	Acetonitrile
AFP-L3	α -fetoprotein-L3
AUC	Area under the curve
BPH	Benign prostatic hyperplasia
CAM	Carbamidomethylation
CE	Collision energy
CID	Collision-induced dissociation
cps	Counts per second
CV	Coefficient of variation
CXP	Cell exit potential
DRE	Digital rectal examination
DMS	Differential ion mobility mass spectrometry
DP	Decustering potential
DTT	Dithiothreitol
ECLIA	Electrochemiluminescence immunoassay
ELISA	Enzyme-linked immunosorbent assay
ELLA	Enzyme-linked lectin assay
EP	Entrance potential
EPI	Enhanced product ion scan
ER	Endoplasmic reticulum
ESI	Electrospray ionization
FA	Formic acid
FDA	Food and Drug Administration
Fuc	Fucose
fuc-PSA	core-fucosylated PSA
GlcNAc	N-acetylglucosamine
GS	Gleason score
HILIC	Hydrophilic interaction chromatography

HPLC	High-performance liquid chromatography
HRMS	High-resolution mass spectrometry
IAM	Iodoacetamide
IA-MS	Immunoaffinity mass spectrometry
IgG	Immunoglobulin G
ISF	In-source fragmentation
KLK3	Kallikrein-3
LLOD	Lower limit of detection
LLOQ	Lower limit of quantification
MALDI	Matrix-assisted laser desorption/ionization
MRM	Multiple reaction monitoring
MS	Mass spectrometry
MSIA	Mass spectrometric immunoassay
n/a	not applicable
NP	Normal phase
OX	Oxidation
PBS	Phosphate buffered saline
PCa	Prostate cancer
PCA3	Prostate Cancer Antigen 3
PHI	Prostate Health Index
PSA	Prostate-specific antigen
PTM	Post-translational modification
ROC	Receiver operating characteristic
RP	Reversed phase
Sia	Sialic acid
SIL	Stable isotope labeled
SIM	Selected ion monitoring
SISCAPA	Stable isotope standards and capture by anti-peptide antibodies
SRM	Selective reaction monitoring
TFA	Trifluoroacetic acid

TMT	Tandem mass tag
TOF	Time of flight
TQMS	Triple quadrupole mass spectrometry
TRUS	Transrectal ultrasound
TURP	Transurethral resection of the prostate

Abstract

Recently, certain glycan structures of glycoproteins such as site-specific core-fucosylation have attracted attention as they can be associated with several diseases, including cancer. For example, changes in prostate-specific antigen (PSA) glycosylation pattern have been described in prostate cancer (PCa), which is among the most frequently diagnosed cancer types in men worldwide. However, sensitive and selective methods for analysis of very low-concentrated individual glycoproteins in complex matrices, such as serum, are rare and defined glycan structures, which might serve as potential cancer markers, are hard to detect by common methods, including immunoassays.

In the first part of this work, a mass spectrometry-based strategy for the simultaneous analysis of core-fucosylated and total PSA in the low ng/mL concentration range in human serum was developed. The final sample preparation workflow comprised an immunoaffinity capture step to enrich total PSA from human serum using anti-PSA antibody coated magnetic beads followed by consecutive two-step on bead partial deglycosylation with endoglycosidase F3 and tryptic digestion prior to LC-MS/MS analysis. The method was shown to be linear from 0.5 to 60 ng/mL total PSA concentrations and allows the simultaneous quantification of core-fucosylated PSA down to 1 ng/mL and total PSA lower than 0.5 ng/mL. The imprecision of the method over two days ranged from 9.7-23.2 % for core-fucosylated PSA and 10.3-18.3 % for total PSA depending on the PSA level. The feasibility of the method in native sera was shown using three human specimens making it a useful tool for the analysis of comprehensive patient cohorts in order to study if core-fucosylated PSA may serve as a more specific biomarker compared to conventional total and free PSA. Furthermore, the described strategy could be used to monitor potential changes in site-specific core-fucosylation of other low-concentrated glycoproteins, which could serve as improved markers ("marker refinement") in cancer research.

In the second part of this work, the previously developed LC-MS/MS-based strategy was used for multiplex analysis of core-fucosylated PSA and total PSA levels in sera from 50 benign prostatic hyperplasia (BPH) and 100 PCa patients of different aggressiveness (Gleason scores 5-10) covering the critical grey area (2-10 ng/mL) in PCa diagnosis. The objective of this study was to evaluate whether the core-fucosylation determinant of serum PSA may serve as refined marker for differentiation between non-aggressive from aggressive PCa and identification of BPH. The data showed that the ratio core-fucosylated PSA to total PSA (%-fuc-PSA) was decreased in aggressive PCa (Gleason score > 6) in comparison to non-aggressive PCa (Gleason score ≤ 6) and yielded a 5 to 8 % increase in the area under the curve (AUC = 0.60) than the currently used total PSA (AUC = 0.52) and %-free PSA (AUC = 0.55) tests. In contrast, both core-fucosylated PSA and %-fuc-PSA had no diagnostic value for differentiation of BPH from PCa. In summary, a higher tendency for differentiation of non-aggressive and aggressive PCa was obtained using %-fuc-PSA compared to conventional diagnostic PCa markers. Therefore, %-fuc-PSA should be further investigated e.g. in larger patient cohorts or by more precise methods whether it could be clinically used in PCa diagnosis.

Zusammenfassung

Bestimmte Glykanstrukturen von Glykoproteinen, wie z.B. spezifische Fucosylierung am Glykankern (Kern-Fucosylierung), haben unlängst das Interesse geweckt, da sie mit verschiedenen Krankheiten, u.a. Krebs, in Verbindung gebracht werden können. So wurden beispielsweise für Prostatakrebs, eine der weltweit am häufigsten diagnostizierten Krebsarten bei Männern, veränderte Glykosylierungsmuster des Prostata-spezifischen Antigens (PSA) beschrieben. Sensitive und selektive Methoden zur Bestimmung von sehr niedrig konzentrierten, individuellen Glykoproteinen aus komplexen Matrices wie Serum sind jedoch selten und definierte Strukturen von Glykanen, die als mögliche Krebsmarker dienen könnten, sind mit bekannten Methoden, wie immunologischen Tests, schwer nachzuweisen.

Im ersten Teil dieser Arbeit wurde eine massenspektrometrische Methode für die simultane Analyse von Kern-Fucosyliertem und gesamt PSA (*total PSA*) im niedrigen ng/mL Konzentrationsbereich in humanem Serum entwickelt. Der finale Probenvorbereitungsablauf umfasste einen Immunoaffinitätsschritt mit anti-PSA Antikörper beschichteten magnetischen Partikeln, um *total PSA* aus humanem Serum anzureichern. Anschließend wurden zwei nacheinander folgende Schritte auf den mit PSA beladenen magnetischen Partikeln durchgeführt. Einer kontrollierten Teildglykosylierung mit Endoglykosidase F3 folgte ein tryptischer Verdau vor der eigentlichen LC-MS/MS Messung. Die Methode ist in einem Konzentrationsbereich von 0,5-60 ng/mL *total PSA* linear und erlaubt die simultane Quantifizierung von bis zu 1 ng/mL Kern-Fucosyliertem PSA und weniger als 0,5 ng/mL *total PSA*. Die Präzision der Methode, gemessen über zwei Tage, lag abhängig vom PSA Level bei 9,7-23,2 % für Kern-Fucosyliertes PSA und 10,3-18,3 % für *total PSA*. Die Eignung der Methode zur Anwendung in nativen Seren wurde anhand von drei Patientenproben gezeigt. Dies macht die Methode zu einem nützlichen Hilfsmittel für die Analyse von größeren Patientenkohorten, um zu untersuchen, ob Kern-Fucosyliertes PSA als Marker mit höherer Spezifität als konventionelles *total PSA* und freies PSA fungieren könnte. Außerdem könnte die beschriebene Methode genutzt werden, um mögliche Veränderungen in der spezifischen Kern-Fucosylierung von anderen, niedrig konzentrierten Glykoproteinen zu erforschen, die als verbesserte Marker dienen könnten („*marker refinement*“).

Im zweiten Teil dieser Arbeit wurde die vorher entwickelte LC-MS/MS Methode zur simultanen Konzentrationsbestimmung von Kern-Fucosyliertem und *total PSA* in Patientenproben angewendet. Die Proben stammten dabei von 50 Patienten mit Benigner Prostatahyperplasie (BPH) und 100 Patienten mit unterschiedlich stark differenziertem Prostatakarzinom (Gleason Scores 5-10). Die *total PSA* Level der Probanden lagen im kritischen Grau-Bereich (2-10 ng/mL) für die Diagnose von Prostatakrebs. Ziel dieser Studie war es zu evaluieren, ob Kern-Fucosyliertes PSA in Serum als verbesserter Marker zur Differenzierung von nicht-aggressivem und aggressivem Prostatakrebs bzw. zur Identifizierung von BPH dienen könnte. Die Ergebnisse zeigten, dass das Verhältnis von Kern-Fucosyliertem und *total PSA* (%-fuc-PSA) bei aggressivem Prostatakrebs (Gleason score > 6) gegenüber nicht-aggressivem Prostatakrebs (Gleason score ≤ 6) erniedrigt war. Zudem wurde mit %-fuc-PSA eine Steigerung der Fläche unter der Kurve (Englisch: *Area under the curve*, AUC = 0,60)

von 5-8 % im Vergleich zu gegenwärtig verwendeten Tests wie *total PSA* (AUC = 0,52) und %-freies PSA (AUC = 0,55) beobachtet. Im Gegensatz dazu hatten sowohl Kern-Fucosyliertes PSA als auch %-fuc-PSA keinen diagnostischen Wert zur Differenzierung zwischen BPH und Prostatakrebs. Zusammenfassend lässt sich sagen, dass im Vergleich zu konventionellen Prostatakrebsmarkern mit %-fuc-PSA tendenziell eine etwas höhere Unterscheidung von aggressivem und nicht-aggressivem Prostatakrebs erzielt wurde. Daher sollte weiter untersucht werden, ob %-fuc-PSA einen klinischen Nutzen in der Prostatakrebsdiagnose hat, sei es z.B. in größeren Patientenkohorten oder mithilfe von präziseren Methoden.

Chapter I

Aim of the thesis

Chapter I: Aim of the thesis

Glycoproteins are functional molecules in organisms involved in several biological processes such as cell-signaling, cell-cell interaction, immune recognition, cell proliferation and differentiation [1]. Dysfunctions in these processes are frequently associated with altered glycoproteins, hence making them excellent biomarker candidates for disease monitoring. However, glycoprotein analysis in complex biological fluids such as serum is challenging as they often possess very low concentrations compared to numerous other high-abundant matrix proteins such as albumin or immunoglobulin (IgG). The extensive glycan heterogeneity of glycoproteins represents an additional challenge and leads to the requirement for specialized set of tools for their study. In this work, the glycoprotein prostate-specific antigen (PSA) served as an ideal example as its native serum concentrations usually are in the low ng/mL concentration range which in fact is approximately 6-8 orders of magnitude lower than the most abundant proteins in serum. Moreover, alterations in PSA glycosylation pattern such as terminal sialylation or site-specific core-fucosylation have been reported in prostate cancer (PCa) cell lines, prostate tissue, seminal fluid, urine, and serum samples with elevated PSA levels, frequently by means of lectin-based assays [2-5].

The aim of the first part of this work was to develop a mass spectrometry (MS)-based strategy for the simultaneous analysis of both site-specific core-fucosylated and total PSA in the low ng/mL concentration range in human serum. For this purpose, several sub-goals were pursued including (1) evaluation of various enzymes for protein cleavage and selective glycan trimming, (2) testing of different solid support materials and capture reagents for immunoaffinity enrichment to ensure purification of the sample, (3) selection of suitable high-performance liquid chromatography (HPLC) columns for retention of target peptides and separation of interfering compounds generated during the sample preparation process, (4) identification of suitable surrogate peptides and their respective mass transitions representing the target analytes, and (5) tuning of analyte-specific MS parameters in order to achieve the maximum sensitivity. Following method development and optimization, the final workflow was characterized in terms of linear range, lower limit of detection (LLOD), lower limit of quantification (LLOQ), and assay imprecision, and the feasibility of the method in native sera was shown using three human specimens.

The aim of the second part of this work was to evaluate whether core-fucosylated PSA might serve as potential biomarker for differentiation of non-aggressive and aggressive PCa and for identification of other prostatic diseases such as benign prostatic hyperplasia (BPH). For this purpose, a large number of patient samples ($n = 150$) was analyzed applying the previously developed LC-MS/MS method. Patient samples were classified into three groups according to their clinical diagnosis and the Gleason score (GS) grading system: (1) BPH, (2) non-aggressive PCa ($GS \leq 6$), and (3) aggressive PCa ($GS > 6$). Total PSA levels obtained in this refinement study were compared to results from electrochemiluminescence immunoassay (ECLIA) using a Bland Altman plot and Deming regression. Statistical data evaluation was performed by receiver operating characteristic (ROC) curves and box plot diagrams.

Chapter II

Theoretical part

Chapter II: Theoretical part

1. Biological samples – Focus on blood and its fractions

A wide variety of biological sample types may be collected from human origin including blood, tissue, urine, saliva, semen, bone marrow, cell lines, exhaled air, feces, and hair. Of particular interest for routinely analysis are those sample types that can be collected most conveniently and efficiently, and at the lowest cost for large population-based studies. The most common sample types for these studies are blood, tissue, urine, and saliva [6]. In this work, serum which was previously isolated from whole blood was used as sample matrix. Hence, basic information such as functions, composition, processing, and storage of blood and its fractions is given below.

Blood, which is circulated by the heart through the vascular system, has several major functions. It transports oxygen, nutrients (such as amino acids, fatty acids, glucose) and cells to and removes waste materials (such as carbon dioxide, urea, lactic acid) away from body tissues. Blood is responsible for the regulation of pH, temperature and water content of cells. Tissue damages are indicated by transport of hormones through the blood serving as a messenger system. Immune defense and coagulation are stimulated by biochemical cascades and complex coagulation pathways initiated by blood compounds. The average human adult has a blood volume of roughly 5 L, which accounts for 6-8 % of the human body weight. Whole blood consists of plasma and blood cells in a composition of approximately 55 to 45 % in healthy conditions. Blood plasma is composed of nearly 92 % water and 7 % plasma proteins by volume and contains trace amounts of glucose, electrolytes, hormones, and gases. The total plasma protein concentration usually ranges from 60 to 85 g/L [7]. However, individual protein concentrations can differ by 10 orders of magnitude with interleukin-6 (0-5 pg/mL) at the low abundance and albumin (35-50g/L) at the high abundance end of the protein landscape (Figure 1) [8].

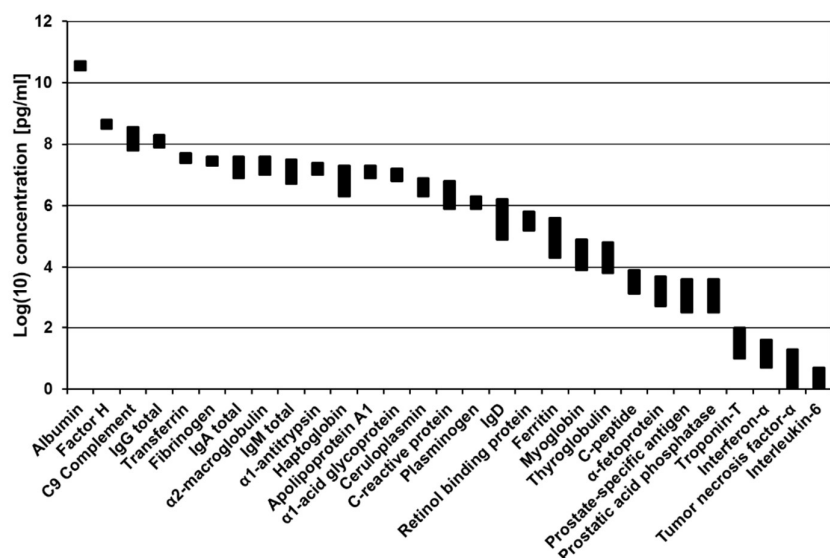


Figure 1: Reference intervals for 29 plasma proteins plotted on a log(10) scale spanning 12 orders of magnitude. Reproduced and modified from [8].

Blood cells, also known as corpuscles or formed elements, represent mainly red blood cells (erythrocytes), white blood cells (leukocytes) and platelets (thrombocytes). The proportion of blood occupied by red blood cells is referred to as the hematocrit, and is normally within the range of 36-48 % in females and 40-53 % in males [9]. These values can be changed in diseases such as anemia (depressed hematocrit) or polycythemia (elevated hematocrit). Whole blood is often fractionated by centrifugation before being analyzed and stored. While plasma is obtained from an anticoagulated blood sample, serum isolation requires no anticoagulants. After centrifugation of anticoagulated blood, white blood cells and platelets build the so-called buffy coat (<1 %) between the upper, straw yellow plasma layer and the lower, bright red layer consisting of red blood cells. If coagulated blood is processed, the buffy coat forms a cell clot with red blood cells and is not amenable to separate analysis (Figure 2). Therefore, depending on the intended analysis and the required blood fraction, it should be considered whether blood is collected anticoagulated or coagulated. In addition, anticoagulant effects need to be respected to avoid certain problems in laboratory applications. For example, EDTA as anticoagulant is preferred for hematology testing but interferes with calcium assays due to its chelating character [10]. Blood fractions can serve for different intended uses. Whole blood, buffy coat and cell clots representing suitable sources for DNA are preferably used in genomic studies whereas serum and plasma are the preferred sample types in proteomics, although analytical results may be different in both specimen [11]. This could probably be due to protein binding to the cell clot formed during coagulation which causes a decrease in free protein serum concentration. Improper storage conditions can also lead to coagulation and protein precipitation and therefore affect blood stability. To reduce these effects, repetitive freeze-thaw cycles should be avoided, the temperature at which blood is collected may be important and stabilizing agents might be necessary to preserve distinct analytes.

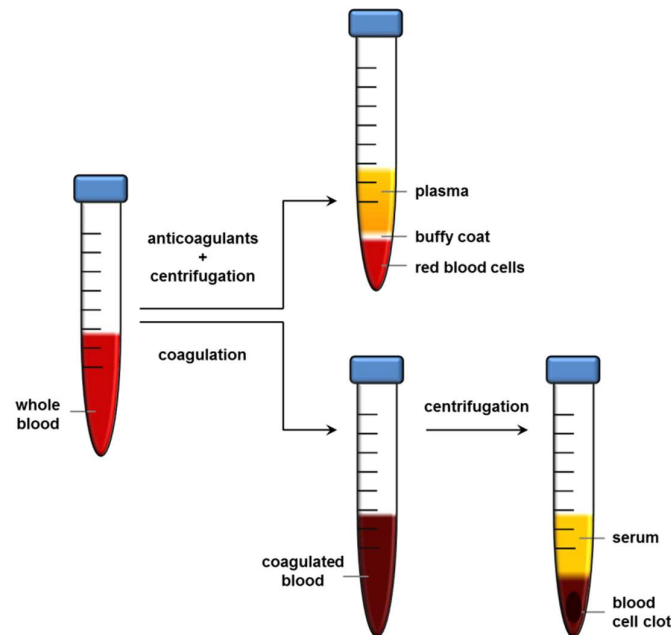


Figure 2: Preparation of plasma (upper path) and serum (lower path) by centrifugation of whole blood previously treated with or without anticoagulants, respectively.

2. Structure of proteins

2.1. Amino acids – Building blocks of proteins

Proteins are linear biopolymers constituted of monomer subunits known as amino acids. As the name indicates, each amino acid contains an amine ($-\text{NH}_2$) and a carboxyl ($-\text{COOH}$) functional group attached to one central carbon atom, the α -carbon. The remaining two bonds of this α -carbon atom are generally satisfied by a hydrogen ($-\text{H}$) atom and a side chain ($-\text{R}$ group) specific to each amino acid. Depending on the $-\text{NH}_2$ and $-\text{COOH}$ functional groups' positions, α -, β -, γ - or δ -amino acids exist. In nature, α -amino acids are of particular importance. Therefore, in the following context the term *amino acid* is used to refer specifically to the α -form. According to the polarity of their side chains amino acids can be classified into four groups: (1) non-polar, (2) polar/uncharged, (3) acidic, and (4) basic amino acids. Among these groups a broad variety of residues including aliphatic, aromatic, heterocyclic, hydroxylic, carboxylic, amidic, and sulfur containing side chains can be distinguished which leads to the unique and manifold functionality of proteins. Twenty amino acids encoded by the universal genetic code are occurring in natural proteins. These so-called proteinogenic amino acids are abbreviated by three-letter or single-letter notations as depicted in Table 1 [12, 13]. All proteinogenic amino acids are chiral molecules due to the configuration of the α -carbon atom with four different ligands, except glycine as it contains two hydrogen atoms on the α -carbon atom. The absolute stereochemistry can be indicated by (L) and (D) designators in which only (L)-amino acids are present in human proteins.

Table 1: Name, three-letter, single-letter and structure of the 20 proteinogenic amino acids classified according to their polarity.

1. Non-polar amino acids

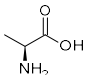
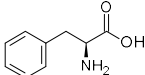
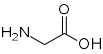
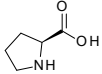
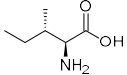
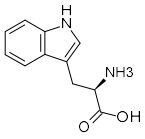
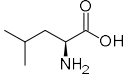
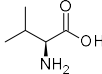
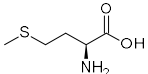
Alanine	Ala	A		Phenylalanine	Phe	F	
Glycine	Gly	G		Proline	Pro	P	
Isoleucine	Ile	I		Tryptophan	Trp	W	
Leucine	Leu	L		Valine	Val	V	
Methionine	Met	M					

Table 1 continued: Name, three-letter, single-letter and structure of the 20 proteinogenic amino acids classified according to their polarity.**2. Polar/uncharged amino acids**

Asparagine	Asn	N		Serine	Ser	S	
Cysteine	Cys	C		Threonine	Thr	T	
Glutamine	Gln	Q		Tyrosine	Tyr	Y	

3. Acidic amino acids

Aspartic acid	Asp	D		Glutamic acid	Glu	E	
---------------	-----	---	--	---------------	-----	---	--

4. Basic amino acids

Lysine	Lys	K		Histidine	His	H	
Arginine	Arg	R					

2.2. The peptide bond

When the α -carboxyl group of one amino acid reacts with the α -amine group of a second amino acid, a covalent bond, the peptide bond, is formed thereby releasing a molecule of H_2O (condensation reaction). Depending on the number of amino acids linked together one can distinguish oligopeptides (2-20 amino acids), polypeptides (21-50 amino acids), and proteins (> 50 amino acids). However, the boundary is not well defined and can overlap in meaning. Due to resonance effects the peptide bond possesses partial double bond characteristics resulting in a very stable, planar geometry in which two amino acids are fixed in either *cis*- or *trans*-conformation. Most peptides are in *trans*-conformation, where the two α -carbon atoms are on opposite sides of the peptide bond, as there is less steric hindrance between side chains attached to α -carbon atoms. Even though the geometry of the peptide bond is fixed, single bonds on either side of the α -carbon atoms can rotate allowing for flexibility in protein folding.

2.3. Levels of protein structures

Generally four levels of protein structures are differentiated: primary, secondary, tertiary and quaternary structures. The primary structure is the amino acid sequence assembled in a particular order in a protein. The sequence of a protein is written from the amino terminus (N-terminus, left) to the carboxyl terminus (C-terminus, right). For instance, the amino acid sequence of prostate-specific antigen (PSA, Uni-ProtKB P07288) starts with methionine (M) at the N-terminus and ends with proline (P) at the C-terminus (Figure 3).

10	20	30	40	50
MWVPVVFLTL	SVTWIGAAPL	ILSRIVGGWE	CEKHSQPWQV	LVASRGRAVC
60	70	80	90	100
GGVLVHPQWV	LTAAHCI RNK	SVILLGRHSL	FHPEDTGQVF	QVSHSFPHPL
110	120	130	140	150
YDMSLLKNRF	LRPGDDSSHD	LMLRLSEPA	ELTDAVKVMD	LPTQEPALGT
160	170	180	190	200
TCYASGWGSI	EPEEF LTPKK	LQCVDLHVIS	NDVCAQVHPQ	KVTKFMLCAG
210	220	230	240	250
RWTGGKSTCS	GDSGGPLVCN	GVLQGITSWG	SEPCALPERP	SLYTKVVHYR
260				
KWIKDTIVAN	P			

Figure 3: Amino acid sequence of prostate-specific antigen (PSA, Uni-ProtKB P07288) illustrated as single-letter code.

The secondary structure corresponds to local folded structures within the protein due to interactions between amino hydrogen and carboxyl oxygen atoms of the backbone. The most common types of secondary structures are alpha helices and beta sheets. In alpha helices, a helical structure is formed by hydrogen bonds in which each turn contains around 3.6 amino acids [14]. Side chains are directed to the outside of the helix where they are free to interact. In beta sheets, segments of the polypeptide chain line up parallel or anti-parallel to each other, forming a sheet-like structure by hydrogen bond interactions. Side chains protrude below or above the sheet's plane. Different secondary structure elements, also known as protein domains, can be present in a single protein molecule linked by turns and flexible loops. The tertiary structure refers to the overall, three-dimensional structure of a protein. The spatial arrangement is maintained by different interactions between the side chains of the amino acids. Both non-covalent interactions such as hydrophobic interactions, dipole-dipole interactions, hydrogen bonds, and ionic bonding as well as covalent disulfide bridges, established between two cysteine residues, contribute to the tertiary structure. The conformational structure of proteins is also affected by the surrounding medium. For instance, in aqueous medium non-polar residues will cluster in the inside of a protein, whereas polar amino acids are presented on the outside to interact with water molecules. Some proteins possess multiple polypeptide chains with defined tertiary structures, which are also called subunits. These subunits can interact together by similar interactions that were mentioned for tertiary structures forming the quaternary structure.

3. N-linked glycosylation of proteins

3.1. Biosynthesis of N-glycans and their major structural types

After protein biosynthesis by ribosomes, proteins may undergo post-translational modification (PTM) such as acetylation, phosphorylation, lipidation, amidation, methylation, and glycosylation which further increase the structural complexity of proteins. This section describes only N-linked glycosylation of proteins including steps in their synthesis and processing, potential N-glycosylation sites, and their major structural classes. Strategies for analysis of N-glycosylated proteins including their isolation, purification, separation and detection is reserved for the next section.

In the first phase, N-glycan synthesis of all eukaryotes begins on the cytoplasmic side of the endoplasmic reticulum (ER) membrane by the transfer of 2-N-acetylglucosamine-1-phosphate (GlcNAc-1-P) from uridine diphosphate N-acetylglucosamine (UDP-GlcNAc) to the membrane-bound precursor dolichol phosphate (Dol-P), forming dolichol pyrophosphate N-acetylglucosamine (GlcNAc-P-P-Dol). Subsequently, a second N-acetylglucosamine (GlcNAc) and five mannose (Man) residues are transferred step-by-step to GlcNAc-P-P-Dol by specific glycosyltransferases to generate $\text{Man}_5\text{GlcNAc}_2\text{-P-P-Dol}$ on the cytoplasmic side of the ER. By a mechanism that is not fully understood, the $\text{Man}_5\text{GlcNAc}_2\text{-P-P-Dol}$ precursor flips across the ER membrane bilayer. The glycan structure, which is now exposed to the lumen of the ER, is further extended by addition of four Man and three glucose (Glc) residues. In total, fourteen sugars were sequentially added to the Dol-P precursor. Next, the entire glycan structure ($\text{Glc}_3\text{Man}_9\text{GlcNAc}_2$) is transferred by oligosaccharyltransferase (OST) to asparagine ($\text{GlcNAc}\beta 1\text{-Asn}$ linkage) in nascent protein regions that have translocated into the ER [15]. It must be noted that not all asparagine residues can accept an N-glycan but only those within the receptive NXT/S motifs where X is a variable amino acid except proline. However, the presence of the consensus tripeptide is not always sufficient to conclude that an asparagine residue is N-glycosylated, as protein folding plays an important role in the regulation of N-glycosylation. Sometimes, unfolding of the polypeptide chain might be required in order to expose respective sequons for carbohydrate attachment [16].

In the second phase, a series of processing reactions trims the 14-N-glycan. In the ER, Glc residues are removed by α -glucosidases I and II to give $\text{Man}_9\text{GlcNAc}_2\text{Asn}$. The majority of glycoproteins exits the ER towards the Golgi apparatus with either eight or nine Man residues, depending on whether they were processed by ER α -mannosidase I. Mature glycoproteins, which are not processed in the following *cis*-Golgi compartment, possess N-glycans referred to the oligomannose N-glycan type. In the *cis*-Golgi compartment, glycan trimming continues in which three Man residues are removed by α -mannosidases IA and IB forming $\text{Man}_5\text{GlcNAc}_2\text{Asn}$, which is a key intermediate for the biosynthesis of hybrid and complex N-glycans initiated in the *medial*-Golgi compartment. Here, N-acetylglucosaminyltransferase GlcNAc-TI adds an GlcNAc residue to the core of $\text{Man}_5\text{GlcNAc}_2\text{Asn}$. Next, terminal Man residues are removed by α -mannosidase II to form $\text{GlcNAcMan}_3\text{GlcNAc}_2\text{Asn}$. Hybrid N-glycans will be formed, if this step does not occur. A second GlcNAc residue is added to the Man core by the action of N-acetylglucosaminyltransferase GlcNAc-TII to yield

GlcNAc₂Man₃GlcNAc₂Asn, the precursor for all biantennary, complex N-glycans. Additional branches can be added at the core mannoses to yield tri- and tetra-antennary N-glycans. Further modifications, such as addition of fucose (Fuc) to the core, elongation of branching with galactose (Gal), or capping of branches by sialic acid (Sia), mostly occur in the *trans*-Golgi compartment. Biosynthesis of N-glycans leads to a myriad of oligosaccharides, as this process is non-template-driven involving the availability of several enzymes and substrates without any proofreading machinery. Three major structural classes of N-glycans attached to mature proteins at the NXT/S motifs can be distinguished (Figure 4). (1) Oligomannose-type glycans contain only two GlcNAc and a variable number of Man and sometimes also Glc residues, (2) complex-type glycans are composed of GlcNAc, Gal, Fuc, Sia and sometimes also GalNAc residues in addition to the pentasaccharide core, and (3) hybrid-type glycans combine the characteristics of both oligomannose- and complex-type glycans [17].

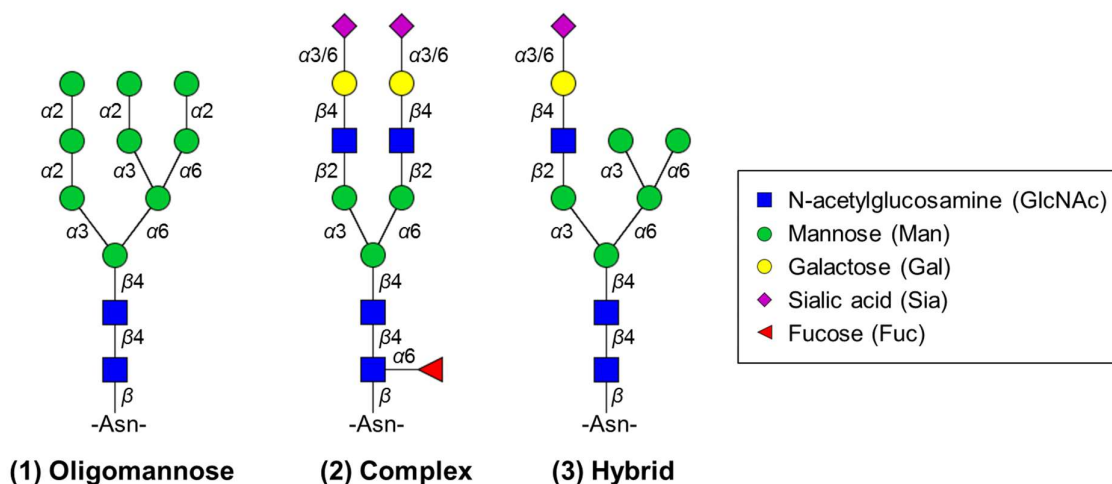


Figure 4: Three major structural classes of N-glycans in mature proteins: (1) Oligomannose-, (2) complex-, and (3) hybrid-type oligosaccharides and their specific linkages. Each N-glycan type contains the common pentasaccharide core Man₃GlcNAc₂Asn. Reproduced and modified from [15].

3.2. Strategies for analysis of protein N-glycosylation

Analysis of protein N-glycosylation can be performed at the levels of intact glycoproteins, glycopeptides and free oligosaccharides. A general overview of the wide landscape of methods and tools aiming for these targets is given in this section.

3.2.1. Analysis of intact glycoproteins

One of the first steps in isolation and analysis of intact glycoproteins is the usage of gel electrophoresis such as sodium dodecyl sulfate polyacrylamide gel electrophoresis (SDS-PAGE). In gel electrophoresis, glycoproteins are separated according to their size and/or charge depending on the utilized gel conditions. Although complete separation is often not feasible due to the heterogeneous glycan patterns, gel electrophoresis may be used as preparative technique prior to the use of other methods. For instance, subsequent application of lectins, which are highly specific for

carbohydrates moieties, may enable improved detection and characterization of glycosylation patterns of electro-blotted proteins [18]. Several lectins exist with different selectivities such as Fuc-binding lectins e.g. *Aleuria aurantia lectin* (AAL), *Ulex europaeus agglutinin* (UEA), Sia-binding lectins e.g. elderberry lectin from *Sambucus nigra* (SNA), *Maackia amurensis hemoagglutinin* (MAH), Man-binding lectins e.g. *Concanavalin A* (ConA), and GlcNAc-binding lectins e.g. *Wheat germ agglutinin* (WGA). A higher resolving power of glycoforms can be provided by capillary electrophoresis (CE) whereas CE does not allow per se elucidation of attached glycan structures [19]. Mass spectrometric detection of individual glycoproteins is difficult due to the extensive microheterogeneity of their glycan moieties. Resolution of small glycoproteins with a limited number of glycans has been achieved by the use of matrix-assisted laser desorption/ionization time-of-flight (MALDI-TOF) mass spectrometry (MS) [20]. Larger proteins with multiple glycosylation sites and heterogeneous glycosylation patterns usually lead to broad and unresolved peaks as shown in Figure 5 using the example of prostate-specific antigen (PSA). Normally, electrospray ionization (ESI)-MS is also faced with severe problems in intact glycoprotein analysis including less efficient ionization, adduct formation and data complexity due to multiple ion species. In this context, the use of lectins bound to appropriate supporting materials like magnet beads, micro-columns or membranes also allows for isolation, fractionation and separation of glycoproteins according to their glycan structures [5, 21, 22]. Additional information on the number of glycosylation sites and attached glycan types can be obtained by combining MS- or lectin-based approaches with previous treatment of target glycoproteins using specific endo- and exo-glycosidases.

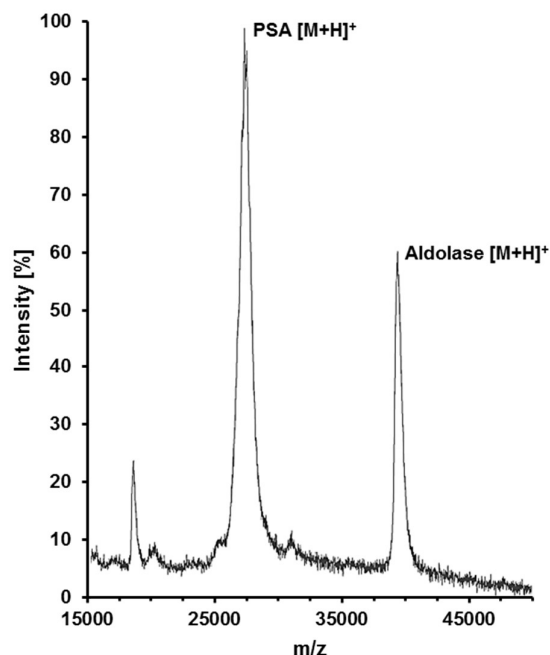


Figure 5: Matrix-assisted laser desorption/ionization time-of-flight (MALDI-TOF) mass spectrum of the native glycoprotein prostate-specific antigen (PSA) leading to a broad and unresolved peak in the mass range of 26-29 kDa. Aldolase (m/z 39,112 Da) was used as internal mass calibrator.

3.2.2. Analysis of glycopeptides

Prior to glycopeptide analysis, specific or non-specific cleavage of glycoproteins is required which yields a mixture of different peptides and glycopeptides. The resulting peptide length depends on the glycoprotein's amino acid sequence and the specificity of the cleavage reagent. Different proteolytic enzymes and chemical reagents for specific protein cleavage together with their preferred cleavage sites are summarized in Table 2. One of the most common proteases in protein digestion for MS-based applications is trypsin, which offers some major advantages such as good availability, high specificity, an optimal average peptide length of ~14 amino acids, and typically the presence of at least two defined positive charges at the N-terminus as well as at the C-terminal Arg or Lys residues, rendering tryptic peptides well suited for ESI-MS [23]. Non-specific cleavage e.g. by pronase provides glycans only containing one amino acid or very short peptide backbones [17]. Alternatively, chemical reagents such as cyanogen bromide (CNBr) or hydroxylamine may be used as important tools for selective cleavage of proteins. In contrast to enzymatic cleavage, chemical treatment usually targets residues and specific dipeptide linkages that occur at low frequencies in proteins resulting on average in fewer peptides being larger in size compared to those produced by standard protease treatment [24]. Glycoproteins can be completely denatured by reduction e.g. with dithiothreitol (DTT) and alkylation e.g. with iodoacetamide (IAM) to ensure accessibility of cleavage reagents. However, it has to be considered that protein cleavage might be sterically hindered in highly glycosylated proteins.

Table 2: Proteolytic and chemical cleavage reagents for specific protein digestion and their respective cleavage sites.

Cleavage	Reagent	Preferred cleavage site*
Proteolytic	Trypsin	C-terminus of arginine and lysine residues
	Chymotrypsin	C-terminus of tryptophan, tyrosine, phenylalanine, leucine, methionine, and histidine residues
	Pepsin (pH = 1.3)	C- and N-terminus of phenylalanine, leucine, tyrosine, and tryptophan residues
	Protease Arg-C	C-terminus of arginine residues
	Protease Glu-C	C-terminus of glutamic acid residues
	Protease Lys-C	C-terminus of lysine residues
	Protease Asp-N	N-terminus of aspartic acid residues
Chemical	Cyanogen bromide (CNBr)	C-terminus of methionine residues
	2-Iodosobenzoic acid (IBA)	C-terminus of tryptophan residues
	Hydroxylamine	Asparagine-glycine peptide bonds
	Formic acid (FA)	Aspartic acid-proline peptide bonds

* Enzyme specific exceptions not considered

After glycoprotein cleavage, glycopeptide identification is still challenging for several reasons. First, glycopeptides usually represent only a minor proportion within the generated total peptide mixture. Second, glycopeptides often possess lower signal intensities than non-glycosylated peptides, mainly because glycopeptide signals are distributed across several species carrying different glycan structures. Third, glycopeptides may suffer from low ionization efficiency and ion suppression in the presence of other peptides, especially if glycans are capped by negatively charged sialic acid residues [25]. To avoid these challenges, several additional techniques can be applied in parallel or sequentially. As mentioned before, the use of lectin-affinity capture enables discrimination between glycosylated and non-glycosylated peptides. Depending on their specificity, lectins can function as structure-specific selectors or allow for binding of multiple glycan types [26, 27]. Hydrophilic interaction chromatography (HILIC) can also be applied for separation of hydrophilic glycopeptides from more hydrophobic peptides [28]. Furthermore, size exclusion chromatography (SEC) may be useful for fractionation of peptide mixtures according to their size [29]. Carbohydrate residues, previously oxidized with periodate, can be coupled to hydrazine beads followed by peptide release using peptide-N-glycosidase F (PNGaseF) [30]. This method could serve as additional strategy in glycopeptide analysis, although information on the oligosaccharide structure is lost. Glycopeptides may be identified in samples measured before and after enzymatic release of either the whole glycan or defined carbohydrate moieties [31]. The latter can also be used for elucidation of the carbohydrate constitution by calculation of mass differences if the glycopeptide contains only one glycosylation site. Most commonly used glycosidases are shown in Figure 6. Different MS fragmentation techniques can be employed to determine glycan structures, glycan attachment sites and peptide sequences. For instance, collision-induced dissociation (CID) in triple quadrupole MS instruments leads predominantly to fragmentation of glycosidic linkages which are more labile compared to peptide bonds, hence primarily revealing information on the glycan composition [32]. In contrast, applying electron capture dissociation (ECD) in Fourier transform (FT)-MS or electron transfer dissociation (ETD) in ion trap instruments, the peptide backbone is preferably fragmented leaving glycan structures intact [33, 34]. Thus, a combination of these fragmentation techniques leads to complementary information.

3.2.3. Analysis of glycans

Similar to protein cleavage, glycan release can be accomplished by enzymatic and chemical methods in which different reagents are employed compared to proteolysis. The usage of peptide-N-glycosidase F (PNGaseF) enables complete N-glycan removal, except for those containing $\alpha(1,3)$ -linked Fuc attached to the reducing terminal GlcNAc residue [35]. In contrast, this type of glycan can be removed by PNGaseA. Both amidases cleave the linkage between GlcNAc and Asn which converts Asn into Asp. The resulting mass shift of +0.98 Da can be used to identify respective attachment sites in glycoproteins or -peptides with a single N-glycosylation site. Endo- β -N-acetylglucosaminidases cleave the glycosidic bond between the first and the second GlcNAc residue of the chitobiose core, leaving a single GlcNAc residue still bound to the peptide backbone. Glycosidases of this enzyme classification possess different substrate specificities [36]. Endo H and F1 preferably cleave oligomannosidic and most hybrid-type chains, while Endo F2 and

F3 liberate certain complex-type glycans. Exoglycosidases such as sialidase, α -fucosidase, α/β -mannosidase, β -N-acetylhexoaminidase, and β -galactosidase cleave non-reducing terminal Sia, Fuc, Man, GlcNAc, and Gal residues, respectively, and can be used for enzymatic glycan sequencing. Hence, information can be obtained on the glycan composition, on the anomeric linkages and, at least with certain available enzymes, on the monomeric linkage positions [17]. An overview of suitable endo- and exoglycosidases for glycan analysis is illustrated in Figure 6. The enzymatic release of glycans is applicable to glycoproteins in solution, in gel after gel electrophoresis, directly on the MALDI-target plate or bound to affinity reagents [37-39]. For chemical release, hydrazinolysis and β -elimination under harsh conditions are the most common procedures producing intact N-glycans with a free reducing terminus, but disruption of the peptide chain has to be considered as an inevitable drawback [40, 41].

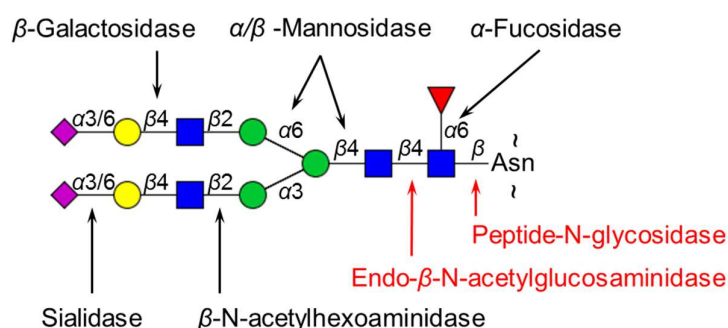


Figure 6: A biantennary N-glycan is shown with different exoglycosidases (black) only acting on terminal sugars and endoglycosidases (red) removing intact N-glycans. Reproduced and modified from [15].

As glycan detection is hampered by interconversion of anomeric forms of the reducing sugar, the lack of chromophores and low ionization efficiency by MS, several possible labeling reactions generating respective glycan derivatives have been developed such as reductive amination, Michael addition, and hydrazide labeling [42-44]. By reductive amination of the reducing end-aldehyde group, amine-based labels such as 2-aminopyridine (PA) and 2-aminobenzamide (2-AB) can be incorporated into the glycan structure. For Michael addition, the active methylene group of a label reagent like 1-phenyl-3-methyl-5-pyrazolone (PMP) reacts with the reducing end of a glycan, followed by a reversible 1,4-Michael addition of a second label molecule under basic conditions [45]. The considerable risk of loss of sialic acids in acidic medium in case of reductive amination reactions can be avoided [46]. In hydrazide labeling, the hydrazine label such as benzohydrazide is attached to the end-aldehyde group of a glycan forming a hydrazone under weak acidic conditions [47]. Glycans may be not only derivatized by chromophores and fluorophores facilitating detection after chromatographic separation but also by ionizable functional groups, thus improving sensitivity in MS-based detection.

Glycan derivatization may be also required as saccharides are very hydrophilic structures primarily due to numerous hydroxyl groups, and thus analysis by reversed phase (RP) high-performance liquid chromatography (HPLC) is challenging. In order to achieve retention on hydrophobic stationary phases, glycans can be permethylated or are often labeled with hydrophobic tags such as 2-AB [48, 49]. For analysis of complex glycan mixtures, several other techniques have been employed enabling separation of isobaric and isomeric glycan species, of which MS-based differentiation is still a cumbersome task. Ion exchange chromatography (IEC) has been used for many years for separation of glycans based on the number of charged groups and to a minor extent on the glycan size [50]. The widely used mode of IEC for the analysis of glycans is high-performance anion-exchange chromatography (HPAEC) coupled with pulsed amperometric detection (PAD) and MS [51-53]. In normal phase (NP)-HPLC, glycan elution times generally increase with sugar size due to elevated hydrophilic interactions between glycans and the stationary phase [54]. HILIC is considered as a variant of NP-HPLC as it also utilizes a stationary phase which is more polar than the initial mobile phase. When this type of separation system is applied, glucose oligomers (dextran ladder) are often utilized for the calibration of retention time relying on certain conditions such as pH, salt concentration, and temperature. Porous graphitized carbon (PGC) columns fractionate oligosaccharides mainly due to hydrophobic interactions and are widely employed for efficient separation of glycan isomers and closely related compounds [55]. As described before, lectin affinity chromatography also offers a tool for fractionation of complex glycan mixtures into structurally subsets according to the lectin specificity. Lastly, capillary electrophoresis (CE) separates charged analytes according to their migration velocity in an electric field placed across the ends of a capillary column [17]. All of the aforementioned separation techniques differ partially or complete in their separation mechanism, and thus represent complementary methodologies which can be used in conjunction helping to provide substantial information on N-glycan structures. Advancements of mass spectrometry in terms of sensitivity, together with the capability for direct coupling to many separation methods mentioned above, has made MS a key technology for analysis of N-linked glycosylation. Understanding of N-glycan composition and its structural features is important as N-glycosylation influences glycoprotein properties such as protein folding, solubility, antigenicity, and recognition by other proteins. Consequently, alterations in glycosylation patterns affect a variety of biological processes and may lead to human diseases [15]. However, protein N-glycosylation analysis in low concentration ranges in biological samples is often impeded by the small amounts of sample available and the enormous structural glycan heterogeneity.

4. Hybrid immunoaffinity mass spectrometry (IA-MS)

The aforementioned challenges accompanied with the analysis of protein N-glycosylation in biological samples might be tackled by combining the advantages of traditional immunoassays (IA) with latest MS-based technology, called hybrid immunoaffinity mass spectrometry (IA-MS). In this section, first the principles of IA and triple quadrupole mass spectrometry (TQMS) are briefly described together with their pros and cons for large biomolecule analysis. Then, the main drivers and opportunities of hybrid IA-MS-based assays are discussed.

4.1. Immunoassays (IA)

IA are widely used for bioanalysis of large molecules through the use of antibodies specific to an analyte (antigen-capture). Numerous variations of IA have been developed which can be classified into heterogeneous and homogeneous assays, respectively. While heterogeneous IA contain multiple steps such as binding, separation, and washing, homogeneous IA are operated simply by mixing the reagents and sample without additional steps prior to detection of the analyte of interest. Both assay types can be performed in either competitive or non-competitive mode depending on nature of the analyte, availability of antibodies and label reagents, and analytical requirements. In the competitive mode, the sample analyte and a labeled analyte compete for the binding to a limited amount of anti-analyte antibody bound to a solid support such as test tubes or 96-well plates. After equilibration and separation, the label activity on the solid phase is measured e.g. by radiation, fluorescence or enzymes. The obtained signal is inversely proportional to the analyte concentration in the sample (Figure 7a) [56]. In the non-competitive mode, also called sandwich assay, two antibodies are required which bind to non-overlapping epitopes on the analyte molecules. One of the two antibodies is used as analyte capture antibody, whereas the second one is labeled and used for detection. The analyte in the sample is allowed to specifically bind to the capture antibody which is immobilized onto a solid phase. After washing away of other sample constituents, the analyte-antibody-complex is incubated with an excess of the labeled detection antibody, which binds to another epitope on the analyte molecule. After washing, the label activity can be measured directly or indirectly by means of substrates depending on the label type linked to the detection antibody (Figure 7b) [56]. Among a variety of different signal generating labels including radioactive isotopes, DNA reporters, electrochemiluminescent tags, fluorescent probes or metal chelates, enzymes are the most common labels employed in IA-based methods, frequently called enzyme-linked immunosorbent assays (ELISA) [57-62]. The major advantages of these assays in large biomolecule analysis are the ease of use, the possibility to fully automate the method, high throughput, and very low limits of detection. However, the development of antibodies specific to different epitopes of the antigen is often time-consuming and expensive. Moreover, IA have narrow dynamic ranges and suffer from limited selectivity due to antibody cross-reactivity which may result in lack of specificity from interferences and high-background levels [63].

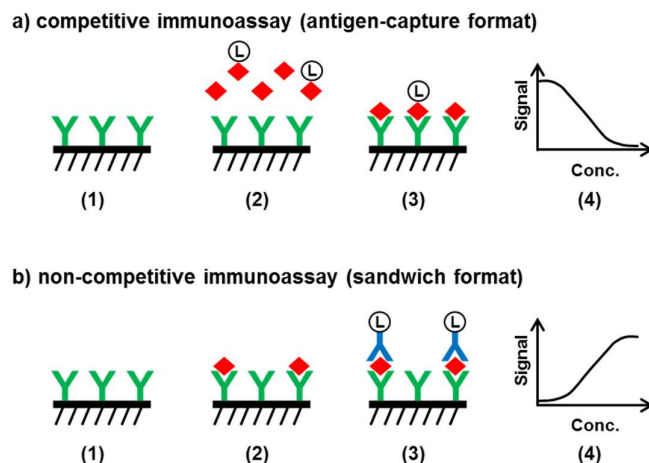


Figure 7: Schematic representation of two different immunoassay designs:

a) Competitive immunoassay including (1) solid support coating with capture antibodies, (2) sample loading and competitive reaction of sample analyte and labeled analyte, (3) capture of sample analyte and labeled analyte after washing, and (4) reading label activity and relating signal to analyte concentration.

b) Non-competitive immunoassay including (1) solid support coating with capture antibodies, (2) sample loading and capture of analyte, (3) addition of detection antibody and binding to analyte, and (4) reading label activity and relating signal to analyte concentration.

4.2. Triple quadrupole mass spectrometry (TQMS)

With the introduction of electrospray ionization (ESI) in the late 1980's, it has become possible to hyphenate high-performance liquid chromatography with mass spectrometry for the analysis of biological macromolecules such as proteins, peptides, and nucleic acids because ESI does not induce their fragmentation [64]. After ionization, quantitative analysis of generated ions has been dominated by triple quadrupole mass spectrometry (TQMS) due to its broad dynamic range and superior sensitivity over other MS analyzers including high-resolution mass spectrometers (HRMS) or time of flight (TOF) instruments [65-67]. A TQMS analyzer consists of two quadrupole mass filters (Q1 and Q3) in tandem, separated by a quadrupole collision region (Q2), and can be operated in different scan modes allowing for simple MS or MS/MS data collection. The most selective scan mode is referred to as multiple reaction monitoring (MRM) or selected reaction monitoring (SRM). In MRM the first quadrupole (Q1) selects ions of interest, so called precursor ions, previously generated in the ion source. The second quadrupole (Q2) filled with a collision gas e.g. nitrogen is used as a collision cell to fragment precursor ions into product ions. The third quadrupole (Q3) is set to allow only specified product ions to pass. Hence, defined precursor/product ion pairs (mass transitions) are conducted to the MS detector, which typically is an electron multiplier. A schematic overview of a TQMS analyzer operating in MRM mode is illustrated in Figure 8.

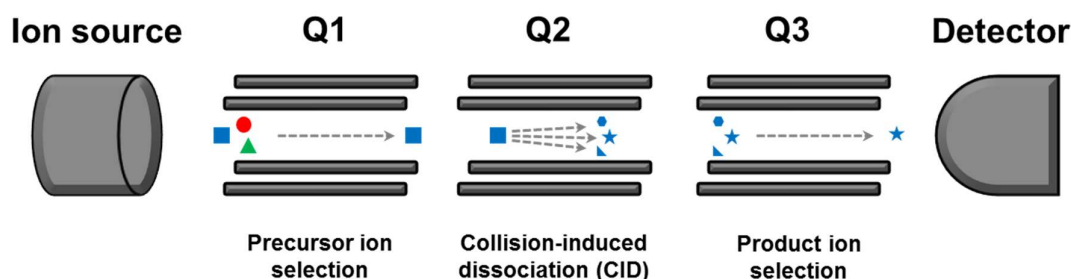


Figure 8: Schematic overview of a triple quadrupole mass spectrometer (TQMS) operating in multiple reaction monitoring (MRM) scan mode.

While TQMS instruments exhibit excellent sensitivity in MRM mode, they tend to be limited in mass resolution and possess low mass detection ranges. The upper mass limit of state-of-the-art instruments is approximately at 2000 m/z [68]. For the measurement of protein targets, thus, a bottom-up approach is commonly used in which intact proteins are subjected to proteolytic cleavage and resulting surrogate peptides are analyzed by tandem MS. Using collision-induced dissociation (CID) characteristic peptide fragments can be observed which are denoted as a-, b-, and c-ions, when the charge is retained on the N-terminal side of the fragmented peptide, and x-, y-, and z-ions when the charge is retained on the C-terminal side [69]. The most common peptide fragments observed in low energy collisions (collision energy < 200 eV) are a-, b- and y-ions, as depicted in Figure 9. In comparison to traditional IA-based methods, LC-MS-based assays benefit from less method development time, wider dynamic ranges, ability of multiplex analysis, and improved specificity, whereas the expertise to operate complex LC-MS instrumentation and the low throughput limits wider adoption of the technique [63]. In addition, with LC-MS, analysis of large molecules at low ng/mL levels in biosamples is challenging without pre-enrichment, mainly due to ion suppression from high-abundant proteins in the sample [70].

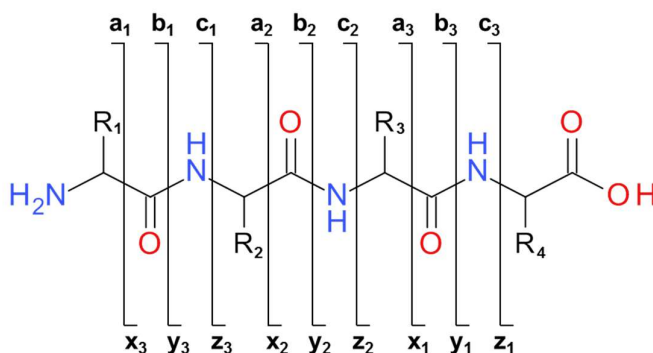


Figure 9: Characteristic fragmentation pattern of a tetrapeptide observed in collision-induced dissociation (CID)-MS.

4.3. Opportunities of hybrid IA-MS-based assays

Both traditional IA and latest LC-MS/MS are essential technologies being used in large molecule bioanalysis but each technique is associated with individual pros and cons as mentioned before. Major limitations in specificity or sensitivity can be tackled by combining both technologies allowing for efficient sample purification and immunoaffinity enrichment of large molecules prior to highly selective LC-MS/MS-based analysis. For this purpose, different formats of immunoaffinity enrichment methods have been developed in which antibody-coated microbeads such as agarose or magnetic beads have been the most widely applied tools [71]. Affinity capturing has also been performed in 96-well plates, on chips, on columns, and on pipette tips [72-75]. Antibodies can be immobilized onto solid support materials using different strategies including simple physical adsorption, covalent binding, biotin-streptavidin interaction, DNA directed orientation, or protein A/G capturing [76]. Another driver for hybridizing IA with MS may be that only one specific antibody is needed to enrich target proteins compared to ELISA which requires two antibodies against different epitopes. Moreover, the antibody selectivity is of less priority due to the final selection by MS [70]. This significantly reduces time and costs in assay development. Besides antibodies against intact proteins, another approach uses anti-peptide antibodies together with stable isotope standards (SIS), known as stable isotope standards and capture by anti-peptide antibodies (SISCAPA) workflow. An alternative option for protein capturing complementary to antibodies represents the use of aptamers which are chemically synthesized, single-stranded oligonucleotides forming a complex three-dimensional structure [77]. If affinity enrichment is conducted on protein level, proteolytic digestion can be performed either after elution of captured proteins in solution or directly on the solid support material where the target protein is still immobilized. As LC-MS/MS possess the ability of multiplex analysis, simultaneous detection of multiple peptides and even biotransformation products including metabolites is feasible [78, 79]. Assay automation has enabled the screening of large number of samples, which is a required step in biomarker evaluation due to the large variations across populations [80]. This might offer the adoption of hybrid IA-MS from early biomarker discovery to high throughput clinical applications. As shown, hybrid IA-MS provides new opportunities to keep up with the increasing demand for selective and very sensitive analysis of biologicals such as therapeutic monoclonal antibodies, antibody drug conjugates (ADC), fusion proteins, and biomarkers with specific isoforms or post-translational modifications (PTMs).

Chapter III

**Development of an LC-MS/MS-based strategy
for analysis of site-specific core-fucosylation
of prostate-specific antigen (PSA) in the low
ng/mL range in human serum**

Chapter III: Development of an LC-MS/MS-based strategy for analysis of site-specific core-fucosylation of prostate-specific antigen (PSA) in the low ng/mL range in human serum

1. Introduction

1.1. The role of human protein glycosylation

Among protein post-translational modifications (PTMs), glycosylation is a frequently occurring and functionally important one involved in many physiological processes including cell adhesion, receptor activation, protein folding and immune response [81-84, 108]. Estimates suggest that approximately half of all mammalian proteins are glycosylated [85, 108]. Protein glycosylation is not a template-driven process such as DNA, RNA or protein synthesis, but is rather controlled by complex enzymatic pathways during protein passage through the endoplasmic reticulum and Golgi compartments. The activity of those enzymes depends on factors including their quantity, localization and substrate availability, which can largely vary based on differences in tissue, cell type and disease state [86-88, 108]. Even under non-malignant conditions this greatly increases the complexity of protein glycosylation, resulting in extensive molecular micro- and macroheterogeneity of glycoproteins. The disturbance of this equilibrium in disease often leads to altered glycosylation of individual glycoproteins expanding the degree of heterogeneity beyond their natural forms [89, 108]. This offers the potential for glycoproteins to serve as markers for a variety of biological processes. Fucose (Fuc), galactose (Gal), glucose (Glc), mannose (Man), N-acetylglucosamine (GlcNAc), N-acetylgalactosamine (GalNAc) and sialic acid (Sia) are the primary building blocks of a diverse set of human N- and O-glycan structures. Core-fucosylation, consisting of an $\alpha(1,6)$ -Fuc modification on the innermost GlcNAc residue of the N-glycan core structure, has attracted attention, because it can be linked to various types of cancers such as hepatocellular carcinoma, pancreatic cancer, lung cancer and prostate cancer (PCa) [4, 90-92, 108].

1.2. Prostate-specific antigen (PSA)

Prostate-specific antigen (PSA), also known as Kallikrein-3 (KLK3), is a 28-32 kDa glycoprotein composed of 237 amino acids. According to the NXT/S motif for N-glycosylation (if X is not proline), PSA possesses a single N-glycosylation site at Asn-69. In blood, PSA circulates in two predominant forms, either as free PSA or complexed to $\alpha 1$ -antichymotrypsin and $\alpha 2$ -macroglobulin [93, 108]. PSA is almost exclusively secreted by epithelial cells of the prostate gland, which makes PSA a highly organ-specific biomarker [2, 108]. PSA blood levels of 10 ng/mL or higher indicate the risk of cancer, and prostate biopsy is usually recommended [94, 108]. However, PSA is not a cancer-specific biomarker because PSA blood levels do not efficiently distinguish between PCa and other prostatic diseases, such as benign prostatic hyperplasia (BPH) and prostatitis, especially in the so called “grey area” ranging from 4-10 ng/mL [95, 108]. In addition, PSA serum levels cannot differentiate between indolent and aggressive PCa [96, 108]. As a consequence, PSA screening resulted in tremendous

over-diagnosis and over-treatment during the last decades [97, 108]. Several groups proposed that altered glycosylation might increase the diagnostic potential of PSA [98, 108]. Defined changes in the fucosylation degree of PSA in cancer samples have been described using different lectin-based approaches. For example, Fukushima *et al.* showed in a 40-sample cohort that $\alpha(1,2)$ -fucosylated total PSA levels were higher in sera of PCa patients than in sera of BPH patients with more than 95 % probability [99, 108]. The $\alpha(1,2)$ -fucosylated form of free PSA was shown by Dwek *et al.* to be increased in sera of cancer patients with 92 % specificity and 69 % sensitivity for PCa over BPH [93, 108]. In contrast, a significant decrease with 90 % sensitivity and 95 % specificity in $\alpha(1,6)$ -core-fucosylated total PSA was found by Llop *et al.* in high-risk PCa that differentiated BPH and low-risk PCa from high-risk PCa patients in a 73-sample cohort in which total PSA concentrations ranged from 4.14 to 109.7 ng/mL [4, 108].

1.3. Approaches for the analysis of core-fucosylated proteins

Although glycoprotein research has been improved by advancements in mass spectrometry (MS), core-fucosylation analysis in complex matrices remains challenging as concentrations of individual glycoproteins are usually very low due to glycan microheterogeneity at multiple glycosylation sites. Furthermore, representative glycopeptides have decreasing ionization efficiencies with glycan branching and sialylation and notably suffer from ion suppression from co-eluting non-glycopeptides during electrospray ionization (ESI) [100, 108]. Several methods have been applied to overcome these challenges using large scale glycoprotein or glycopeptide enrichment steps, for example, lectin affinity chromatography, peroxidase oxidation prior to hydrazide coupling or hydrophilic interaction chromatography [30, 90, 108]. In contrast, specific enrichment of individual glycoproteins using IgG depletion followed by immunoprecipitation has been performed on high-abundance glycoproteins such as ceruloplasmin and $\alpha 2$ -macroglobulin [91, 101, 108]. Enriched and purified glycoproteins or glycopeptides are commonly enzymatically treated by endoglycosidases for complete or partial cleavage of their glycans and are analyzed by tandem MS with or without previous labeling [102, 103, 108]. Core-fucosylation analysis at the glycan level is usually achieved by using peptide-N-glycosidase F (PNGaseF) cleaving N-glycans from purified proteins or from biological mixtures [104, 108]. This enzymatic release additionally allows for indirect identification of N-glycosylation sites of glycoproteins by deamidation of asparagine to aspartic acid providing a mass shift of +0.98 Da. However, information linking multiple glycosylation sites to its respective glycan structures is lost. Other enzyme-based strategies using galactosidases, sialidases or endo- β -N-acetylglucosaminidases retain site-specific information as these enzymes do not remove the complete glycan [105, 108]. In addition, glycan microheterogeneity of partially truncated glycopeptides is simplified and ionization efficiency is increased compared to intact glycopeptides, making partial deglycosylation a useful tool in core-fucosylation analysis.

All of the examples mentioned above have been limited to the core-fucosylation analysis of high-abundance and highly purified glycoproteins or applied large scale screenings of core-fucosylated serum proteomes. By applying glycoproteome-wide studies, disease-specific modifications of a single,

low-concentrated glycoprotein cannot be monitored. The analysis of individual modifications may be a more effective biomarker refinement strategy as the discovery of the core-fucosylated α -fetoprotein (AFP-L3) approved for the early diagnosis of hepatocellular carcinoma by the Food and Drug Administration (FDA) recently showed [106, 108]. Alternative, non-MS-based strategies for core-fucosylation analysis use enzyme-linked lectin assays (ELLA). These types of assays are based on a similar principle to the common enzyme-linked immunosorbent assay (ELISA) technique, in which the capture or detection antibody or both are replaced by a lectin. Approaches involving antibody-based capture of low-concentrated glycoproteins and subsequent detection of their fucosylation by lectins have been employed [4, 93, 108]. Major challenges with ELLA are the inherent glycosylation of the capture/ detection antibody or non-specific binding by high-abundance glycoproteins from human matrices, which can cause a non-specific background signal by lectin detection, obscuring the analyte signal of interest. Furthermore, simultaneous measurement of total glycoprotein levels and corresponding core-fucosylated subpopulations is not feasible. Outside the biological context, lectins have low affinity for their target glycans as multivalent interactions are missing [107, 108]. This makes glycosylation analysis in the low concentration range more difficult.

In this chapter, a hybrid immunoaffinity mass spectrometry (IA-MS) based approach for the simultaneous quantification of total PSA levels and its core-fucosylated subpopulation in the low ng/mL concentration range in human serum was developed [108]. Challenges in lectin-based approaches including weak affinity for low-concentrated targets could be tackled by combining the sensitivity of immunoassays with the specificity of mass spectrometric detection. Here, the glycoprotein PSA served as an ideal example as its native serum concentrations usually are very low. The heart of the method was a magnetic bead-based immunoaffinity enrichment step followed by consecutive partial deglycosylation and proteolytic digestion while PSA was still captured by the immunoaffinity complex. Following, surrogate peptides of total PSA and core-fucosylated PSA were analyzed by LC-MS/MS. Based on calibration curves of total and core-fucosylated PSA, the linear range, lower limit of detection (LLOD), lower limit of quantification (LLOQ) and imprecision expressed as coefficient of variation (CV) were evaluated [108].

2. Experimental section

2.1. Reagents and materials

Streptavidin-coated magnetic particles (Ref. 11641786001), biotinylated monoclonal antibodies PSA30 against free PSA, PSA10, PSA36 and PSA66 against total PSA (= free and complexed PSA), total PSA CalSet II (Ref. 04485220190), sialidase from *Clostridium perfringens* (Ref. 11585886001), protease Arg-C from *Clostridium histolyticum* (Ref. 11370529001), protease Arg-C activation solution (Ref. 11370529001), proteinase K from *Pichia pastoris* (Ref. 03115887001), 2-Amino-2-(hydroxymethyl)propane-1,3-diol (TRIS, Ref. 10708976001) and universal diluent (Ref. 11732277122) were obtained from Roche Diagnostics GmbH (Mannheim, Germany). Endoglycosidase F3 (Endo F3) from *Elizabethkingia meningosepticum* and endoglycosidase F2 (Endo F2) from *Elizabethkingia miricola* were obtained from Ludger Ltd (Oxfordshire, UK). IgGZERO® Endo S from *Streptococcus pyogenes* AP1 and GlycINATOR® Endo S2 from *Streptococcus pyogenes* M49 were obtained from Genovis Inc. (Cambridge, USA). Remove-iT® Endo S from *Streptococcus pyogenes* was purchased from New England Biolabs (Ipswich, USA). Thermolysin and elastase were received from Promega (Madison, USA). Phosphate buffered saline (PBS), triethylammonium bicarbonate buffer (TEAB), 2-[4-(2-hydroxyethyl)piperazin-1-yl]ethanesulfonic acid (HEPES), trypsin from porcine pancreas, α -chymotrypsin from bovine pancreas, pepsin from pig gastric mucosa, tween 20, 1,4-dithiothreitol (DTT), iodoacetamide (IAM) and ammonium bicarbonate (ABC) were purchased from Sigma-Aldrich (St. Louis, USA). TMT duplex isobaric label reagent set containing TMT-126 and TMT-127 label reagent was purchased from Thermo Fisher Scientific (Waltham, USA). Di-sodium hydrogen phosphate, sodium dihydrogen phosphate, di-potassium hydrogen phosphate, potassium dihydrogen phosphate, sodium chloride and calcium chloride, anhydrous sodium acetate, potassium hydroxide and glacial acetic acid were obtained from Merck (Darmstadt, Germany). Acetonitrile (ACN), trifluoroacetic acid (TFA) and formic acid (FA) were all ULC/MS grade and purchased from Biosolve (Dieuze, France). Hydrochloric acid (HCl) was obtained from Bernd Kraft GmbH (Duisburg, Germany). Deionized water (18.2 m Ω cm) was prepared with a Milli-Q® Plus integral water purification system for ultrapure water from Merck Millipore (Darmstadt, Germany). PSA purified from human seminal fluid was purchased from Scripps Laboratories (San Diego, USA). Peptides LSEPAELTDAVK (single-letter amino acid code), SVILLGR and a mixture of glycopeptides N(GlcNAc)K and N(GlcNAc+Fuc)K were synthesized in house at Roche Diagnostics GmbH (Penzberg, Germany). MS tune solutions including 2.0 e-7 M polypropylene glycol and ES tuning mix were obtained from AB Sciex (Darmstadt, Germany).

2.2. Instruments and equipment

Microcon® centrifugal filter were purchased from Merck Millipore (Carrigtwohill, Ireland). Protein LoBind tubes, 96-deepwell plates, pipette tips and combitips advanced were obtained from Eppendorf (Hamburg, Germany). Mass spectrometric immunoassay disposable automation research tips (MSIA™ D.A.R.T.'S™) coated with streptavidin were purchased from Thermo Fisher Scientific

(Waltham, USA). HPLC vials and 0.1 mL micro inserts were obtained from VWR (Radnor, USA). 0.35 mL micro inserts were obtained from WICOM (Heppenheim, Germany).

Unless stated otherwise, the following instruments and equipment were used. Samples were incubated on a ThermoMixer C from Eppendorf (Hamburg, Germany) or in a drying oven Typ B 6030 from Heraeus instruments (Hanau, Germany). For sample drying a vacuum concentrator 5301 from Eppendorf was used. Samples were weighed with a Research RC 210 P MC1 analytical scale from Sartorius (Utting, Germany). MSIA tip-based experiments were performed using a Finnpiptette™ Novus i Multichannel Electronic Pipette from Thermo Fisher Scientific (Waltham, USA). Magnet particle separation was achieved using a DynaMag™-2 Magnet from Thermo Fisher Scientific. Samples were centrifuged using a centrifuge 5417R from Eppendorf. Multipette® stream and pipettes Reference® 2 were also from Eppendorf. LC-MS/MS analysis was performed using an Infinity 1290 UHPLC from Agilent Technologies (Santa Clara, USA) equipped with a G4220A binary pump, a G4226A autosampler, a G1316C thermostatted column compartment and a G1330B thermostat. The MS instrument was a QTRAP 6500 equipped with TurboV™ Ion Source from AB Sciex (Darmstadt, Germany) which was initially tuned and calibrated according to the manufacturer's instructions using polypropylene glycol, ES Tuning Mix and Tuning Mix Solvent from AB Sciex. Q1 and Q3 resolution was set to 0.7 ± 0.1 amu full width at half height at a scan rate of 10 Da/s, referred to as unit resolution in MRM mode. Chromatographic separation of tryptic surrogate peptides was performed using an XBridge Amide column (130 Å, 3.5 µm, 2.1 x 100 mm). Surrogate peptides generated by digestion of PSA using protease Arg-C were separated using an Acquity UPLC BEH C18 column (130 Å, 1.7 µm, 2.1 x 150 mm). Both columns were obtained from Waters (Milford, USA).

2.3. PSA spiked-in serum samples and human specimen

For method optimization and characterization, total PSA CalSet II was used containing calibrator 1 and 2 consisting of human PSA (Scripps Laboratories) in female serum matrix at 0 ng/mL and 60 ng/mL, respectively. Both calibrators were mixed and spiked if applicable with PSA purified from human seminal fluid (Scripps Laboratories) resulting in different concentrations of total PSA. Prior to preparing PSA spiked-in serum samples, N-glycans of human PSA from Scripps Laboratories were analyzed by LC-MS to give a rough estimation about the fucosylation degree of this material. N-glycan analysis revealed two major N-glycan peaks corresponding to a biantennary complex structure (A2G2S2, Oxford notation name) with and without core-fucose in a proportion of 78 % and 32 %, respectively. Furthermore, non-fucosylated and fucosylated PSA previously separated by lens culinaris agglutinin (LCA) lectin affinity chromatography using PSA from Scripps Laboratories as raw material were diluted in universal diluent and combined accordingly, resulting in different ratios of non-fucosylated to fucosylated PSA. These solutions were spiked into PSA-free female serum resulting in final total PSA concentrations of 10 ng/mL and different ratios of non-fucosylated to fucosylated PSA (100:0, 75:25, 50:50, 25:75 and 0:100). Three anonymized human specimen with total PSA concentrations of 2.35, 7.20 and 7.30 ng/mL and three PSA-free female sera were provided in-house by Roche Diagnostics GmbH (Penzberg, Germany) for feasibility studies. Total PSA

concentrations of PSA spiked-in serum samples and human specimen were measured using commercially available Elecsys® total PSA electrochemiluminescence immunoassay (ECLIA) assays on the **cobas e 601** system (Roche Diagnostics GmbH, Penzberg, Germany) as described previously [59]. All procedures in this study involving human sera were conducted according to the Declaration of Helsinki [108].

2.4. Endoglycosidase selection

Endoglycosidase selection was performed based on partial deglycosylation of intact PSA according to the following protocols:

IgGZERO® Endo S:

10 µL of a 1 µg/µL PSA solution in H₂O (Scripps Laboratories), 38 µL of a 10 mM sodium phosphate buffer containing 150 mM sodium chloride at pH 7.4 and 2 µL (80 units) IgGZERO® Endo S were mixed and incubated at 37 °C overnight.

GlycINATOR® Endo S2:

10 µL of a 1 µg/µL PSA solution in H₂O (Scripps Laboratories), 38 µL of a 10 mM sodium phosphate buffer containing 150 mM sodium chloride at pH 7.4 and 2 µL (80 units) GlycINATOR® Endo S2 were mixed and incubated at 37 °C overnight.

GlycINATOR® Endo S2 and Sialidase:

10 µL of a 1 µg/µL PSA solution in H₂O (Scripps Laboratories), 30 µL of a 2 mM potassium phosphate buffer at pH 6.1 and 5 µL (0.1 units) Sialidase were mixed and incubated at 37 °C overnight. Next, 3 µL 20 mM potassium hydroxide, 2 µL H₂O and 2 µL (80 units) GlycINATOR® Endo S2 were added, mixed and incubated at 37 °C overnight.

Remove-iT® Endo S:

10 µL of a 1 µg/µL PSA solution in H₂O (Scripps Laboratories), 5 µL of a 500 mM sodium phosphate buffer at pH 7.5, 34 µL H₂O and 1 µL (200 units) Remove-iT® Endo S were mixed and incubated at 37 °C overnight.

Remove-iT® Endo S and Sialidase:

10 µL of a 1 µg/µL PSA solution in H₂O (Scripps Laboratories), 5 µL of a 500 mM sodium acetate buffer containing 50 mM CaCl₂ at pH 5.5, 29 µL H₂O, 5 µL (0.1 units) Sialidase and 1 µL (200 units) Remove-iT® Endo S were mixed and incubated at 37 °C overnight.

Endo F2:

10 µL of a 1 µg/µL PSA solution in H₂O (Scripps Laboratories), 10 µL of a 250 mM sodium acetate buffer at pH 4.5, 28 µL H₂O and 2 µL (0.01 units) Endo F2 were mixed and incubated at 37 °C overnight.

Endo F3:

10 μ L of a 1 μ g/ μ L PSA solution in H₂O (Scripps Laboratories), 10 μ L of a 250 mM sodium acetate buffer at pH 4.5, 28 μ L H₂O and 2 μ L (0.01 units) Endo F3 were mixed and incubated at 37 °C overnight.

Endo F2 and Endo F3:

10 μ L of a 1 μ g/ μ L PSA solution in H₂O (Scripps Laboratories), 10 μ L of a 250 mM sodium acetate buffer at pH 4.5, 26 μ L H₂O, 2 μ L (0.01 units) Endo F2 and 2 μ L (0.01 units) Endo F3 were mixed and incubated at 37 °C overnight.

Endo F3 and Sialidase:

10 μ L of a 1 μ g/ μ L PSA solution in H₂O (Scripps Laboratories), 25 μ L of a 100 mM sodium acetate buffer at pH 5.0, 8 μ L H₂O, 5 μ L (0.1 units) Sialidase and 2 μ L (0.01 units) Endo F3 were mixed and incubated at 37 °C overnight.

Endo F3 in TRIS/HCl buffer:

10 μ L of a 1 μ g/ μ L PSA solution in H₂O (Scripps Laboratories), 25 μ L of a 100 mM TRIS/HCl buffer containing 10 mM CaCl₂ at pH 7.8, 28 μ L H₂O and 2 μ L (0.01 units) Endo F3 were mixed and incubated at 37 °C overnight.

All endoglycosidase treated PSA solutions were separated on an Acquity UHPLC system (Waters, Milford, USA) equipped with a Zorbax C8 column (Agilent Technologies, Santa Clara, USA) and analyzed on a LCT Premier (Waters, Milford, USA) in-house at Roche Diagnostics GmbH (Penzberg, Germany).

2.5. Protease and surrogate peptide selection

In silico digestion of PSA (Uni-ProtKB P07288) was performed by the PeptideMass tool [109] which is available online at the ExPASy Bioinformatics Resource Portal. PSA cleavage was simulated using different enzymes including trypsin, Lys-C, protease Arg-C, Asp-N, Glu-C, chymotrypsin, pepsin, proteinase K, elastase and thermolysin using the following settings: no missed cleavages and cysteines in reduced form.

For *in vitro* digestion, 50 μ L of a 1 μ g/ μ L PSA solution in H₂O (Scripps Laboratories) were partially deglycosylated by adding 10 μ L (0.05 units) Endo F3 and 140 μ L of a 50 mM sodium acetate buffer at pH 4.5. The mixture was incubated overnight at 37 °C. Following partial deglycosylation, 10 μ L of the Endo F3 treated PSA solution were pipetted on a 10 kDa cut-off Microcon® centrifugal filter and 50 μ L of a 100 mM ABC buffer at pH 8.0 were added. After centrifugation at 12,500 rpm for 30 min, 50 μ L of a 100 mM ABC buffer at pH 8.0 containing 50 μ g PPS and 5 μ L of a 10 mM DTT solution were added. The mixture was incubated at 50 °C for 30 min. After cooling to RT, reduced PSA was carboxymethylated by adding 5 μ L of a 55 mM IAM solution and mixed at 37 °C for 30 min in the dark.

The mixture was centrifuged at 12,500 rpm for 30 min and the Microcon® vial, containing the flow through, was replaced by a new Microcon® vial. In total, fourteen preparations were executed in this way in order to test seven different enzymes each at two different PSA-to-enzyme ratios (10:1 and 100:1) according to the following protocols:

Trypsin

50 µL of a 50 mM ABC buffer at pH 8.0 containing 50 µg PPS and 5 µL of a 0.05 µg/µL trypsin solution (PSA-to-enzyme ratio 10:1) or 5 µL of a 0.005 µg/µL trypsin solution (PSA-to-enzyme ratio 100:1), respectively, were added and incubated overnight at 37 °C.

Elastase

50 µL of a 50 mM TRIS/HCl buffer at pH 9.0 and 5 µL of a 0.05 µg/µL elastase solution (PSA-to-enzyme ratio 10:1) or 5 µL of a 0.005 µg/µL elastase solution (PSA-to-enzyme ratio 100:1), respectively, were added and incubated overnight at 37 °C.

Proteinase K

50 µL of a 50 mM TRIS/HCl buffer at pH 9.0 and 5 µL of a 0.05 µg/µL proteinase K solution (PSA-to-enzyme ratio 10:1) or 5 µL of a 0.005 µg/µL proteinase K solution (PSA-to-enzyme ratio 100:1), respectively, were added and incubated overnight at 37 °C.

Thermolysin

50 µL of a 50 mM TRIS/HCl buffer at pH 8.0 containing 0.5 mM CaCl₂ and 5 µL of a 0.05 µg/µL thermolysin solution (PSA-to-enzyme ratio 10:1) or 5 µL of a 0.005 µg/µL thermolysin solution (PSA-to-enzyme ratio 100:1), respectively, were added and incubated overnight at 37 °C.

Protease Arg-C

45 µL of a 100 mM TRIS/HCl buffer at pH 7.8 containing 10 mM CaCl₂, 5 µL activation solution containing 50 mM DTT and 5 mM EDTA, and 5 µL of a 0.05 µg/µL protease Arg-C solution (PSA-to-enzyme ratio 10:1) or 5 µL of a 0.005 µg/µL protease Arg-C solution (PSA-to-enzyme ratio 100:1), respectively, were added and incubated overnight at 37 °C.

Pepsin (pH = 1.3)

48 µL of a 50 mM ABC buffer at pH 8.0 containing 50 µg PPS, 2 µL 2M HCl and 5 µL of a 0.05 µg/µL pepsin solution (PSA-to-enzyme ratio 10:1) or 5 µL of a 0.005 µg/µL pepsin solution (PSA-to-enzyme ratio 100:1), respectively, were added and incubated overnight at 37 °C.

Chymotrypsin

50 µL of a 100 mM TRIS/HCl buffer at pH 7.8 containing 10 mM CaCl₂ and 5 µL of a 0.05 µg/µL chymotrypsin solution (PSA-to-enzyme ratio 10:1) or 5 µL of a 0.005 µg/µL chymotrypsin solution (PSA-to-enzyme ratio 100:1), respectively, were added and incubated overnight at 37 °C.

After incubation, all samples were centrifuged at 12,500 rpm for 30 min. 2 μ L FA were added to the flow through to stop digestion and incubated for 1 h at 37 °C, except of samples containing pepsin, which were heated to 90 °C for 15 min to stop digestion. Prior to LC-MS/MS analysis, 5 μ L of the samples were diluted with 25 μ L H₂O containing 0.1 % FA (v/v). Diluted samples were separated using a Dionex UltiMate 3000 nano LC system equipped with Nanospray™ Flex ion source, a FLM-3300B flow manager, a LPG-3300MB micro pump, a WPS-3000TPL RS autosampler (all devices from Thermo Fisher Scientific, Waltham, USA) and a temperature controller ET1312 (Enda, Istanbul, Turkey) used as external column oven. The column used was a PepSwift™ monolithic polymer column (200 μ m x 5 cm, Polystyrene/Divinylbenzol) and operated at a flow of 2 μ L/min. The mobile phase A was 0.05 % TFA in H₂O (v/v) and mobile phase B was 0.05 % TFA in acetonitrile (v/v). The analytical gradient lasted for 45 min where solvent B was held for 3 min at 0 %. The composition of solvent B was increased from 0 to 30 % in 30 min, followed by washing where solvent B was increased to 80 % in 1 min and held for 5 min. For column re-equilibration, solvent B was decreased to 0 % in 1 min and held for 5 min. The injection volume was 1 μ L, the flush volume was 7 μ L and the loop overfill was 2 μ L. Full loop injection mode was applied. Prior to sample injection the loop was washed twice with 100 μ L 50 % acetonitrile in H₂O (v/v). MS analysis was performed using a LTQ/FT Ultra mass spectrometer (Thermo Fisher Scientific, Waltham, USA) operated in positive ionization mode. The nano ESI (NSI) spray voltage and capillary voltage were set to 3.5 kV and 48 V, respectively. Collision-induced dissociation (CID) fragmentation was applied at 35 % of the normalized collision energy. Mass spectra were acquired in data-dependent manner using a full scan in the mass range of m/z 300 to 2000 and a resolution of 100,000 followed by CID MS/MS which was performed on the three most intensive ions using dynamic exclusion.

Spectra of two enzymatic preparations (PSA-to-enzyme ratio 10:1 and 100:1) were combined and searched automatically by Proteome Discoverer™ software (Version 1.3, Thermo Fisher Scientific) with SEQUEST using the following settings: (1) two maximum missed cleavage sites were allowed, (2) precursor mass tolerance was 10 ppm and fragment mass tolerance was 0.8 Da, (3) dynamic modifications i.e. methionine oxidation (+15.995 Da), asparagine glycosylation with GlcNAc (+203.079 Da) and with GlcNAc + Fuc (+349.137 Da), (4) static modification i.e. cysteine carbamidomethylation (+57.021 Da), (5) an in-house database was used containing PSA (Uni-ProtKB P07288), (6) trypsin, elastase, thermolysin, proteinase K, protease Arg-C, pepsin or chymotrypsin were selected as digestion enzymes. Peptide identification data was assessed manually using XCalibur™ software (Version 2.2, Thermo Fisher Scientific) and compared to *in silico* data. Based on these results, surrogate peptides suitable for quantification of total and core-fucosylated PSA were chosen prior to analyte-specific MS parameter optimization.

2.6. Analyte-specific MS parameter tuning

Suitable surrogate peptides, generated by protease Arg-C and trypsin digestion of PSA, were selected for quantification of total and core-fucosylated PSA. For this purpose, analyte-specific MS parameters i.e. transitions, declustering potential (DP), entrance potential (EP), collision energy (CE) and cell exit potential (CXP) were optimized. In this work, surrogate peptides generated by protease Arg-C were not available as synthetic standard peptides whereas tryptic surrogate peptides were synthesized in-house. Thus, two different procedures were used for analyte-specific MS parameter optimization. Both procedures are described below.

2.6.1. Tuning of surrogate peptides generated by protease Arg-C digestion

10 μL of a 1 $\mu\text{g}/\mu\text{L}$ PSA solution in H_2O (Scripps Laboratories) were partially deglycosylated using GlycINATOR® Endo S2 followed by protease Arg-C digestion similar to the procedures described in the previous chapter. Prior to LC-MS/MS analysis, digested PSA was diluted in H_2O containing 0.1 % FA (v/v) to a final concentration of 1.48 $\mu\text{g}/\text{mL}$ relating to the initial PSA weight. Chromatographic separation was performed using the Infinity 1290 UHPLC equipped with an Acquity UPLC BEH C18 column. The column oven temperature was set to 50 $^{\circ}\text{C}$ and the injection volume was 5 μL . The flow rate was set to 0.4 mL/min and mobile phases consisted of water containing 0.1 % FA (v/v) as eluent A and acetonitrile containing 0.1 % FA (v/v) as eluent B. The gradient started with 100 % eluent A for 2 min and was then decreased to 65 % eluent A within 30 min. Then, the percentage of eluent A was decreased to 5 % linearly within 1 min and held for 2 min. Afterwards eluent A was increased again to 100 % within 0.1 min and the column was re-equilibrated for 4.9 min at this percentage. In total, each run took 40 min taking into account the column re-equilibration time.

Using a QTRAP 6500 MS, enhanced product ion (EPI) scans of different precursor ions were performed and product ions were monitored in the mass range from 200 to 1000 Da as shown in Table 3. The scan rate was set to 10,000 Da/s and measurements were performed in positive ionization mode. The pause time between mass ranges was 1.5 ms, resolution in Q1 was set to unit resolution and a dynamic fill time of the linear ion trap was applied. Source parameters were adjusted as follows: curtain gas = 30 psi; collision gas = 12 psi; ion spray voltage = 3500 V; temperature = 450 $^{\circ}\text{C}$; gas 1 = 50 psi; gas 2 = 70 psi. Analyte-specific MS parameters were uniform for each precursor: DP = 100 V, EP = 10 V and CE = 7 V. After each LC-MS/MS run, the CE was increased by 3 V, while the other parameters were held constant. This resulted in nine different LC-MS/MS runs applying CE values of 7, 10, 13, 16, 19, 22, 25, 28 and 31 V.

Table 3: Peptide sequences generated by protease Arg-C digestion of total PSA and their respective precursor ions with charge states.

Peptide generated by protease Arg-C digestion	Precursor ion [Da]	Charge state
KWIKDTIVANP	642.9	2+
KWIKDTIVANP	428.9	3+
PSLYTKVVHYR	681.9	2+
PSLYTKVVHYR	454.9	3+
N(GlcNAc)KSVILLGR	1202.7	1+
N(GlcNAc)KSVILLGR	601.9	2+
N(GlcNAc)KSVILLGR	401.6	3+
N(GlcNAc+Fuc)KSVILLGR	674.9	2+
N(GlcNAc+Fuc)KSVILLGR	450.3	3+

For multiple reaction monitoring (MRM), a MRM method was created based on the most sensitive precursor/product ion pairs and their respective CE values identified in the EPI scan experiments (Table 9). The dwell time of each transition was 100 ms and the pause time between single transitions was set to 5 ms. Q1 and Q3 resolution was set to 0.7 ± 0.1 amu full width at half peak height at a scan rate of 10 Da/s, which is referred to as unit resolution in MRM mode. Source parameters were used as described in the EPI scan experiments. The initial analyte-specific MS parameters were as follows: DP = 100 V, EP = 10 V and CXP = 20. The CE values were analyte-specific as shown in Table 4. Chromatographic settings were similar as described in the EPI scan experiments but this time using an improved gradient which started with 90 % eluent A for 2 min and was then decreased to 70 % eluent A within 30 min. Then, the percentage of eluent A was decreased to 5 % linearly within 1 min and held for 2 min. Afterwards eluent A was increased again to 100 % within 0.1 min and the column was re-equilibrated for 4.9 min at this percentage. For this experiment, 5 μ L of a 1.48 μ g/mL digested PSA solution were injected, which was the same solution as used in the EPI scan experiments. Several LC-MS/MS runs were performed based on the described MRM method, but each time one of the initial analyte-specific MS parameters was varied (CE \pm 2 V, CXP \pm 5 V, DP set to 25, 50, 75 or 125 V, EP set to 7, 8 or 9 V), resulting in several slightly differing LC-MS/MS runs. This procedure was repeated using further parameter variations in order to obtain final optimized analyte-specific MS parameters of PSA peptides generated by protease Arg-C (Table 10).

Table 4: Most sensitive transitions and their respective CE values identified in EPI scan experiments.

Peptide generated by protease Arg-C digestion	Charge state	Precursor ion [Da]	Product ion [Da]	Collision energy [V]
KWIKDTIVANP	2+	642.9	585.3	19
KWIKDTIVANP	3+	428.9	528.3	10
KWIKDTIVANP	3+	428.9	585.3	10
PSLYTKVVHYR	2+	681.9	574.3	28
PSLYTKVVHYR	3+	454.9	589.3	13
PSLYTKVVHYR	3+	454.9	633.4	13
N(GlcNAc)KSVILLGR	2+	601.9	757.5	25
N(GlcNAc+Fuc)KSVILLGR	2+	674.9	601.9	22
N(GlcNAc+Fuc)KSVILLGR	2+	674.9	757.5	22

2.6.2. Tuning of surrogate peptides generated by tryptic digestion

Analyte-specific MS parameters of tryptic PSA peptides, including transitions, DP, EP, CE and CXP, were automatically tuned in terms of signal intensity carrying out the compound optimization feature of the Analyst software (Version 1.6.2, AB Sciex) scanning for the ten most intensive transitions. For this purpose, pure peptide solutions of LSEPAELTDAVK, SVILLGR and a mixture of glycopeptides N(GlcNAc)K and N(GlcNAc+Fuc)K were directly infused into the QTRAP 6500 MS via T-fitting at a concentration of 1 µg/mL solved in 70 % acetonitrile in H₂O containing 0.1 % FA (v/v) accompanied by a constant LC flow consisting of 70 % acetonitrile in H₂O containing 0.1 % FA (v/v) at a flow rate of 0.3 mL/min. DMS and MS3 parameters as well as source parameters were optimized manually using the same T-Fitting arrangement as mentioned before. Furthermore, 10 µg of peptide LSEPAELTDAVK as well as 10 µg of the glycopeptides N(GlcNAc)K and N(GlcNAc+Fuc)K were labeled using 20 µg TMT-126 and incubated overnight at RT. Analyte-specific MS parameters of TMT-labeled peptides at concentrations of 4 µg/mL were automatically tuned in the same manner as unlabeled peptides.

2.7. Immunoaffinity enrichment

2.7.1. MSIA tip-based approach

Initially, streptavidin-coated MSIA tips were prewashed with 200 μ L PBS buffer by repetitive up and down pipetting (175 μ L pipetted volume, 20 cycles) using a Finnpiptette™ Novus i Multichannel Electronic Pipette (Thermo Fisher Scientific, Waltham, USA). A volume of 125 μ L of biotinylated PSA36 antibody solution at 10 μ g/mL was loaded into a 500 μ L Protein LoBind 96-deepwell plate. 100 μ L of that solution were drawn through the streptavidin-coated pipette tip for enrichment (400 cycles). Afterwards, a washing step using 200 μ L PBS was incorporated to remove unbound anti-PSA antibodies (175 μ L pipetted volume, 20 cycles). 100 μ L of serum samples were loaded into the 96-deepwell plate prior to immunoaffinity capture. The PSA enrichment was performed by repeatedly aspirating and dispensing 75 μ L of serum sample through the antibody-bound streptavidin-coated pipette tips (1000 cycles). Following, the tips were rinsed stepwise with 200 μ L PBS buffer containing 0.1 % Tween 20 followed by 200 μ L PBS in order to remove unbound serum contaminants (175 μ L pipetted volume, 20 cycles each).

2.7.2. Magnet bead-based approach

By means of a magnet separator 100 μ g (100 μ L) streptavidin-coated magnetic particles were washed with 10 mM (100 μ L) PBS buffer in order to remove storage buffer containing 50 mM HEPES, 0.1 % BSA, 0.1 % chloracetamide and 0.01 % methyl-isothiazolone. Next, supernatant was removed, 1 μ g (100 μ L) biotinylated anti-PSA antibody PSA36 was added to washed streptavidin-coated magnetic particles and incubated for 10 min at 25 °C. Again, the supernatant was removed and streptavidin-coated magnetic particles were washed with 10 mM (100 μ L) PBS buffer in order to remove unspecific-bound antibodies. 100 μ L of serum samples were added to antibody-bound streptavidin-coated magnetic particles and incubated for 10 min at 25 °C. Supernatant was removed. After incubation, magnetic particles were washed with 10 mM (100 μ L) PBS containing 0.05 % Tween followed by 10 mM (100 μ L) PBS [108].

2.8. Partial deglycosylation and digestion

2.8.1. Protease Arg-C-assisted approach using MSIA tips (in solution protocol)

Following immunoaffinity capture, enriched PSA was eluted manually into a clean 0.5 mL Protein LoBind tube by repetitive (20 cycles) up and down pipetting of 25 μ L elution buffer consisting of 40 % acetonitrile and 0.4 % TFA in H₂O (v/v). Next, a volume of 40 μ L of a 200 mM TRIS/HCl buffer at pH 7.5 containing 10 mM CaCl₂ was added to the 0.5 mL Protein LoBind tube and mixed. Afterwards, 2 μ L (0.01 units) Endo F3 in 20 mM TRIS-HCl buffer at pH 7.5 were added and incubated at 37 °C overnight. The next day, 60 μ L of 200 mM TRIS/HCl buffer at pH 7.5 containing 10 mM CaCl₂ and 10 μ L protease Arg-C solution containing 1.4 ng/ μ L protease Arg-C, 200 mM TRIS/HCl, 10 mM CaCl₂, 25 mM DTT and 2.5 mM EDTA were added and incubated at 37 °C overnight. Finally, samples were dried in a vacuum concentrator for 3.5 h at 45 °C and redissolved in 25 μ L 10 % acetonitrile in H₂O containing 0.1 % FA (v/v) prior to LC-MS/MS analysis.

2.8.2. Trypsin-assisted approach using MSIA tips (on tip protocol)

Following immunoaffinity enrichment, 2 μL (0.01 units) Endo F3 and 8 μL 100 mM sodium acetate buffer at pH 4.5 were pipetted into a 0.5 mL LoBind tube. The entire mixture was loaded onto the emptied streptavidin-coated pipette tip, still capturing the antibody-PSA complex. The pipette tip was placed into the 0.5 mL LoBind tube and incubated in a drying oven at 37 °C overnight. Next, the Endo F3 containing solution was discarded and the pipette tip was washed automatically with 200 μL ABC buffer at pH 8.0 (175 μL pipetted volume, 20 cycles). Then, 10 μL of a 0.1 $\mu\text{g}/\mu\text{L}$ trypsin solution in 100 mM ABC buffer at pH 8.0 were loaded onto the emptied pipette tip. The pipette tip was placed into a 0.35 mL HPLC micro insert (WICOM) and incubated in a drying oven at 37 °C overnight. The trypsin solution containing on tip digested proteins including PSA was discarded and the pipette tip was washed with 20 μL of acetonitrile containing 0.1 % FA (v/v) kept in a separate 0.5 mL LoBind tube (10 μL pipetted volume, 20 cycles). The eluate of the separate 0.5 mL LoBind tube was added to the volume of the HPLC Micro Insert prior to LC-MS/MS analysis.

2.8.3. Trypsin-assisted approach using magnet beads (on bead protocol)

Following immunoaffinity enrichment, partial deglycosylation and proteolytic digestion were performed stepwise while PSA was still captured by the immunoaffinity complex. First, 0.01 units (50 μL) Endo F3 in 100 mM sodium acetate buffer at pH 4.5 were added to the washed magnetic particles and incubated for 3 h at 37 °C. Supernatant was removed and magnetic particles were washed with 100 mM (100 μL) ABC buffer at pH 8.0. Secondly, 1 μg (50 μL) trypsin in 100 mM ABC buffer at pH 8.0 was added and incubated overnight (20.5 h) at 37 °C. Finally, supernatant was transferred to a new vial, dried for 2.5 h at 45 °C in a vacuum concentrator, and redissolved in 30 μL 70 % acetonitrile in H_2O containing 0.1 % FA (v/v) prior to LC-MS analysis [108].

2.9. LC-MS/MS analysis

2.9.1. RPLC-MS/MS analysis of protease Arg-C derived PSA peptides

After sample preparation, samples were analyzed by LC-MS/MS using an Infinity 1290 UHPLC. The MS instrument was a QTRAP 6500 MS equipped with TurboV™ Ion Source. MS measurements were carried out in positive ionization mode using the following source parameters: curtain gas = 30 psi; collision gas = medium; ion spray voltage = 3500 V; temperature = 450 °C; gas 1 = 50 psi; gas 2 = 70 psi. Q1 and Q3 resolution was set to 0.7 ± 0.1 amu full width at half peak height at a scan rate of 10 Da/s, which is referred to as unit resolution in MRM mode. Analyte-specific MS parameters i.e. transitions, dwell time, DP, EP, CE, and CXP were optimized and are listed in Table 10. One MRM transition of each of the two peptides N(GlcNAc+Fuc)KSVILLGR (m/z 674.9/601.9) and KWIKDTIVANP (m/z 428.9/585.3) was selected to quantify fucosylated PSA and total PSA, respectively. Pause time between single MRM transitions was set to 5 ms. Chromatographic separation was performed using the Acquity UPLC BEH C18 column at a flow rate of 0.4 mL/min. The injection volume was 20 μL and the column oven temperature was set to 50 °C. The mobile phases consisted of water containing 0.1 % FA (v/v) as eluent A and acetonitrile containing 0.1 % FA (v/v) as

eluent B. The gradient started with 90 % eluent A for 2 min and was then decreased to 84 % eluent A within 13 min. Then, the percentage of eluent A was decreased to 5 % linearly within 1 min and held for 2 min. Afterwards eluent A was increased again to 90 % within 0.1 min and the column was re-equilibrated for 4.9 min at this percentage. In total, each run took 23 min taking into account the column re-equilibration time [108].

2.9.2. HILIC-MS/MS analysis of tryptic PSA peptides

After sample preparation, samples were analyzed by LC-MS/MS using an Infinity 1290 UHPLC. The MS instrument was the QTRAP 6500 MS equipped with TurboV™ Ion Source. MS measurements were carried out in positive ionization mode using the following source parameters: curtain gas = 30 psi; collision gas = high; ion spray voltage = 4500 V; temperature = 450 °C; gas 1 = 50 psi; gas 2 = 70 psi. Q1 and Q3 resolution was set to 0.7 ± 0.1 amu full width at half peak height at a scan rate of 10 Da/s, which is referred to as unit resolution in MRM mode. Analyte-specific MS parameters i.e. transitions, dwell time, DP, EP, CE, and CXP were optimized and are listed in Table 13. One MRM transition of each of the two peptides N(GlcNAc+Fuc)K (m/z 464.2/261.2) and LSEPAELTDAVK (m/z 636.9/943.4) was selected to quantify core-fucosylated PSA and total PSA, respectively. Pause time between single MRM transitions was set to 5 ms. Chromatographic separation was performed using the XBridge Amide column at a flow rate of 0.3 mL/min. The injection volume was 20 μ L and the column oven temperature was set to 50 °C. The mobile phases consisted of water containing 0.1 % FA (v/v) as eluent A and acetonitrile containing 0.1 % FA (v/v) as eluent B. The gradient started with 90 % eluent B and was decreased to 50 % eluent B within 10 min. Then, the percentage of eluent B was decreased to 0 % linearly within 3.1 min and held for 0.9 min. Afterwards eluent B was increased again to 90 % within 0.1 min and column was re-equilibrated for 5.9 min at this percentage. In total, each run took 20 min taking into account the column equilibration time [108].

2.9.3. Multiple reaction monitoring cubed (MRM³)

Analysis in MRM³ mode was carried out in positive ionization mode using an ion spray voltage of 5500 V. The TurboV™ Ion Source was operated at 450 °C. The curtain gas flow was set to 50 psi and auxiliary gas 1 and 2 were set to 50 and 70 psi, respectively. The resolution in Q1 was adjusted to 0.7 ± 0.1 amu full width at half peak height, referred to as unit resolution. The Q3 entry barrier was set to 8 V. Linear ion trap (LIT) fill time and excitation time were set to 100 and 25 ms, respectively. MS/MS parameters used to fragment 1st precursor ions to 2nd precursor ions in Q2 are described in Table 13. Specified 2nd precursor ions were collected, isolated and further fragmented in LIT using parameters listed in Table 5. The resulting fragment ions were trapped into LIT prior to being scanned out and detected.

Table 5: MRM³ parameters of four surrogate peptides.

Target	Surrogate peptide	1 st Precursor ion [Da]	2 nd Precursor ion [Da]	Product ion scan [Da]	AF2 start- stop [V]	AF3 start- stop [V]	EXB start- stop [V]
Non-fucosylated PSA	N(GlcNAc)K / N(GlcNAc+Fuc)K	464.2	261.1	60-250	0.12-0.18	2.119- 2.710	-152.8 to -145.3
Fucosylated PSA	N(GlcNAc+Fuc)K	610.3	464.2	200-280	0.06-0.14	2.555- 2.804	-147.3 to -144.2
Total PSA	LSEPAELTDAVK	636.8	943.6	400-930	0.1-0.13	3.177- 4.825	-139.5 to -118.7
Total PSA	SVILLGR	379.3	579.4	150-550	0.09-0.09	2.399- 3.643	-149.3 to -133.6

AF2 = excitation energy used to fragment isolated 2nd precursor ions in the LIT

AF3 = trap radio frequency amplitude applied to Q3 when scanning the ions out of the LIT

EXB = exit barrier used to mass-selectively eject ions from the LIT

2.10. Data acquisition and analysis

Instrument control, data acquisition, data processing and data analysis were performed using Analyst software (Version 1.6.2, AB Sciex). In order to characterize the developed method the dwell time was set to 100 ms for each analyte generating sufficient data points per peak (> 25) for accurate quantification. The IntelliQuan integration algorithm was used for automatic peak integration and MRM spectra were processed with a smoothing width factor of 3 points. In case of inadequate peak detection and integration, peaks were integrated manually. Calibration curves were generated by plotting peak areas (y) against analyte concentrations (x). In case of samples containing different amounts of non-fucosylated and fucosylated PSA the peak area ratio of N(GlcNAc+Fuc)K to LSEPAELTDAVK was plotted against the relative amount of fucosylated PSA ranging from 0 to 100 % [108].

3. Results and discussion

3.1. Endoglycosidase selection

Preliminary experiments were performed to find an efficient endoglycosidase which allows partial deglycosylation of PSA between the two N-acetylglucosamine (GlcNAc) residues in the diacetylchitobiose core of the oligosaccharide linked to Asn-69. The aim was to generate a truncated PSA glycoprotein containing one GlcNAc residue with or without fucose (Fuc) that could be easily distinguished from PSA forms with complex glycan structures using ESI-MS. Five different endoglycosidases were tested including IgGZERO® Endo S from *Streptococcus pyogenes* AP1, GlycINATOR® Endo S2 from *Streptococcus pyogenes* M49, Remove-iT® Endo S from *Streptococcus pyogenes*, Endo F2 from *Elizabethkingia miricola* and Endo F3 from *Elizabethkingia meningosepticum*. Endoglycosidase treatment was performed using native PSA as described in chapter III section 2.4 and the enzymatic activity was evaluated based on mass spectra which were screened for partially deglycosylated PSA and non-deglycosylated PSA. Representative mass spectra are shown in Figure 10. Besides five different endoglycosidases, different enzyme mixtures were tested. In addition, enzyme amounts and reaction buffers were varied. The results of these experiments are summarized in Table 6.

Table 6: Overview of experiments using different endoglycosidases and conditions.

Experiment	with Sialidase	Endoglycosidase amount per µg PSA [units]	Efficiency
IgGZERO® Endo S		8	-
Remove-iT® Endo S		8	-
GlycINATOR® Endo S2 (3h incubation)		8	+
Endo F2		0.01	+
GlycINATOR® Endo S2		8	++
Remove-iT® Endo S	x	200	+++
GlycINATOR® Endo S2	x	8	+++
Endo F3		0.01	+++++
Endo F3 (3 h incubation)		0.01	+++++
Endo F3	x	0.01	+++++
Endo F3 (3x amount)		0.03	+++++
Endo F3 + Endo F2		0.02	+++++
Endo F3 in TRIS/HCl at pH 7.8		0.01	++++

Taking into account that native PSA possesses five disulfide bonds linking amino acid positions 31-173, 50-66, 152-219, 184,198 and 209-234, the molecular weight of PSA without glycans, signal peptide and propeptide is 26,079 Da. Therefore, native PSA with a GlcNAc residue (+203 Da) or GlcNAc+Fuc residue (+349 Da) possesses a molecular weight of 26,282 Da or 26,428 Da, respectively. As shown in Figure 10, native PSA treated with IgGZERO® Endo S and

Remove-iT® Endo S showed no difference compared to untreated PSA, indicating that these two endoglycosidases possess no enzymatic activity on native PSA. The other endoglycosidases GlycINATOR® Endo S2, Endo F2 and Endo F3 showed enzymatic activity on native PSA, indicated by the generated target peak at m/z 26,428 Da, in which Endo F3 showed superior activity compared to all other endoglycosidases tested in this study.

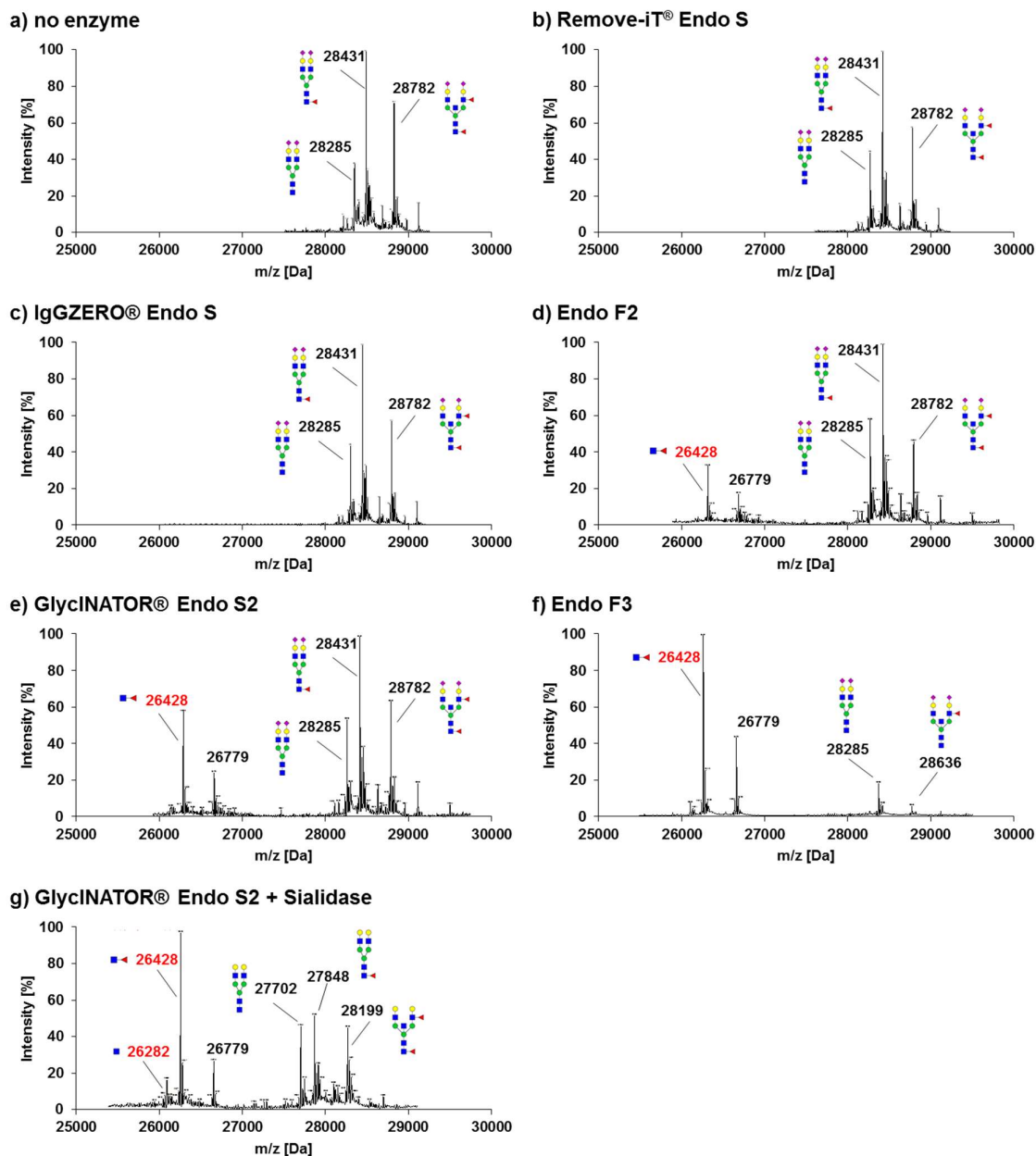


Figure 10: Representative mass spectra of partially deglycosylated PSA using different endoglycosidases a) no enzyme, b) Remove-iT® Endo S, c) IgGZERO® Endo S, d) Endo F2, e) GlycINATOR® Endo S2, f) Endo F3, and g) GlycINATOR® Endo S2 with Sialidase showing the target peaks at m/z 26,282 Da and m/z 26,428 Da as well as major peaks of non-deglycosylated PSA in the mass range from m/z 27,500 to 29,500 Da. Glycan composition as illustrated is in agreement with previously performed in-house N-glycan analysis by LC-MS.

Furthermore, Endo F3 was the most efficient enzyme regarding incubation time and required enzyme amount per μg PSA (Table 6). The enzyme activity of GlycINATOR® Endo S2 and Remove-iT® Endo S could be improved, when PSA was previously treated by sialidase from *Clostridium perfringens*, which specifically removes terminal $\alpha(2,3)$ -, $\alpha(2,6)$ -, or $\alpha(2,8)$ -linked sialic acids giving a mass shift of -291 Da per sialic acid molecule. It is known that extended structures on glycan chains, such as sulfate, phosphate, poly-*N*-acetyl-lactosamines or sialic acids can render the glycoprotein partially or completely resistant to cleavage by distinct enzymes including endoglycosidases which requires removal of each residue before the respective enzyme will work [110]. Partial deglycosylation using sialidase followed by GlycINATOR® Endo S2 treatment resulted in a PSA species containing one GlcNAc residue (m/z 26,282 Da), which was not detected using the other endoglycosidases. However, enzymatic activity regarding the generation of PSA with GlcNAc+Fuc modification was significantly lower compared to Endo F3. Native PSA treated by sialidase followed by Endo F3 showed no difference to samples exclusively treated by Endo F3. In addition, Endo F3 activity was slightly reduced by using a 100 mM TRIS/HCl buffer containing 10 mM CaCl_2 at pH 7.8 which is in agreement with the manufacturer's documentation specifying the pH optimum at 4.5. Residual peaks particularly at m/z 28,285 Da and m/z 28,636 Da showed that glycan cleavage of native PSA using Endo F3 is not complete. These two major peaks could be assigned to non-fucosylated species by calculation of the m/z difference to native PSA and by previously performed in-house MS-based N-glycan analysis indicating low Endo F3 activity on glycan structures without Fuc, which is consistent with the literature [111].

3.2. Protease and surrogate peptide selection

3.2.1. *In silico* digestion of PSA

For successful quantification of low abundant proteins in complex biosamples, the selection of a highly MS-responsive surrogate peptide is a critical step. Normally, every peptide generated by digestion of the target protein can be considered as a potential surrogate peptide. In contrast, peptide selection for quantification of partially glycosylated PSA is limited to peptides containing the N-glycosylation site at Asn-69. In this study, surrogate peptide candidates were initially sought *by in silico* analysis using the PeptideMass tool that predicts fragment peptides on the basis of the protein's amino acid sequence and the proteolytic enzyme specificity. Based upon *in silico* digestion of PSA (Uni-ProtKB P07288) simulated by using different proteases including trypsin, Lys-C, Lys-N, Arg-C, Asp-N, Glu-C, chymotrypsin, pepsin, proteinase K, elastase, and thermolysin, enzymes were preselected regarding their suitability for usage in laboratory *in vitro* digestion experiments (Table 7).

Table 7: *In silico* digestion of PSA (Uni-ProtKB P07288) simulated by using different enzymes.

Enzyme	Sequence of surrogate peptide without glycan (Number of amino acids) ^a	Molecular weight (monoisotopic) [Da]	Suitable for usage in <i>in vitro</i> digestion experiments of PSA
Trypsin	NK (2)	260.1	with restrictions ^b
Lys-C	HSQPWQVLVASRGRAVCGGV VHPQWVLTAAHCIR NK (37)	4073.2	no
Lys-N	KHSQPWQVLVASRGRAVCGGV LVHPQWVLTAAHCIR N (37)	4073.2	no
Protease Arg-C	NKSVILLGR (9)	998.6	yes
Asp-N	IVGGWECEKHSQPWQVLVASR GRAVCGGVLVHPQWVLTAAHCIR RNKSVILLGRHSLFHPE (60)	6660.5	no
Glu-C	KHSQPWQVLVASRGRAVCGGV LVHPQWVLTAAHCIR NKSVILLG RHSLFHPE (52)	5787.1	no
Chymotrypsin	TAAHCIR NKSVIL (13)	1424.8	with restrictions ^c
Pepsin (pH = 1.3)	TAAHCIR NKSVIL (13)	1424.8	with restrictions ^c
Proteinase K	RNKSV (5)	602.4	with restrictions ^b
Elastase	RNKS (4)	503.3	with restrictions ^b
Thermolysin	IRNKS (5)	616.4	with restrictions ^b

^a N-glycosylation site at asparagine-69 illustrated in bold letter

^b Suitability for usage in *in vitro* digestion of PSA restricted due to peptide length

^c Suitability for usage in *in vitro* digestion of PSA restricted due to cysteine containing peptide sequence

A general criterion concerning surrogate peptide selection is the peptide length ideally comprising 7 to 20 amino acids which enhances the probability to obtain a unique and highly MS-responsive peptide [112]. Although surrogate peptides of PSA generated by trypsin, proteinase K, elastase and thermolysin do not fulfill this recommended criterion, these enzymes were tested in subsequent *in vitro* digestion experiments as the lack of uniqueness may be accomplished by using a highly specific anti-PSA antibody later in the workflow. Proteases Lys-C, Lys-N, Asp-N and Glu-C were excluded from *in vitro* experiments as they generate surrogate peptides containing 37, 52, or 60 amino acids which is far away from the recommended optimum. Peptides of this length would probably result in low MS response due to wide distributed charge states. Furthermore, these peptides contain up to three cysteines which may be susceptible to modification *in vivo* or during sample preparation and analysis. Peptides generated by chymotrypsin and pepsin also containing one cysteine were still included in *in vitro* experiments as the peptide length was in the optimal range and the N-glycosylation site at Asn-69 was centrally located in the sequence. The latter might be beneficial over sequences containing the N-glycosylation site close to the enzymatic cleavage site which could decrease the enzyme activity due to hindered enzyme accessibility. The N-terminal cleavage site of the surrogate peptide generated by protease Arg-C is next to the N-glycosylation site at Asn-69. However, considering the restrictions of the other enzymes mentioned before, protease Arg-C was the preferred enzyme for digestion of PSA after evaluation of *in silico* data.

3.2.2. *In vitro* digestion of PSA

In silico digestion was a useful aid for enzyme preselection but its data had to be confirmed by laboratory experiments as theoretical digestion did not consider unspecific and missed cleavages. The final protease and surrogate peptide selection was based on results generated by *in vitro* digestion of partially deglycosylated PSA prior to peptide mapping by LC-MS/MS as described in chapter III section 2.5. In total, seven preselected enzymes were tested including trypsin, elastase, proteinase K, thermolysin, protease Arg-C, pepsin and chymotrypsin. Comprehensive lists of identified peptides are shown in the appendix. In summary, partially deglycosylated target peptides were only detected in samples treated by protease Arg-C and pepsin generating the glycopeptides N(GlcNAc+Fuc)KSVILLGR and TAAHCIRN(GlcNAc+Fuc)KSVIL, respectively. Non-fucosylated species were not detected which is probably due to low Endo F3 activity on structures without Fuc as described before. In samples digested by trypsin and chymotrypsin respective glycopeptides N(GlcNAc+Fuc)K and TAAHCIRN(GlcNAc+Fuc)KSVIL were not found, while neighboring peptide sequences were detected. The tryptic peptide is a polar dipeptide which was not retained by RPLC and thus was not detectable. In subsequent experiments, this peptide could be identified using hydrophilic interaction chromatography (HILIC) coupled to MS. Theoretical glycopeptides generated by chymotrypsin, elastase, thermolysin and proteinase K digestion could neither be detected by the automatic search algorithm of the Proteome Discoverer™ software nor by manual mass search in total ion chromatograms, which indicates one or more unspecific cleavages.

Trypsin, protease Arg-C and pepsin demonstrated to release partially deglycosylated surrogate peptides from PSA which were detectable by MS, although the enzymatic cleavage sites of protease Arg-C and trypsin were directly next to the N-glycosylation site. As mentioned before, the surrogate peptide generated by pepsin contains one cysteine. Thus, protease Arg-C and trypsin seemed to be more suitable in order to generate surrogate peptides for quantification of partially deglycosylated PSA. For quantification of total PSA using protease Arg-C, two peptides KWIKDTIVANP and PSLYTKVVHYR identified in *in vitro* experiments were selected as surrogate peptide candidates as they fulfill recommended criteria for mass spectrometry-based protein quantification (ideal peptide length, no reactive amino acids, uniqueness, observability by MS) [112]. Peptides LSEPAELTDAVK and SVILLGR were selected as potential tryptic surrogate peptides for total PSA quantification, which are already described in the literature [113, 114]. An overview of selected surrogate peptide candidates for quantification of total PSA and partially deglycosylated PSA using protease Arg-C and trypsin as digestion enzymes is shown in Table 8.

Table 8: Selected surrogate peptide candidates for quantification of total and partially deglycosylated PSA based upon *in silico* and *in vitro* digestion using protease Arg-C and trypsin.

Enzyme	Surrogate peptide candidates for quantification of total PSA	Surrogate peptides for quantification of partially deglycosylated PSA
Protease Arg-C	KWIKDTIVANP	N(GlcNAc+Fuc)KSVILLGR
	PSLYTKVVHYR	N(GlcNAc)KSVILLGR
Trypsin	LSEPAELTDAVK	N(GlcNAc+Fuc)K
	SVILLGR	N(GlcNAc)K

3.3. Protease Arg-C-based approaches

3.3.1. Surrogate peptide selection and MRM parameter optimization

In preliminary experiments potential PSA surrogate peptides generated by protease Arg-C digestion were selected. Following, analyte-specific MS parameters including transitions, DP, EP, CE, and CXP were optimized. As surrogate peptides generated by protease Arg-C were not available as synthetic, pure standard peptides, a systematic procedure based on several LC-MS/MS runs with varying parameters was applied to obtain optimal analyte-specific MS parameters. A schematic overview of the MRM parameter optimization procedure with or without standard peptides is shown in Figure 11.

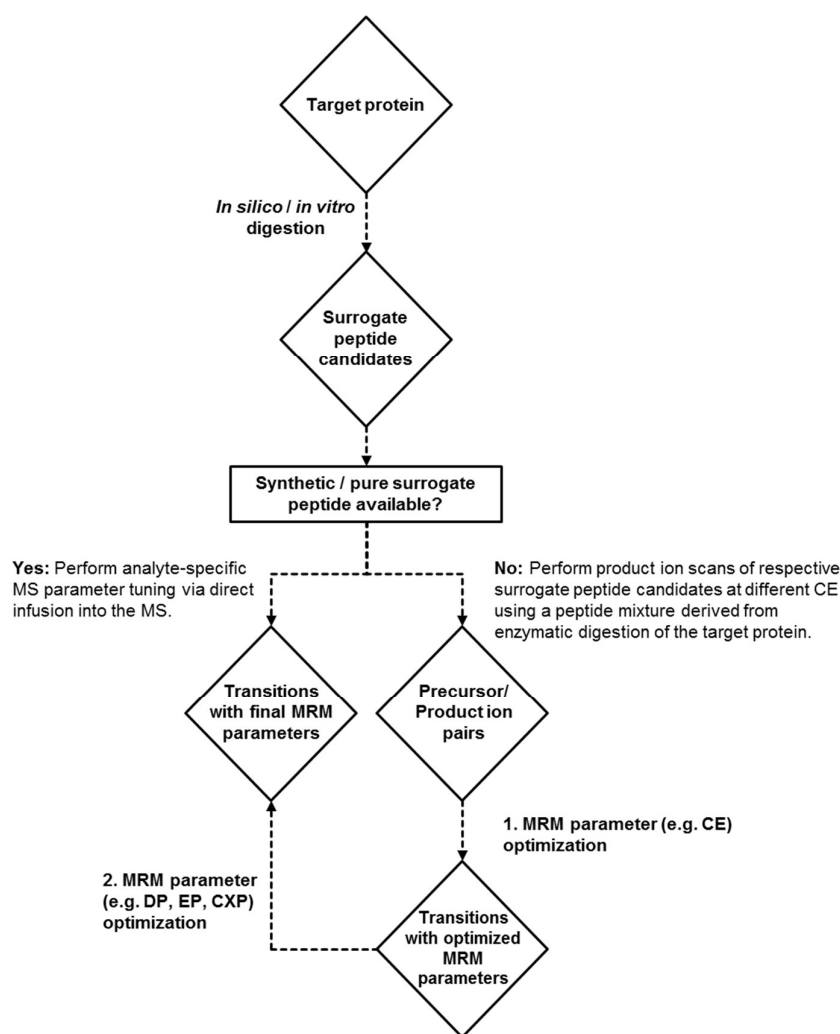


Figure 11: Systematic procedure for MRM parameter optimization with or without standard peptides. Declustering potential = DP, entrance potential = EP, collision energy = CE, and cell exit potential = CXP.

First, enhanced product ion (EPI) scans of selected precursor ions were performed in order to identify sensitive precursor/product ion pairs and their respective CE values (Table 3). For this purpose, MS method parameters were held constant except of CE which was initially set to 7 V and increased by 3 V in each run. The peptides KWIKDTIVANP and PSLYTKVVHYR were selected as surrogate peptide candidates for quantification of total PSA (Table 8). As shown in Figure 12 the most sensitive transition of peptide KWIKDTIVANP was obtained by measuring the triple charge state m/z 428.9 (MH^{+3}) in Q1 and the resulting fragment ion m/z 585.1 (b_{10}^{+2}) in Q3 applying CE of 10 V. Using the double charge state m/z 642.9 Da of peptide KWIKDTIVANP as precursor ion resulted in less lower signal intensities. For peptide PSLYTKVVHYR the most sensitive precursor/product ion pair was m/z 454.9/633.1 (MH^{+3}/y_{10}^{+2}) applying CE of 13 V, while the double charged precursor ion m/z 681.9 (MH^{+2}) signal was less intensive. Single charge states of the two peptides were not amenable to analysis as they exceed the upper mass range of the MS. Comparison of the most sensitive transitions of the two surrogate peptide candidates revealed that transition m/z 428.9/585.1 of peptide KWIKDTIVANP was more sensitive by a factor of 4 over transition m/z 454.9/633.1 of peptide PSLYTKVVHYR. Therefore peptide KWIKDTIVANP was used for final MRM parameter optimization.

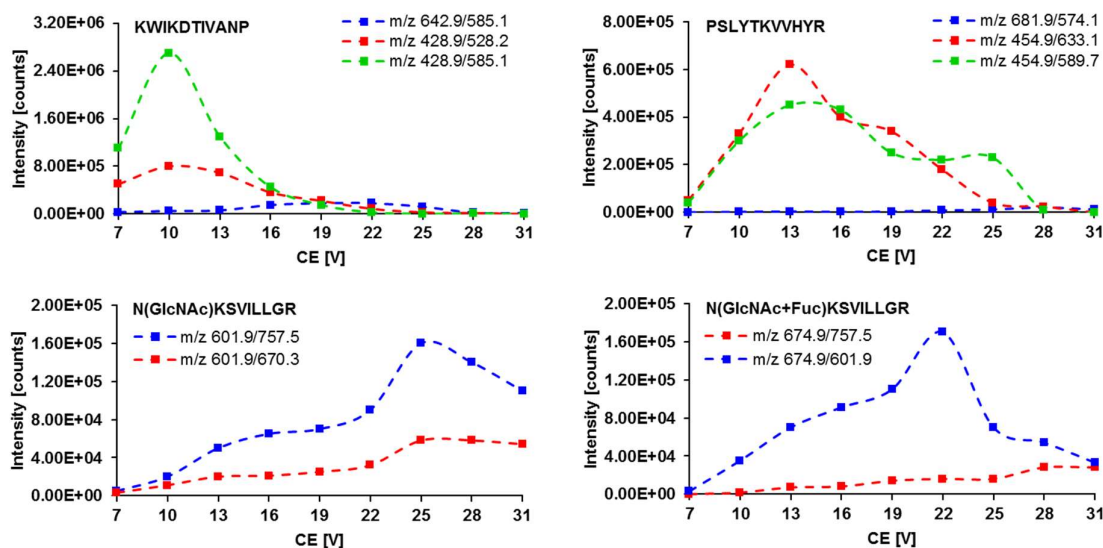


Figure 12: Enhanced product ion (EPI) scans of selected precursor ions of peptides KWIKDTIVANP, PSLYTKVVHYR, N(GlcNAc)KSVILLGR and N(GlcNAc+Fuc)KSVILLGR and their most intensive product ions at different collision energies (CE).

In-source fragmentation (ISF) is a common phenomenon in MS analysis of glycopeptides in which especially the glycosidic bond between GlcNAc and Fuc is labile in dissociation [115]. The most intensive precursor/product ion pair of non-fucosylated PSA was m/z 601.9/757.5 (MH^{+2}/y_7^{+1}) applying CE of 25 V. The precursor ion m/z 601.9 is identical to the double charged ion of fucosylated PSA obtained by in source fragmentation when Fuc is lost ($1347.8 \text{ Da} - 146.1 \text{ Da} = 1201.6 \text{ Da}$; $MH^{+2} = m/z$ 601.9) making differentiation by MS impractical. As chromatographic separation of

N(GlcNAc)KSVILLGR and N(GlcNAc+Fuc)KSVILLGR was not achieved by reversed phase liquid chromatography (RPLC), in this workflow only the glycopeptide N(GlcNAc+Fuc)KSVILLGR was used as surrogate peptide for quantification of core-fucosylated PSA. The most intensive precursor/product ion pair was m/z 674.9/601.9 (MH^{+2}/MH^{+2} minus Fuc) applying CE of 22 V. No signals were detected using single and triple charge states of N(GlcNAc+Fuc)KSVILLGR as precursor ions. Most sensitive transitions and respective CE values of surrogate peptides generated by protease Arg-C are listed in Table 9. Based on these results a multiple reaction monitoring (MRM) method was created. This method was run several times but each run one of the initial analyte-specific MS parameters including DP, EP, CXP and CE was varied resulting in the final MRM parameters shown in Table 10.

Table 9: Most sensitive transitions and their respective CE values identified in EPI scan experiments.

Peptide generated by protease Arg-C digestion	Charge state	Precursor ion [Da]	Product ion [Da]	Collision energy [V]
KWIKDTIVANP	3+	428.9	585.1	10
PSLYTKVVHYR	3+	454.9	633.1	13
N(GlcNAc)KSVILLGR	2+	601.9	757.5	25
N(GlcNAc+Fuc)KSVILLGR	2+	674.9	601.9	22

Table 10: Final MRM parameters of surrogate peptides for quantification of total and core-fucosylated PSA using protease Arg-C as digestion enzyme.

Target	Surrogate peptide	Charge state	Q1 [Da]	Q3 [Da]	DP [V]	EP [V]	CE [V]	CXP [V]
Total PSA	KWIKDTIVANP	3+	428.9	585.3	35	7	14	15
Core-fucosylated PSA	N(GlcNAc+Fuc)KSVILLGR	2+	674.9	601.9	75	9	26	15

3.3.2. Overview of the experimental workflow using MSIA tips

In order to determine total and core-fucosylated PSA in human serum an analytical method was developed comprising immunoaffinity enrichment, two enzymatic steps and LC-MS/MS analysis. The experimental workflow is illustrated in Figure 13 and described in the experimental section. Immunoaffinity enrichment was performed by using biotinylated anti-PSA antibody bound to streptavidin-coated MSIA tips to enrich PSA from complex serum matrix. Enriched PSA was eluted from the pipette tip and partially deglycosylated in solution using Endo F3 to simplify glycan microheterogeneity. Afterwards, surrogate peptides of partially deglycosylated PSA were generated by enzymatic treatment using protease Arg-C as digestion enzyme. Selected peptides were measured by LC-MS/MS using RPLC without additional up-front clean up.

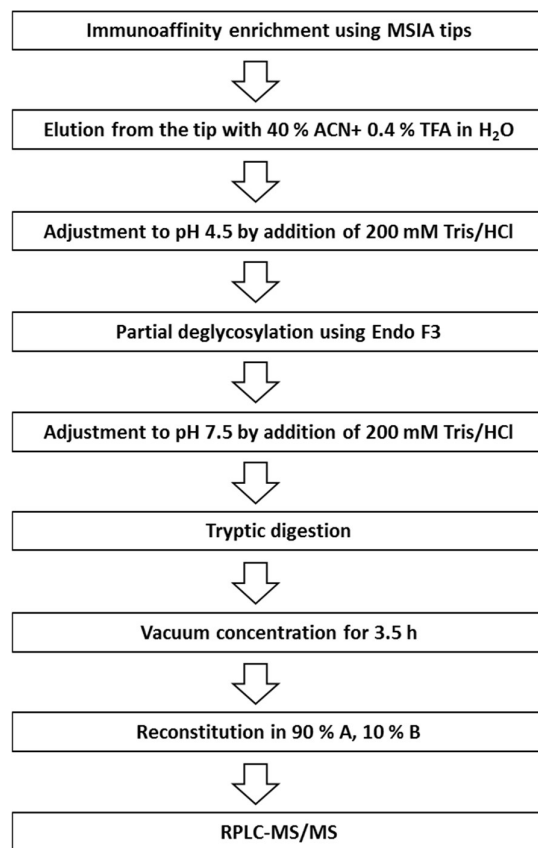


Figure 13: Schematic overview of the experimental workflow for the determination of core-fucosylated and total PSA using a MSIA tip-based and protease Arg-C-assisted LC-MS/MS method.

3.3.3. Determination of core-fucosylated and total PSA in serum samples

Analysis of four female serum samples containing different concentrations of core-fucosylated (0, 15.6, 31.2, 46.8 ng/mL) and total PSA (0, 20, 40 and 60 ng/mL) was performed in order to generate calibration curves by plotting peak areas of peptides N(GlcNAc+Fuc)KSVILLGR and KWIKDTIVANP against respective concentrations (Figure 14).

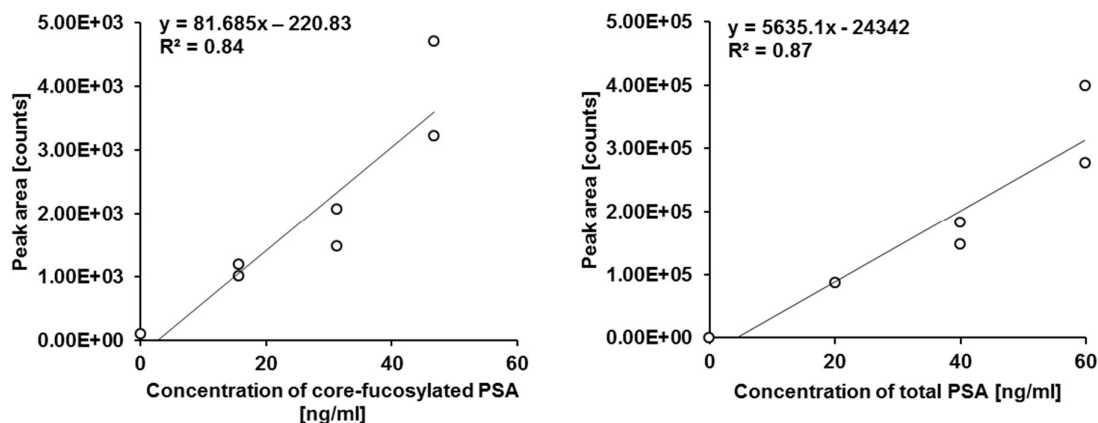


Figure 14: Calibration curves and correlation coefficients R^2 of core-fucosylated (left) and total PSA (right) obtained by plotting peak areas of N(GlcNAc+Fuc)KSVILLGR and KWIKDTIVANP against respective concentrations, $n = 2$.

The most sensitive transition of each peptide was selected for quantification, which means Q1/Q3 ion pairs were m/z 674.9/601.9 and 428.9/585.3 for core-fucosylated and total PSA, respectively. Each concentration was prepared in duplicate followed by analysis as illustrated in Figure 13. Both peptides showed poor linearity over the working range with correlation coefficients $R^2 < 0.90$. In this study peak intensities with a signal-to-noise ratio of 3 and 10 were considered acceptable for determining the LLOD and LLOQ, respectively. The LLOD of core-fucosylated PSA was 15.6 ng/mL and the LLOQ was 46.8 ng/mL whereas the LLOD and LLOQ of total PSA were much lower than 20 ng/mL. More precise values were not determined as it was obviously that core-fucosylated PSA would not meet the required $LLOQ \leq 1$ ng/mL by applying the described workflow. Representative chromatograms for 0, 20 and 60 ng/mL total PSA spiked-in female serum are shown in Figure 15.

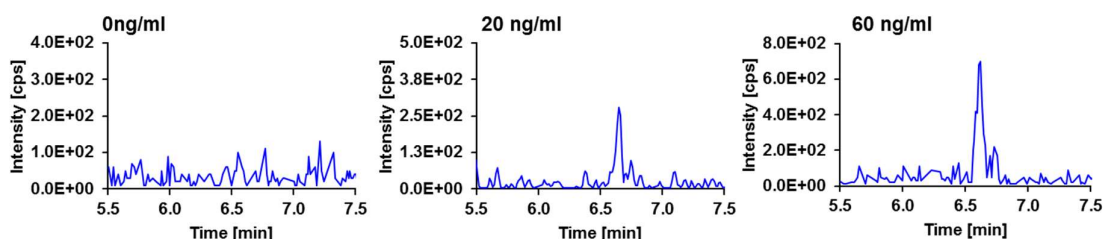
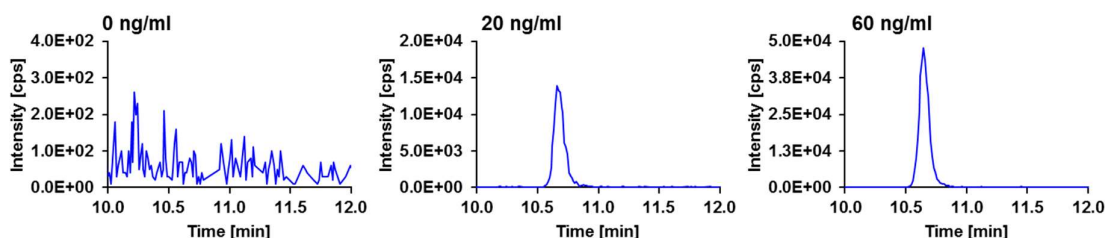
a) core-fucosylated PSA [N(GlcNAc+Fuc)KSVILLGR, m/z 674.9/601.9]b) total PSA [KWIKDTIVANP, m/z 428.9/585.3]

Figure 15: Extracted ion chromatograms of transitions monitored for a) core-fucosylated PSA (N(GlcNAc+Fuc)KSVILLGR, m/z 674.9/601.9) and b) total PSA (KWIKDTIVANP, m/z 428.9/585.3) derived from 0, 20 and 60 ng/mL total PSA spiked-in female serum samples.

3.3.4. Optimization approaches

As the described workflow was limited to measure core-fucosylated PSA in the low ng/mL concentration range, further approaches were conducted to improve the method's sensitivity. Crucial impacts including the antibody type, the order of digestion steps as well as antibody and enzyme amounts were investigated.

3.3.4.1. Antibody type

Four different biotinylated monoclonal antibody fragments were tested in which PSA30-F(ab')₂ binding to epitope 1 captures free PSA and PSA10-Fab' binding to epitope 3a, PSA36-Fab' binding to epitope 6b as well as PSA66-F(ab')₂ binding to epitope 4b capture total PSA [84]. The capture efficiencies of PSA10-Fab' and especially PSA30-F(ab')₂ were lower compared to PSA36-Fab' and PSA66-F(ab')₂ which showed comparable results (Figure 16). These results were supported by data obtained from surface plasmon resonance measurements using a streptavidin modified capture chip (Table 11). Both PSA36-Fab' and PSA66-F(ab')₂ showed high affinity to PSA in the subnanomolar range. By using PSA66-F(ab')₂ the complex stability expressed as $t_{1/2}$ -dissociation, which is the time for a 50 % decline in PSA binding, was superior to the other antibody fragments. The molar ratio indicated the stoichiometric integrity of all antibody fragments. As the method sensitivity could not be improved by using other antibody fragments, PSA36-Fab' fragment was kept as antibody for further experiments.

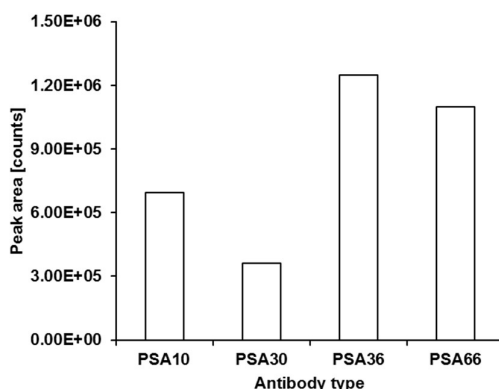


Figure 16: Workflow capture efficiency of four different antibody fragments tested by monitoring total PSA levels (KWIKDTIVANP, m/z 428.9/585.3) using an Endo F3 and protease Arg-C-assisted LC-MS/MS method, $n = 1$.

Table 11: Data obtained by surface plasmon resonance measurements of four different antibody fragments.

Biotinylated antibody fragment	K_D [nM]	$t_{1/2}$ -dissociation [min]	Molar ratio (MR)
PSA30-F(ab') ₂	3.0	16	1.5
PSA10-Fab'	1.0	5	1.0
PSA36-Fab'	0.5	3	0.8
PSA66-F(ab') ₂	0.2	40	1.8

K_D = Affinity constant

$t_{1/2}$ dissociation = halftime of complex dissociation

MR: theoretical F(ab')₂ max. 2.0, Fab' max. 1.0

3.3.4.2. Antibody and enzyme amount

Following antibody selection, respective amounts of antibody (0.25 μ g, 1.25 μ g and 5 μ g), Endo F3 (0.005, 0.01 and 0.02 units) and protease Arg-C (0.28, 1.4, 14, 140 and 500 ng) were tested in separate experiments applying a similar MSIA tip-based LC-MS/MS approach as mentioned in chapter III section 2.7.1. No influence on peak areas of core-fucosylated and total PSA was observed using different Endo F3 and antibody amounts (data not shown). Total PSA monitored by peptide KWIKDTIVANP showed increasing peak areas with increasing amounts of protease Arg-C (Figure 17) in which the optimum was approximately at 140 ng protease Arg-C. In contrast, the most intensive peak of core-fucosylated PSA monitored by glycopeptide N(GlcNAc+Fuc)KSVILLGR was obtained using 14 ng protease Arg-C. Both lower and higher enzyme amounts diminished the peak area significantly. As mentioned before, protease Arg-C used in this work cleaves at the C-terminus of arginine residues but also at the carboxyl side of particular lysines. Using higher amounts of protease Arg-C leads to cleavage at the lysine of peptide N(GlcNAc+Fuc)KSVILLGR into smaller peptide fragments and thus to the loss of signal intensity. Peptide KWIKDTIVANP also possesses potential cleavage sites at two lysine residues but seems to be more stable against trypsin activity. This assumption is supported by data of an aqueous tryptic digest of PSA where the intact peptide

KWIKDTIVANP was also detected (Appendix). Furthermore, trypsin activity seems to be an inherent issue of protease Arg-C as it was also observed in samples treated by Arg-C proteases from four different vendors.

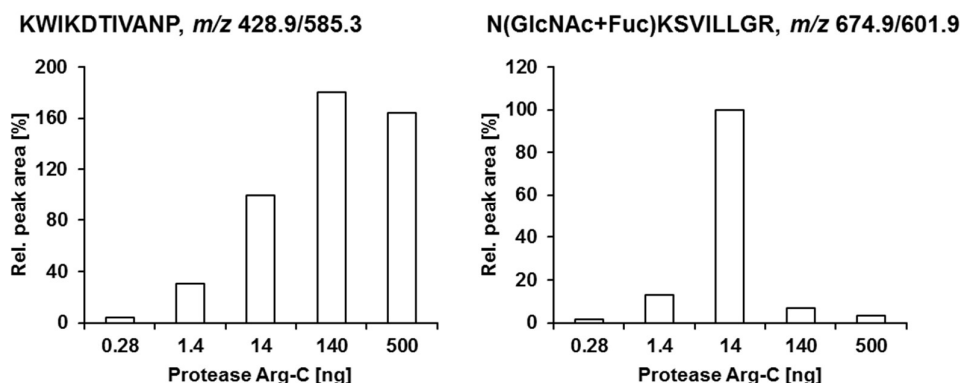


Figure 17: Different protease Arg-C amounts tested by monitoring total PSA (KWIKDTIVANP, m/z 428.9/585.3, left) and core-fucosylated PSA levels (N(GlcNAc+Fuc)KSVILLGR, m/z 674.9/601.9, right) applying a MSIA-based LC-MS/MS approach. Signal intensities are normalized to samples treated with 14 ng protease Arg-C and expressed in %, $n = 1$.

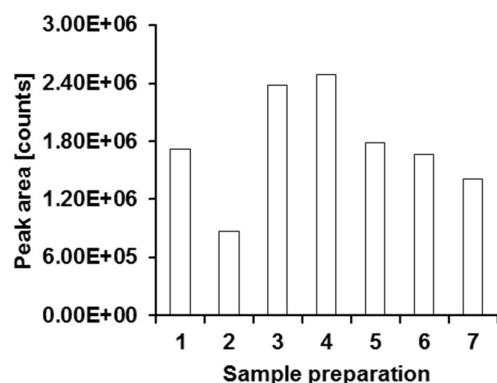
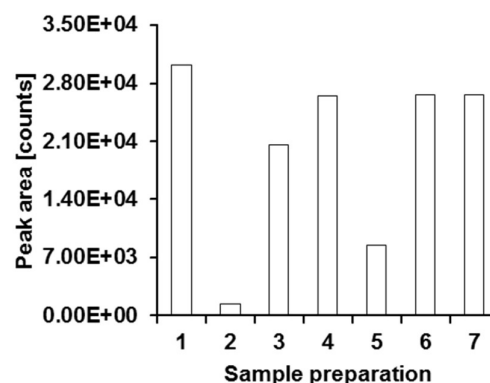
3.3.4.3. Order of digestion and elution steps

Following MSIA tip-based immunoaffinity enrichment, the described method contains an elution step prior to partial deglycosylation in solution using Endo F3 and digestion with protease Arg-C. According to the literature, there seems to be no clear consensus on whether or not the target protein should be eluted from the immobilized antibody prior to digestion [116]. In order to reach the lowest possible limit of quantification for core-fucosylated PSA analysis, several different sample preparation procedures with or without elution were applied as summarized in Table 12. Proteolytic digestion and deglycosylation were executed in solution, on filter or while PSA was still captured on the tip. Furthermore, the order of digestion steps which might also affect the method's sensitivity was investigated.

Deglycosylation of PSA either on filter or immobilized on tip enabled simple buffer exchange prior to proteolytic digestion which was required for optimal enzymatic activity. On the other hand, elution is often accompanied by vacuum concentration and further sample clean up strategies. An additional elution step could be avoided by proteolytic digestion of immobilized PSA as the capture antibody is simultaneously cleaved, thus breaking the antibody-PSA interaction. However, this procedure generates a complex peptide mixture requiring an effective chromatographic separation prior to MS analysis. As shown in Figure 18, filter-based sample preparation procedures were less efficient compared to in solution or on tip workflows especially concerning core-fucosylated PSA which might be due to hindered accessibility of protease Arg-C or unspecific binding of generated peptides to the filter. Comparable results were obtained among workflows conducted in solution or on tip independent of whether deglycosylation or proteolytic digestion was performed first.

Table 12: Overview of seven sample preparation procedures comprising in solution, on tip or on filter digestion and partial deglycosylation.

Sample preparation method	Step 1	Step 2	Step 3
1	Protease Arg-C on MSIA	Wash out	Endo F3 in solution
2	Elution	Protease Arg-C on filter	Endo F3 in solution
3	Elution	Protease Arg-C in solution	Endo F3 in solution
4	Endo F3 on MSIA	Elution	Protease Arg-C in solution
5	Elution	Endo F3 on filter	Protease Arg-C on filter
6	Elution	EndoF3 in solution	Protease Arg-C in solution
7	Endo F3 on MSIA	Protease Arg-C on MSIA	Wash out

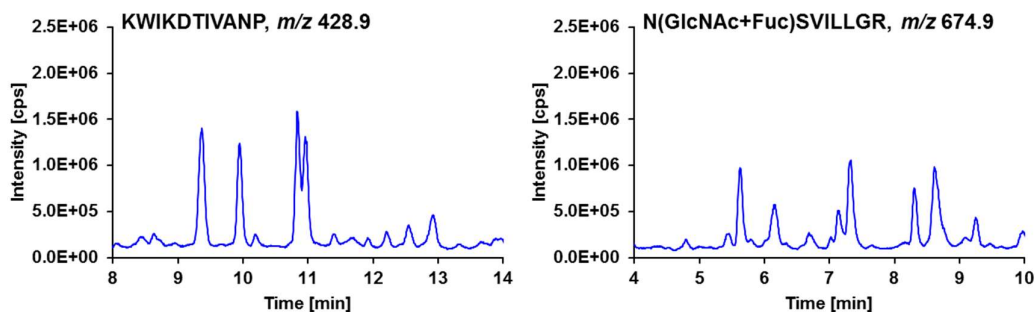
KWIKDTIVANP, m/z 428.9/585.3**N(GlcNAc+Fuc)KSVILLGR, m/z 674.9/601.9****Figure 18:** Peak areas of total PSA (KWIKDTIVANP, m/z 428.9/585.3, left) and core-fucosylated PSA (N(GlcNAc+Fuc)KSVILLGR, m/z 674.9/601.9, right) obtained by applying seven different sample preparation procedures summarized in Table 12, $n = 1$.

3.3.4.4. Multiple reaction monitoring (MRM) compared to selected ion monitoring (SIM)

In selected ion monitoring (SIM) analysis, ions of a selected m/z will reach the detector, except for those lost in transmission through the quadrupole. In contrast, using multiple reaction monitoring (MRM) analysis ions are lost due to transmission through the first and the third quadrupole and due to incomplete fragmentation and different fragmentation ways in the collision cell. Consequently, in a matrix free environment SIM analysis allows for the detection of more ions representing the analyte, and thus can be more sensitive as compared to MRM analysis. As sample preparation in the described method comprises several steps including immunoaffinity enrichment, matrix contaminants might largely be removed. Therefore, SIM mode was compared to MRM mode using a 427 ng/mL total PSA spiked-in female serum sample. As shown in Figure 19, core-fucosylated and total PSA could confidently be detected using MRM mode while no specific analyte signals were detected in

SIM mode. This was probably due to the high baseline noise and co-eluting species obtained in SIM mode indicating that matrix contaminants and other interferences e.g. coming from the streptavidin-coated MSIA tips were not completely removed despite extensive sample preparation.

a) Selected ion monitoring (SIM mode)



b) Multiple reaction monitoring (MRM mode)

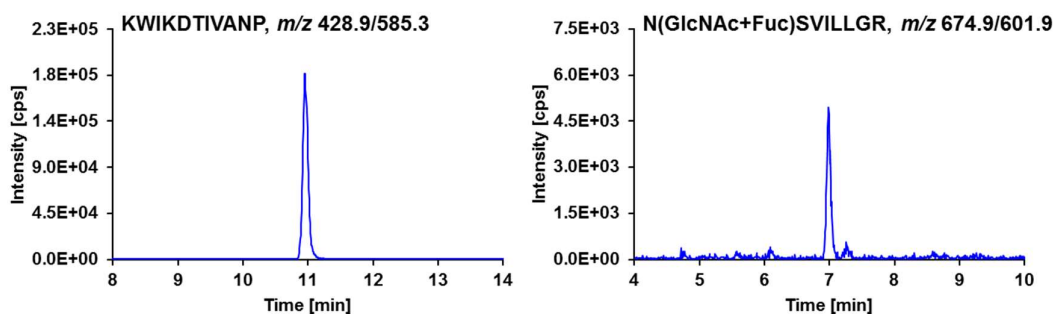


Figure 19: Comparison of a) SIM mode and b) MRM mode analysis of a 427 ng/mL total PSA spiked-in female serum sample monitoring total PSA (KWIKDTIVANP, left) and core-fucosylated PSA (N(GlcNAc+Fuc)KSVILLGR, right).

3.4. From reversed phase to hydrophilic interaction liquid chromatography

The MSIA tip-based workflow using protease Arg-C lacked in sensitivity regarding core-fucosylated PSA most likely due to undesired trypsin activity observed with the usage of protease Arg-C. Other parameters including the antibody type, the enzyme and antibody amounts and the order of digestion steps either had no explicit influence on the method's sensitivity or were already operated in the optimal way. Another disadvantage accompanied with the workflow was that the two glycopeptides N(GlcNAc)KSVILLGR and N(GlcNAc+Fuc)KSVILLGR could not be separated by reversed phase liquid chromatography (RPLC) column (Acquity UPLC BEH C18, 130 Å, 1.7 µm, 2.1 x 150 mm, Waters) used in this workflow. Confident detection of non-fucosylated PSA was impractical due to in-source fragmentation (ISF) of glycopeptide N(GlcNAc+Fuc)KSVILLGR losing Fuc before entering the MS. Hence, protease Arg-C was replaced by trypsin identified as a suitable alternative enzyme in preliminary experiments.

Two RPLC columns (Acquity UPLC BEH C18, 130 Å, 1.7 µm, 2.1 x 150 mm, Waters and Atlantis® T3, 3 µm, 2.1 x 100 mm, Waters) were tested but could not retain the polar dipeptides N(GlcNAc)K and N(GlcNAc+Fuc)K generated by tryptic digestion of PSA. Elution in the column dead volume adversely affects analysis of human samples due to co-eluting endogenous matrix components. Therefore, the column selectivity was switched to hydrophilic interaction chromatography (HILIC) which provides the possibility to effectively separate polar compounds. Among several commercially available HILIC columns XBridge Amide column (130 Å, 3.5 µm, 2.1 x 100 mm, Waters) was selected for further experiments as it showed baseline separation of peptides N(GlcNAc)K, N(GlcNAc+Fuc)K, SVILLGR and LSEPAELTDAVK (Figure 20). The core-fucosylated peptide N(GlcNAc+Fuc)K eluted 20 s later than the related non-fucosylated peptide. This is due to the addition of core-fucose which increases its hydrophilicity. Usually, the weak mobile phase component in HILIC is acetonitrile and samples are ideally dissolved in solutions with the same acetonitrile composition as the mobile phase starting conditions [117]. However, limited solubility of most polar analytes in high organic mixtures is challenging. In order to obtain a good balance between analyte solubility, chromatographic behavior and MS response, a tryptic digest of partially deglycosylated PSA was diluted in six compositions (0-100 %, v/v) of eluent A (H₂O with 0.1 % FA) and eluent B (acetonitrile with 0.1 % FA) and peptides N(GlcNAc+Fuc)K, SVILLGR and LSEPAELTDAVK were monitored by LC-MS/MS (Figure 22-24). Each sample composition was prepared in two concentrations. High concentrations (303 ng/mL PSA) were used for injection of low volumes (5 µL) and vice versa low concentrations (75.75 ng/mL PSA) were used for injection of high volumes (20 µL) resulting in the same analyte amount on column. Samples diluted in 100 % eluent B showed low signals for all three peptides irrespective of the injection volume indicating that peptides were not sufficiently solved. Peptide N(GlcNAc+Fuc)K showed consistent signal intensity, constant retention time and reproducible peak shape among samples containing 80, 60, 40, 20 and 0 % (v/v) eluent B using low injection volumes (Figure 22). Peptide LSEPAELTDAVK showed comparable results among samples containing 80, 60 and 40 % (v/v) eluent B and decreasing peak heights in samples with 20 and 0 % (v/v) eluent B using 5 µL

injection volumes (Figure 23). For peptide SVILLGR most intensive peaks were obtained in sample compositions with 80 and 60 % (v/v) eluent B using low injection volumes (Figure 24). High injection volumes had significantly more impact on peak shapes and signal intensities than low injection volumes. Peptides SVILLGR and LSEPAELTDAVK showed the most intensive peaks at 80 % (v/v) eluent B, while glycopeptide N(GlcNAc+Fuc)K had its optimum at 60 % (v/v) eluent B. Signal heights were clearly reduced and peak shapes of all three peptides were negatively affected caused by sample solvents with lower compositions of eluent B. Portions of peptide SVILLGR and LSEPAELTDAVK were actually eluted in the column dead volume at sample compositions lower than 40 % eluent B.

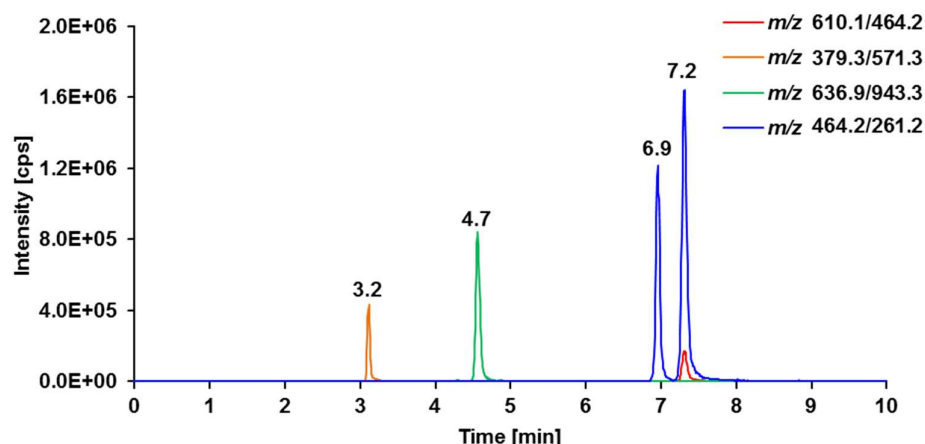


Figure 20: Chromatographic separation of four peptides SVILLGR (3.2 min), LSEPAELTDAVK (4.7 min), N(GlcNAc)K (6.9 min) and N(GlcNAc+Fuc)K (7.2 min), generated by tryptic digestion of PSA using a HILIC XBridge Amide column.

Besides retention of polar analytes, another benefit of HILIC combined with ESI-MS detection is the acetonitrile-rich mobile phase providing favorable conditions for efficient ionization within the MS source resulting in improved sensitivity compared to the highly aqueous mobile phases used in RPLC. In this work, employing HILIC was 2-3 times more sensitive in measuring peptides N(GlcNAc+Fuc)K, SVILLGR and LSEPAELTDAVK compared to RPLC (Figure 21).

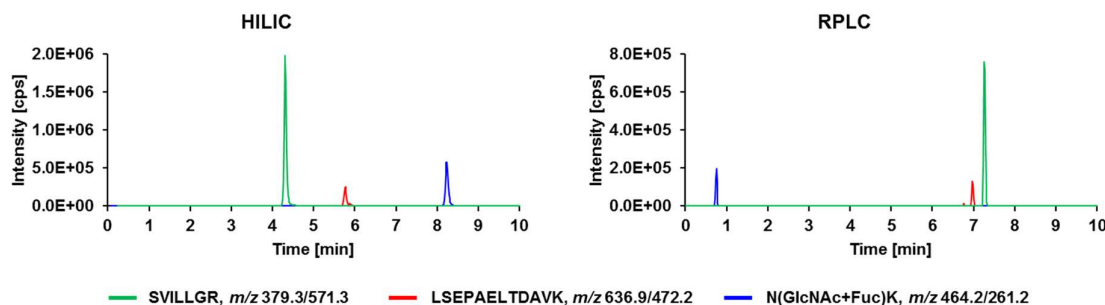


Figure 21: Comparison of three peptides N(GlcNAc+Fuc)K, SVILLGR and LSEPAELTDAVK analyzed by HILIC and RPLC coupled to ESI-MS.

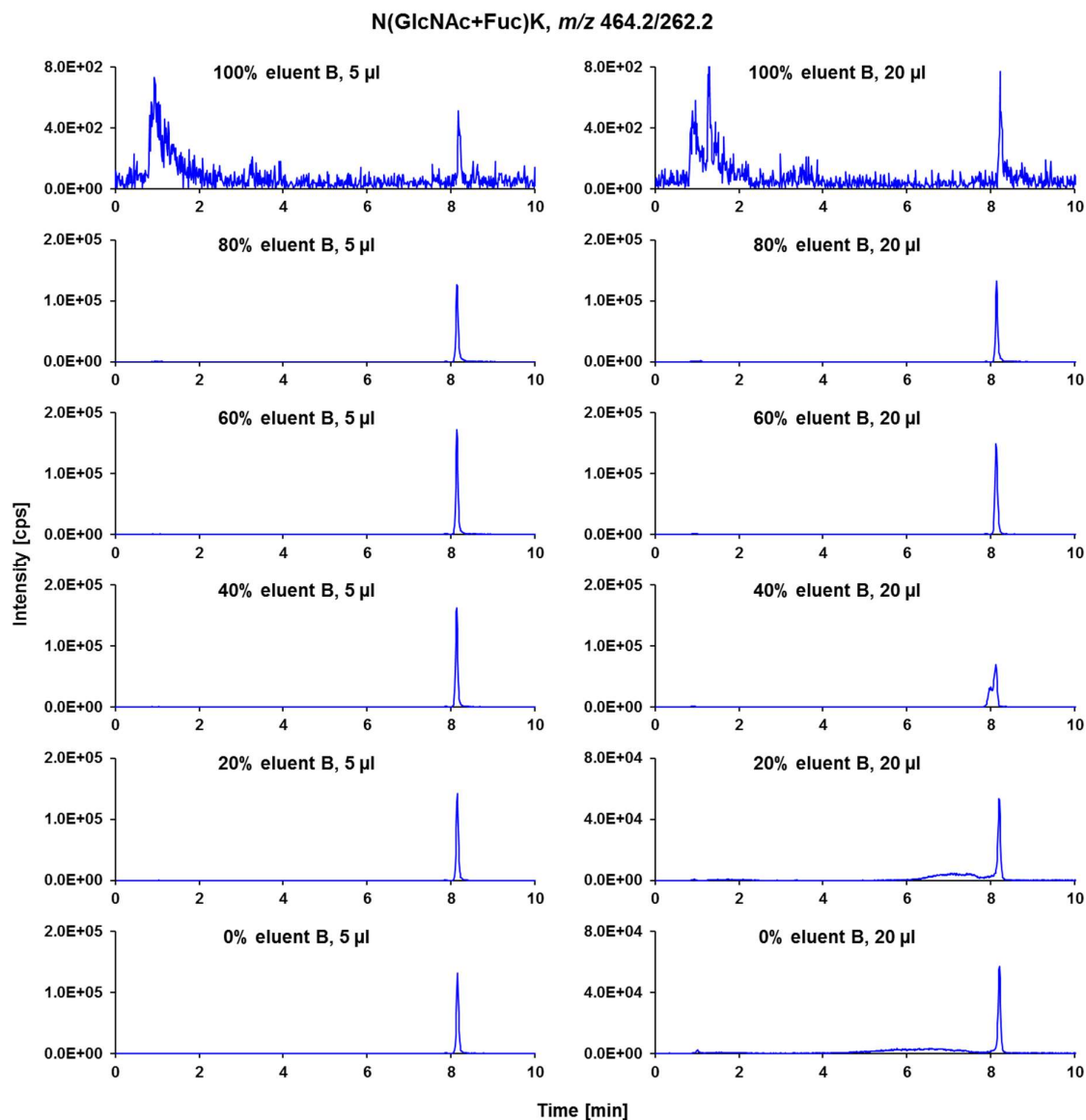


Figure 22: Chromatograms of peptide N(GlcNAc+Fuc)K diluted in different compositions of eluent A and B using 5 μ L (left) and 20 μ L (right) injection volume.

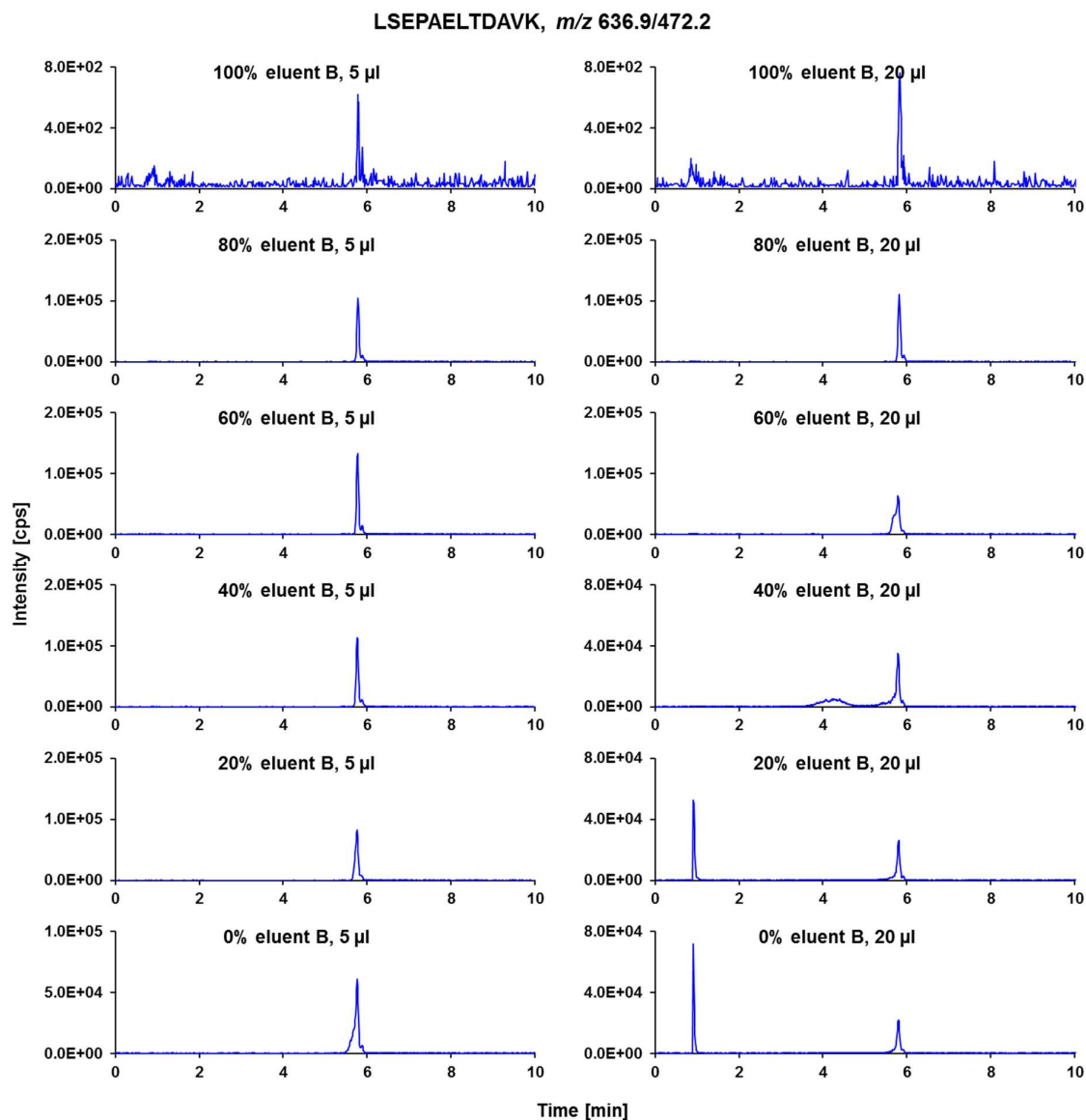


Figure 23: Chromatograms of peptide LSEPAELTDAVK diluted in different compositions of eluent A and B using 5 μ L (left) and 20 μ L (right) injection volume.

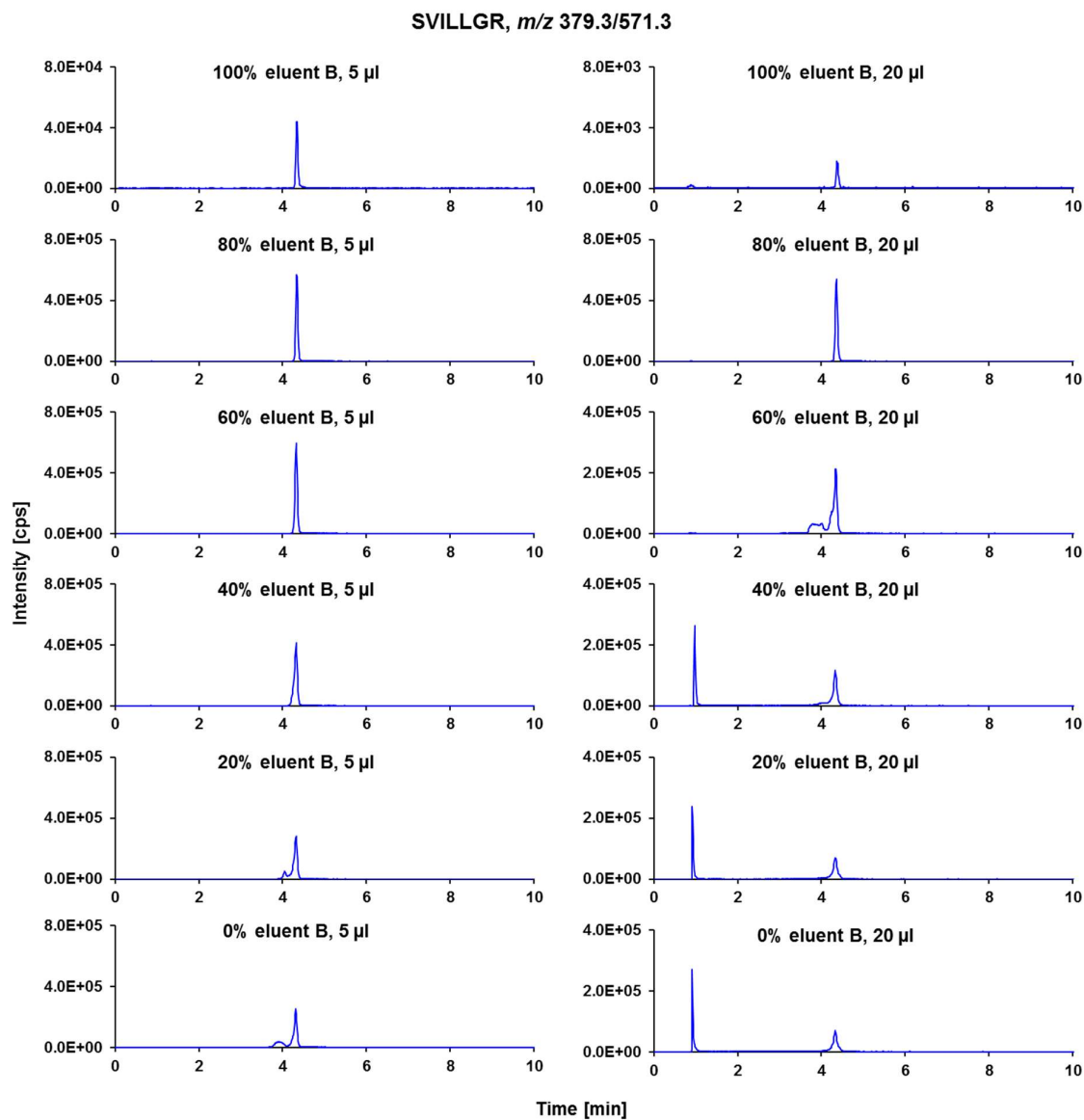


Figure 24: Chromatograms of peptide SVILLGR diluted in different compositions of eluent A and B using 5 μ L (left) and 20 μ L (right) injection volume.

3.5. Trypsin-based approaches

3.5.1. Surrogate peptide selection and analyte-specific MS parameter optimization

In the literature peptides LSEPAELTDAVK and SVILLGR are well-described as excellent representatives of total PSA in human serum. [113, 114] To verify ionization and fragmentation behavior on the instrument used in this work, analyte-specific MS parameters of the two peptides were investigated via T-infusion as mentioned in the experimental section using standard peptides which were synthesized in-house (Roche Diagnostics GmbH, Penzberg, Germany). Obtained results were comparable to that known from the literature [113, 114]. In addition, the same procedure was used to analyze the glycopeptides N(GlcNAc)K and N(GlcNAc+Fuc)K serving for quantification of partially deglycosylated PSA. The final results of peptide MRM parameter optimization are listed in Table 13. The glycopeptide N(GlcNAc+Fuc)K was quantified by measuring transition m/z 464.2/261.1 where m/z 464.2 in Q1 is referred to the intact single charge state m/z 610.1 of N(GlcNAc+Fuc)K without Fuc (146 Da) caused by in-source fragmentation (ISF). As it is shown in Table 13, this is the identical transition as the transition used for the non-fucosylated species N(GlcNAc)K. In practice, some degree of ISF is an inherent phenomenon in ESI-MS of glycopeptides, which could not be avoided in the study. Therefore, the signal intensity of the in-source fragmented species of glycopeptide N(GlcNAc+Fuc)K was maximized by adjusting source parameters, mainly by ion spray voltage, declustering potential and temperature. Differentiation of non-fucosylated and fucosylated PSA was achieved by chromatographic separation applying HILIC as shown in the previous section (Figure 20) [108].

Table 13: Analyte-specific parameters for LC-MS/MS measurement of four surrogate peptides generated by tryptic digestion of PSA. Reproduced from [108].

Target	Surrogate peptide	RT [min]	ISF	Charge state	Q1 [Da]	Q3 [Da]	DP [V]	EP [V]	CE [V]	CXP [V]
Non-fucosylated PSA	N(GlcNAc)K	6.8	no	1+	464.2	261.2	71	10	27	14
Fucosylated PSA	N(GlcNAc+Fuc)K ^a	7.2	yes	1+	464.2	261.2	71	10	27	14
Fucosylated PSA	N(GlcNAc+Fuc)K	7.2	no	1+	610.1	464.2	91	10	33	10
Total PSA	LSEPAELTDAVK	4.7	no	2+	636.9	943.4	71	10	29	44
Total PSA	SVILLGR	3.2	no	2+	379.3	571.3	56	10	17	10

^a differentiation of non-fucosylated PSA and fucosylated PSA was achieved by chromatographic separation as m/z 464.2 in Q1 is referred to the intact single charge state m/z 464.2 of N(GlcNAc)K as well as to the intact single charge state m/z 610.1 of N(GlcNAc+Fuc)K without fucose (146 Da) caused by in-source fragmentation (ISF); GlcNAc = N-Acetylglucosamine, Fuc = fucose, RT = retention time, DP = declustering potential, EP = entrance potential, CE = collision energy, CXP = cell exit potential.

3.5.2. Overview of the experimental workflow using MSIA tips

The trypsin-based workflow using MSIA tips for PSA enrichment was operated as illustrated in Figure 25 and as described in the experimental section. Immunoaffinity enrichment of PSA from human serum was performed in the same way as in the RPLC workflow using protease Arg-C (Figure 13). In contrast, in this workflow enriched PSA was not eluted from the pipette tip. Partial deglycosylation and enzymatic digestion were performed directly on the pipette tip, which allows simple buffer exchange required for maximal activity of Endo F3 and trypsin. Digested PSA was washed out with eluent B directly into a HPLC micro insert generating optimal chromatographic starting conditions. No additional vacuum concentration step was necessary. This procedure was more efficient than the in solution workflow presented in Figure 13 when protease Arg-C was replaced with trypsin and TRIS/HCl with ABC buffer. Beyond that the order of digestion steps was tested in several approaches entailing steps as vacuum concentration, elution and washing which did not lead to sensitivity improvements.

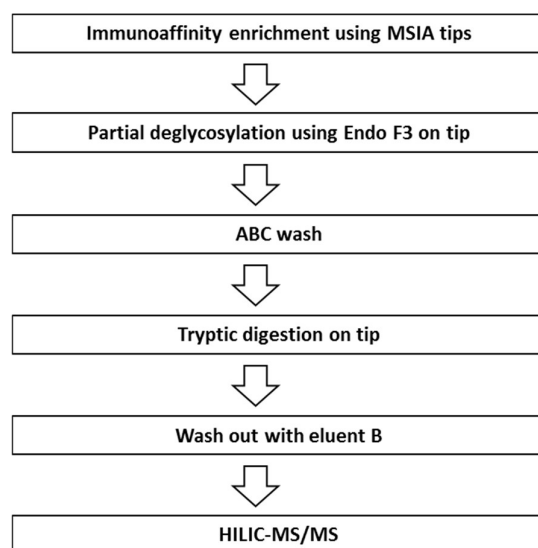


Figure 25: Schematic overview of the experimental workflow for the determination of core-fucosylated and total PSA using a MSIA tip-based and trypsin-assisted LC-MS/MS method.

3.5.3. Determination of partially deglycosylated and total PSA in spiked serum samples

Analysis of six female serum samples containing different concentrations of core-fucosylated (0, 0.78, 1.56, 3.90, 7.80 and 21.8 ng/mL) and total PSA (0, 1, 2, 5, 10 and 25 ng/mL) was performed in order to generate calibration curves by plotting peak areas of peptides N(GlcNAc+Fuc)K (m/z 464.2/261.2), LSEPAELTDAVK (m/z 636.9/943.4) and SVILLGR (m/z 379.3/571.3) against respective concentrations (Figure 26). Each concentration was prepared six times followed by analysis as illustrated in Figure 25. Based on these results the linear range, lower limit of detection (LLOD), lower limit of quantification (LLOQ) and precision over the working range expressed as coefficient of variation (CV) were evaluated.

Peptides N(GlcNAc+Fuc)K and SVILLGR showed poor linearity with correlation coefficients $R^2 < 0.90$ within the working range. In contrast, peptide LSEPAELTDAVK showed good linearity with $R^2 > 0.96$ within 1-25 ng/mL total PSA. As mentioned before, peak intensities with a signal-to-noise ratio of 3 and 10 were considered acceptable for determining the LLOD and LLOQ, respectively. The LLOD value of core-fucosylated PSA monitored by glycopeptide N(GlcNAc+Fuc)K at a retention time of 7.2 min was 2 ng/mL and the LLOQ value was 5 ng/mL. The LLOD of total PSA monitored by peptide LSEPAELTDAVK was lower than 1 ng/mL and the LLOQ was 1 ng/mL. The LLOD of total PSA monitored by peptide SVILLGR was 1 ng/mL and the LLOQ was 2 ng/mL. The assay imprecision for core-fucosylated PSA expressed as CV of six replicates ranged from 9.6 % to 31.4 % depending on the concentration. For total PSA, CVs ranged from 9.1 % to 18.3 % monitored by peptide LSEPAELTDAVK and from 14.1 % to 30.2 % monitored by peptide SVILLGR. In samples without addition of PSA interfering peaks were detected at the respective retention time of core-fucosylated PSA (RT = 7.2 min) and total PSA monitored by SVILLGR (RT = 3.9 min), which impedes robust quantification. Significant background noise (up to 500 cps) was present within the retention window of total PSA monitored by LSEPAELTDAVK (RT = 4.7 min). Representative chromatograms of serum samples containing different concentrations of total PSA are shown in Figure 27.

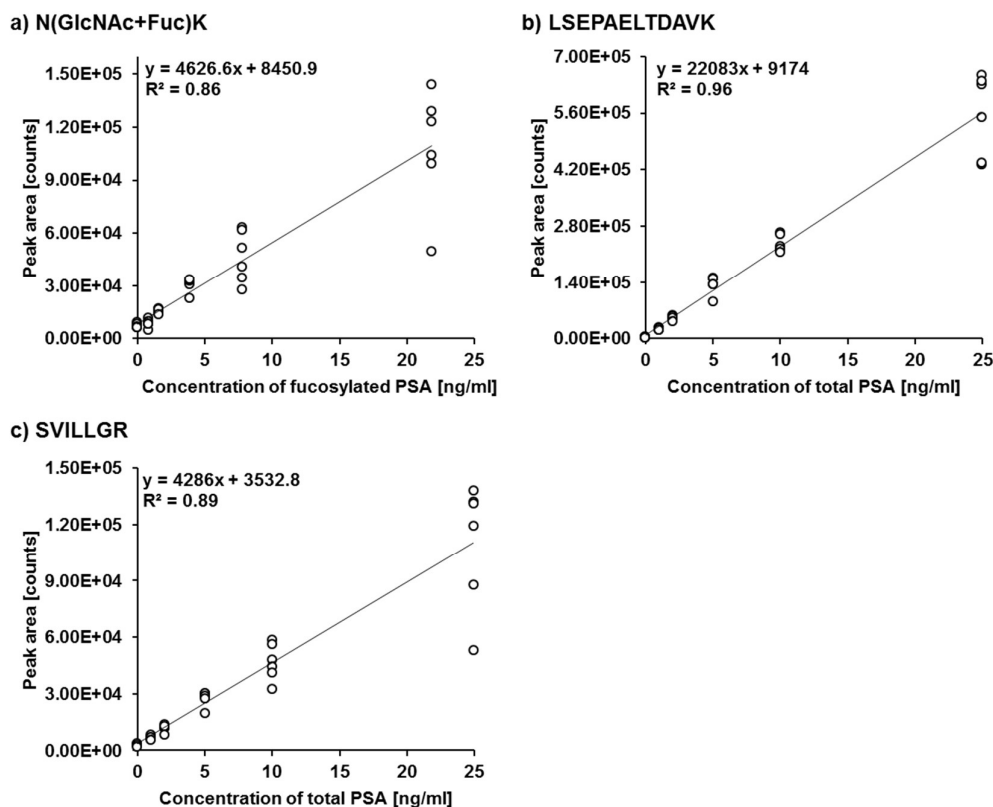


Figure 26: Calibration curves and correlation coefficients R^2 of core-fucosylated and total PSA obtained by plotting peak areas of a) N(GlcNAc+Fuc)K, b) LSEPAELTDAVK, and c) SVILLGR against respective concentrations, $n = 6$.

In terms of total PSA quantification, analysis of peptide LSEPAELTDAVK had a clear advantage over peptide SVILLGR regarding sensitivity and assay imprecision. Thus, peptide SVILLGR was not considered in further experiments. Non-fucosylated PSA monitored by peptide N(GlcNAc)K (m/z 464.2/261.2) at a retention time of 6.8 min could not be detected in the highest concentrated total PSA spiked-in serum sample (25 ng/mL) containing approximately 22 % non-fucosylated PSA as determined by glycan analysis. In a further experiment the LLOD of non-fucosylated PSA was determined to be at 13.2 ng/mL analyzing 0 and 60 ng/mL total PSA spiked-in serum samples (Figure 28). Further parameters of non-fucosylated PSA including linearity, LLOQ and CVs were not performed as the described workflow lacked in sensitivity for non-fucosylated PSA.

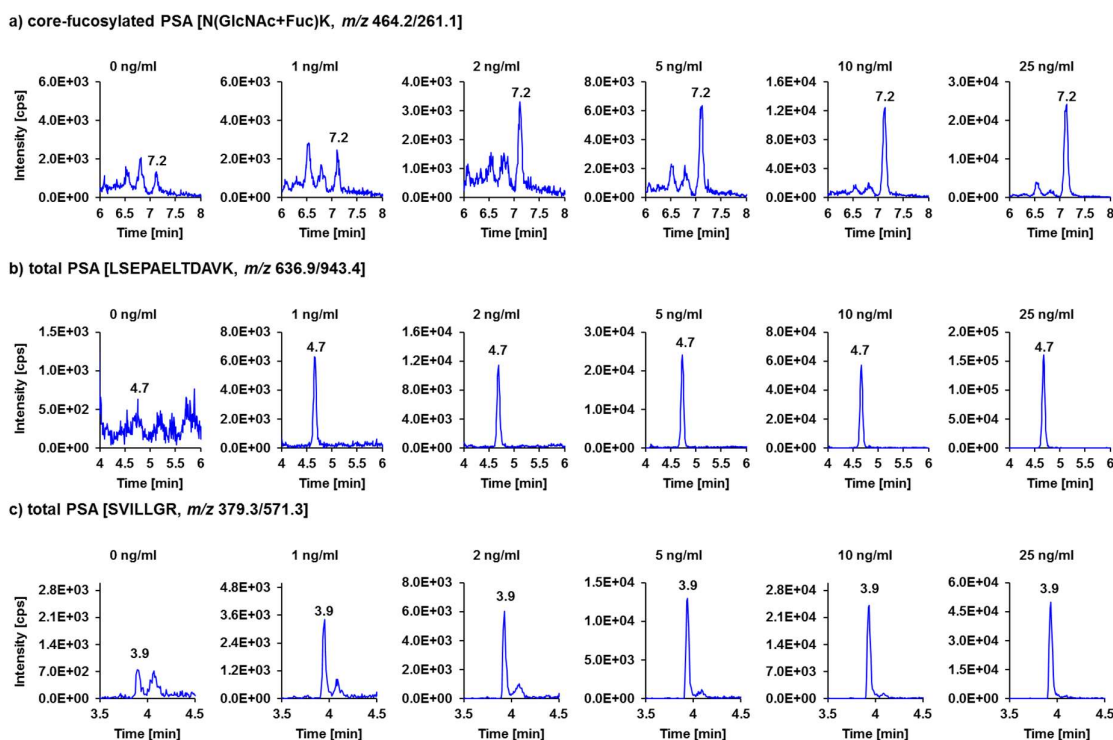


Figure 27: Extracted ion chromatograms of transitions monitored for a) core-fucosylated PSA (N(GlcNAc+Fuc)K, m/z 464.2/261.1), b) total PSA (LSEPAELTDAVK, m/z 636.9/943.4) and c) total PSA (SVILLGR, m/z 379.3/571.3) derived from 0, 1, 2, 5, 10 and 25 ng/mL total PSA spiked-in female serum samples.

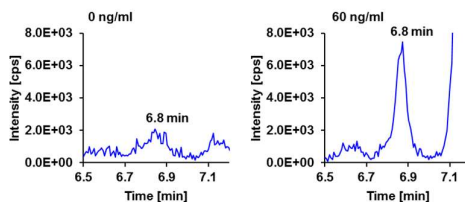
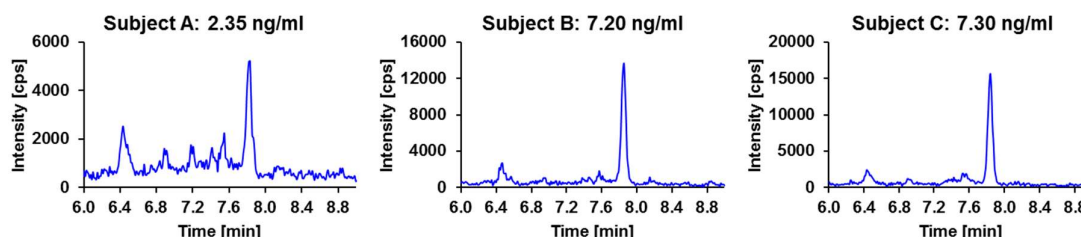


Figure 28: Extracted ion chromatograms of non-fucosylated PSA monitored by peptide N(GlcNAc)K (m/z 464.2/261.1) derived from 0 and 60 ng/mL total PSA spiked-in female serum samples containing 22 % non-fucosylated PSA.

3.5.4. Feasibility of the method in native serum samples

In order to demonstrate the feasibility of the method to detect core-fucosylated and total PSA in native serum samples a small sample set consisting of three human subjects A, B and C containing 2.35, 7.20 and 7.30 ng/mL total PSA was analyzed. As shown in Figure 29 signals of core-fucosylated and total PSA surrogate peptides were obtained in all three samples. Indeed, core-fucosylated PSA was also detected in subject A containing 2.35 ng/mL total PSA, but robust quantification could be problematic due to the low S/N ratio in this concentration range.

a) core-fucosylated PSA [N(GlcNAc+Fuc)K, m/z 464.2/261.1]



b) total PSA [LSEPAELTDAVK, m/z 636.9/943.4]

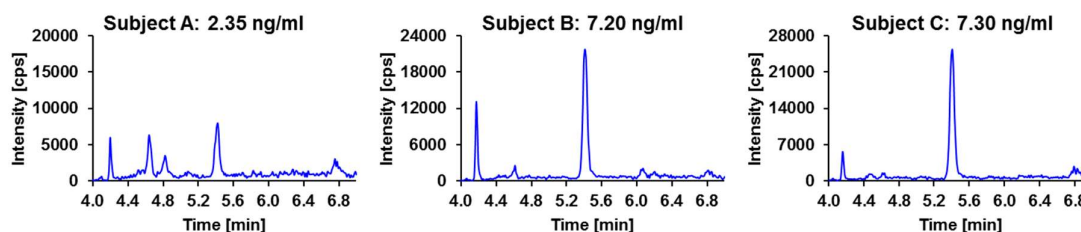


Figure 29: Extracted ion chromatograms of transitions monitored for a) core-fucosylated PSA (N(GlcNAc+Fuc)K, m/z 464.2/261.1) and b) total PSA (LSEPAELTDAVK, m/z 636.9/943.4) derived from three human specimen with total PSA levels of 2.35, 7.20 and 7.30 ng/mL. Reproduced from [108].

Furthermore, three PSA-free female serum matrices were analyzed to test the existence of interfering peaks at respective analyte retention times in native samples derived from different donors. As seen before in the female serum pool used for spiking experiments, with the current workflow interfering peaks were also detected with varying intensities in three female sera without addition of PSA at the respective retention time of core-fucosylated PSA (RT = 7.2 min). In comparison, a PSA-free PBS buffer did not show contamination at 7.2 min indicating that interferences come from serum itself (Figure 30). At the respective retention time of total PSA monitored by LSEPAELTDAVK (RT = 4.7 min), no interfering signals were detected in female sera. As expected, background noise was higher in sera than in PBS buffer. To achieve the required limit of quantification of core-fucosylated PSA further method optimization was performed.

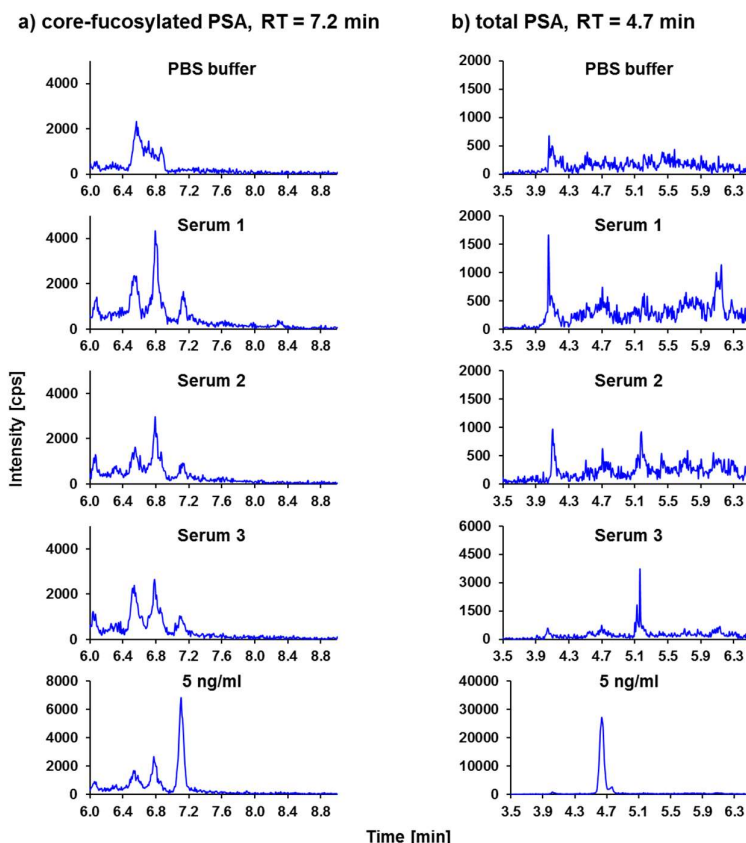


Figure 30: Extracted ion chromatograms of transitions monitored for a) core-fucosylated PSA (N(GlcNAc+Fuc)K, m/z 464.2/261.1) and b) total PSA (LSEPAELTDAVK, m/z 636.9/943.4) derived from PSA-free PBS buffer, three female sera without addition of PSA and a 5 ng/mL PSA spiked-in female serum sample.

3.5.5. Optimization approaches

As the trypsin-based workflow using MSIA tips was still limited to measure partially deglycosylated PSA down to 1 ng/mL in human serum and CV values were rather high, further approaches were conducted to improve the sensitivity and imprecision of the method.

3.5.5.1. Transitions

In particular, reliable quantification of core-fucosylated PSA seemed to be challenging due to the occurrence of interferences at the respective retention time of core-fucosylated PSA in PSA-free human sera. Primary selection of surrogate peptides, charge states and final transitions was performed in terms of signal intensity using aqueous tryptic peptide solutions. This procedure does not take into account challenges associated with the analysis of human samples including chromatographic interferences arising from the serum matrix. Therefore, two samples containing 0 and 10 ng/mL total PSA spiked-in female serum were prepared and analyzed as illustrated in Figure 25. A comprehensive list of different transitions previously obtained by analyte-specific MS parameter optimization representing non-fucosylated, core-fucosylated and total PSA was monitored with or without consideration of in-source fragmentation (Table 14). Despite the interfering peak at the

relevant retention time of core-fucosylated PSA, ion pair m/z 464.2/261.1 was still the favorite transition for quantification of core-fucosylated PSA as the signal-to-noise ratio was significantly higher compared to other transitions monitored in this experiment. The same applies to total PSA monitored by transition m/z 636.9/943.4, which was the most sensitive ion pair among other transitions. Non-fucosylated PSA was still untraceable at such low serum concentrations regardless of which transition was investigated. This is probably due to lower ionization efficiency of the non-fucosylated species and less activity of Endo F3 on glycosylation sites without Fuc.

Table 14: Most intensive transitions of non-fucosylated, fucosylated and total PSA obtained by analyte-specific MS parameter optimization.

Target	Surrogate peptide	RT [min]	ISF	Charge state	Q1 [Da]	Q3 [Da]
Non-fucosylated PSA	N(GlcNAc)K	6.8	no	1+	464.2	84.0
						126.0
						129.0
						209.0
						226.1
						261.2
			no	2+	232.3	84.0
						126.0
						129.0
						204.0
						209.0
						261.2
			yes	1+	261.0 ^a	56.0
						84.0
						129.0
						209.0
Fucosylated PSA	N(GlcNAc+Fuc)K	7.2	no	1+	610.1	84.0
						261.1
						464.2
			no	2+	305.3	75.1
						84.0
						261.1
			yes	1+	464.2 ^b	464.2
						84.0
						126.0
						129.0
						209.0
						261.1
Total PSA	LSEPAELTDAVK	4.7	no	2+	636.9	69.9
						84.0
						183.1
						312.1
						472.3
						943.4

^a m/z 261.0 in Q1 is referred to the intact single charge state m/z 464.2 of N(GlcNAc)K without N-Acetylglucosamine (GlcNAc, 203 Da) caused by in-source fragmentation (ISF).

^b m/z 464.2 in Q1 is referred to the intact single charge state m/z 610.1 of N(GlcNAc+Fuc)K without fucose (Fuc, 146 Da) caused by ISF.

3.5.5.2. Differential ion mobility mass spectrometry (DMS)

Next, differential ion mobility mass spectrometry (DMS) was used by activation of the Selexion® module of the QTRAP 6500 mass spectrometer. DMS offers an additional separation dimension which is orthogonal to the LC separation, and thus might help to remove interfering peaks. DMS parameters of peptides N(GlcNAc+Fuc)K and LSEPAELTDAVK were optimized manually as described in the experimental section and are shown in Table 15. Two samples containing 0 and 10 ng/mL total PSA spiked-in female serum were analyzed as illustrated in Figure 25 with or without additional up-front DMS separation. The application of DMS enabled the reduction of interferences and background noise at the respective retention times of core-fucosylated and total PSA by a factor of 10. On the other hand, the analyte signal intensity was also considerably lowered (Figure 31). Consequently, the S/N ratio of core-fucosylated and total PSA could not be improved by applying up-front DMS separation. In fact, the DMS module seemed to be susceptible to matrix contamination adversely impacting the instruments robustness and making it unsuitable for measurements of large numbers of patient samples.

Table 15: Differential ion mobility mass spectrometry (DMS) parameters of peptides N(GlcNAc+Fuc)K and LSEPAELTDAVK.

Target	Surrogate peptide	RT [min]	ISF	Charge state	Q1 [Da]	Q3 [Da]	COV [V]	DMO [V]	SV [V]
Core-fucosylated PSA	N(GlcNAc+Fuc)K	7.2	yes	1+	464.2	261.2	4.0	5.6	3200
Total PSA	LSEPAELTDAVK	4.7	no	2+	636.9	943.4	7.5	-10.0	3200

GlcNAc = N-Acetylglucosamine, Fuc = fucose, RT = retention time, ISF = in-source fragmentation, COV = compensation voltage, DMO = DMS offset, SV = separation voltage.

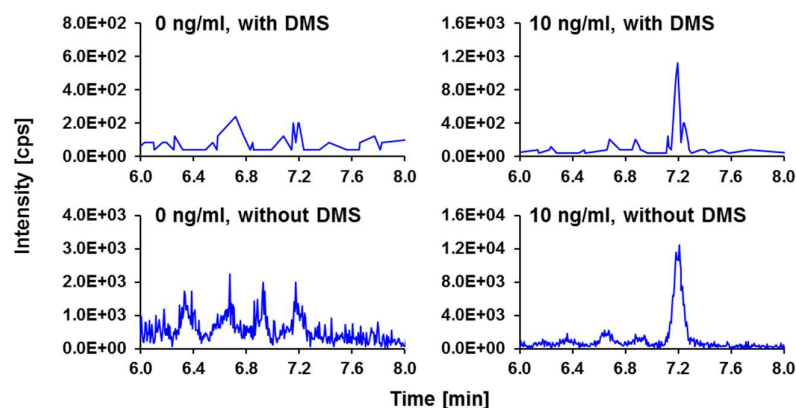
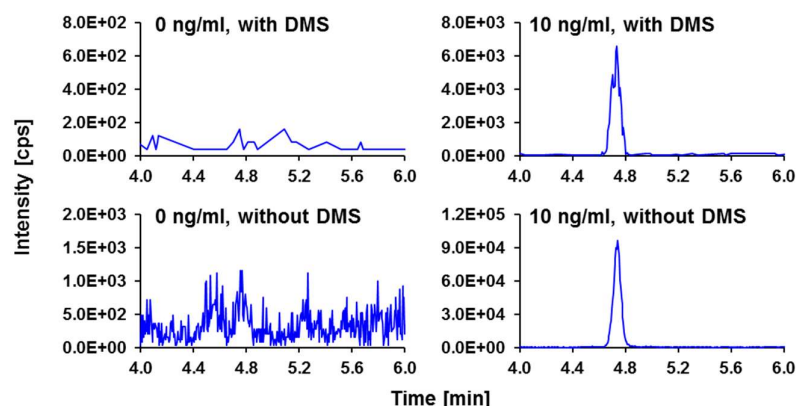
a) core-fucosylated PSA, RT = 7.2 min [N(GlcNAc+Fuc)K, m/z 464.2/261.1]b) total PSA, RT = 4.7 min [LSEPAELTDAVK, m/z 636.9/943.4]

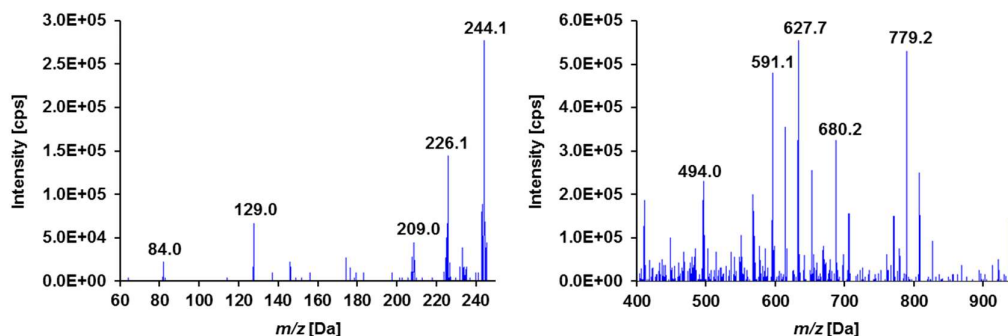
Figure 31: Extracted ion chromatograms of transitions monitored for a) core-fucosylated PSA (N(GlcNAc+Fuc)K, m/z 464.2/261.1) and b) total PSA (LSEPAELTDAVK, m/z 636.9/943.4) derived from 0 and 10 ng/mL PSA spiked-in female serum samples with and without additional up-front DMS separation.

3.5.5.3. Multiple reaction monitoring cubed (MRM³)

Recently, Fortin *et al.* demonstrated that a technique using MS³ reconstructed chromatograms on a signature of secondary precursor ions, termed multiple reaction monitoring cubed (MRM³), enables targeted quantification of protein biomarkers in the low ng/mL range in non-depleted human serum [118]. In order to gain sensitivity and selectivity in this work, MRM³ mode was applied to 0 and 10 ng/mL total PSA spiked-in serum samples. In MRM³ mode secondary precursor ions, previously generated by collision induced dissociation (CID) of primary precursor ions in Q2, were collected in the Q3 linear ion trap (LIT) and subsequently fragmented to product ions by resonant excitation energy as described in the experimental section. Ion chromatograms of core-fucosylated and total PSA were reconstructed from specific product ions which were selected among the most intense MRM³ transitions (Figure 32). Core-fucosylated and total PSA were monitored by MRM³ transition m/z 464.2/261.2/(84.0+129.0+209.0+226.1+244.1) and m/z 636.9/943.4/(494.0+591.1+627.7+680.2+779.2), respectively. These were the most intensive and specific transitions identified in MRM³ spectra. In comparison to MS/MS analysis, by using MRM³ mode the S/N ratio of total PSA could be

enhanced by a factor of 2, while the S/N ratio of core-fucosylated PSA could not be improved. Thus, MRM³ mode was not pursued any further in this work.

a) MRM³ spectra of core-fucosylated PSA (left) and total PSA (right)



b) Reconstructed MRM³ ion chromatograms of core-fucosylated PSA (left) and total PSA (right)

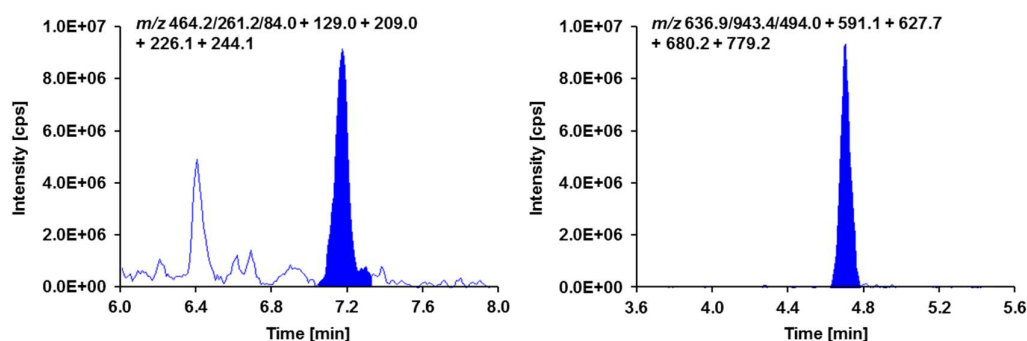


Figure 32: a) MRM³ spectra of core-fucosylated PSA (left) and total PSA (right) and b) reconstructed MRM³ ion chromatograms of core-fucosylated PSA (left) and total PSA (right) derived from a 10 ng/mL total PSA spiked-in serum sample.

3.5.5.4. Derivatization using tandem mass tags (TMT)

Isobaric mass tags are used for multiplex relative quantification by MS allowing for increased sample throughput by generating TMT-labeled analytes which specifically fragment to MS-responsive reporter ions. In this work, tandem mass tag label reagent TMT-126 composed of an amine-reactive NHS-ester group, a spacer arm and an MS/MS reporter was applied to 0, 10 and 20 ng/mL total PSA spiked-in female serum samples in order to overcome chromatographic interferences coming along with the analysis of core-fucosylated PSA. In addition, specific fragmentation channels of labelled target peptides might improve the method's sensitivity and imprecision. Analyte-specific MS parameters of TMT-labeled peptides were automatically tuned in the same manner as unlabeled peptides. The most sensitive transition of TMT-labeled core-fucosylated PSA was m/z 530.8/457.9 in which m/z 530.8 in Q1 is referred to the double charged intact peptide N(GlcNAc+Fuc)K labeled with two molecules TMT-126 (Figure 33).

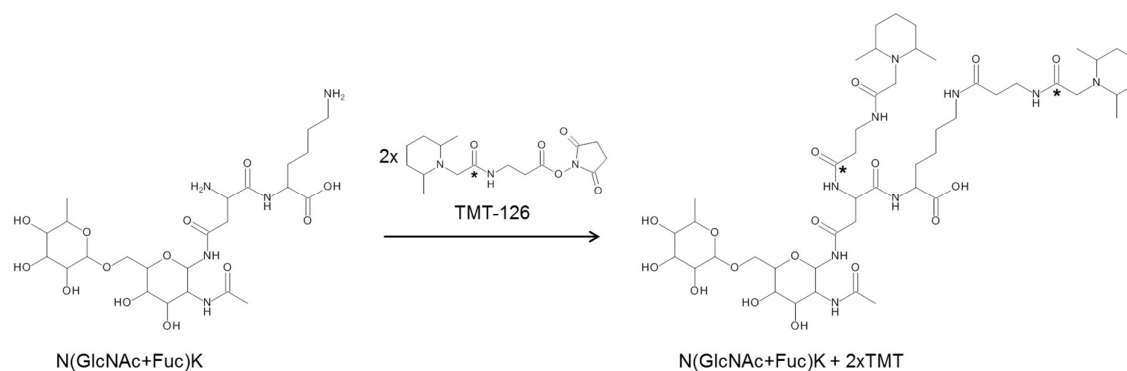


Figure 33: Derivatization of peptide N(GlcNAc+Fuc)K with two molecules TMT-126 (heavy carbon atom indicated by asterisk) at the primary amine residues.

The in-source fragmented species m/z 457.9 where Fuc is lost during the ionization process was observed to a much less extent. As shown in Figure 34 derivatization of core-fucosylated PSA monitored by peptide N(GlcNAc+Fuc)K + 2xTMT was complete indicated by the disappearance of the unlabeled species m/z 464.2/261.1 in 10 and 20 ng/mL total PSA samples. The signal intensity of TMT-labeled core-fucosylated PSA increased linearly with increasing total PSA concentrations and was twice as high ($2.6\text{E}+04$ cps) as the signal intensity of the unlabeled species ($1.3\text{E}+04$ cps). However, in the PSA-free female serum sample interfering peaks were detected at the retention time of TMT-labeled core-fucosylated PSA ($\text{RT} = 5.0$ min) resulting in a lower S/N ratio compared to the unlabeled species. Hence, the usage of TMT-derivatization of PSA could not improve the method's performance.

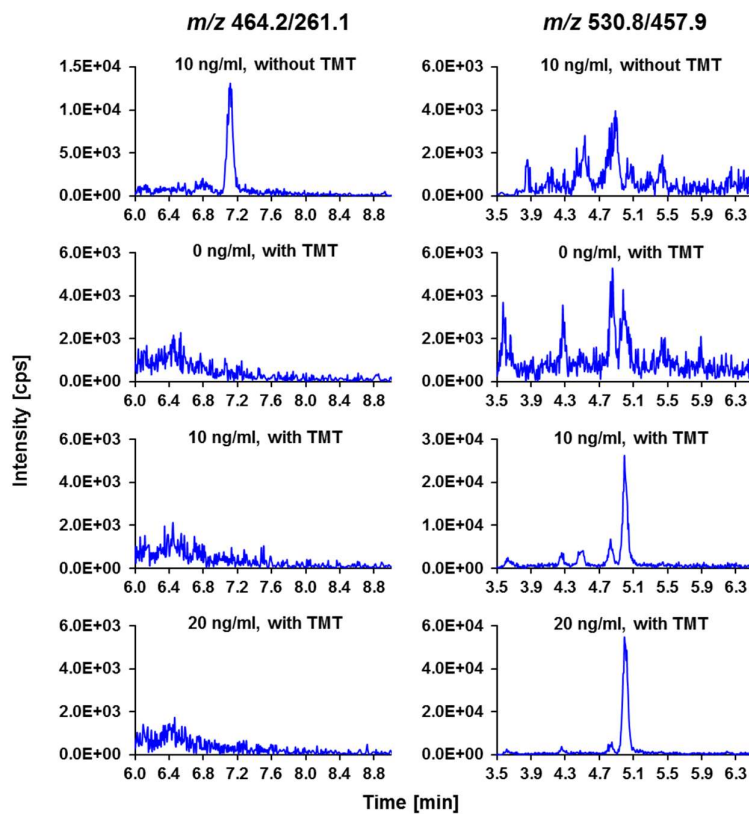


Figure 34: Extracted ion chromatograms of transitions monitored for core-fucosylated PSA (N(GlcNAc+Fuc)K, m/z 464.2/261.1, left) and TMT-labeled core-fucosylated PSA (N(GlcNAc+Fuc)K + 2xTMT, m/z 530.8/457.9, right) derived from 0, 10 and 20 ng/mL PSA spiked-in female serum samples with and without addition of TMT-126.

3.5.6. Overview of the experimental workflow using magnet beads

The trypsin-based workflow using MSIA tips for immunoaffinity enrichment of PSA showed poor linearity and lacked in sensitivity regarding the analysis of core-fucosylated PSA. Furthermore, the assay imprecision was rather high. Approaches such as DMS, MS³ and TMT-derivatization could not improve the method's performance. A barrier for robust quantification of core-fucosylated PSA in the low ng/mL concentration range seemed to be a co-eluting peak derived from a serum compound which might be enriched through unspecific binding to MSIA tips. Therefore, another solid support material was selected for immobilization of the PSA immunoaffinity complex in order to reduce unspecific interaction. A magnetic particle-based workflow was developed and operated as illustrated in Figure 35. Starting with 100 μ L human serum, immunoaffinity enrichment was performed by using biotinylated anti-PSA antibody bound to streptavidin-coated magnetic particles to enrich PSA from complex serum matrix. Enriched PSA, still captured by the immunoaffinity complex, was stepwise partially deglycosylated in order to simplify glycosylation microheterogeneity and tryptically digested to generate surrogate peptides. Following vacuum concentration and reconstitution, appropriate peptides were measured by LC-MS/MS without additional up-front SPE clean up. Other procedures e.g. involving analyte elution and subsequent in solution digestion were less efficient.

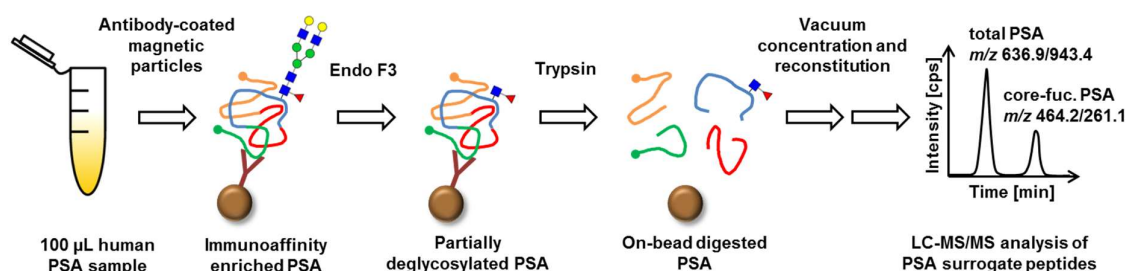


Figure 35: Schematic overview of the experimental workflow for the quantitative analysis of core-fucosylated and total PSA using a magnet bead-based workflow and trypsin-assisted LC-MS/MS method. Reproduced from [108].

3.5.7. Development of the magnet bead-based workflow

3.5.7.1. Optimization of immunoaffinity enrichment

Different amounts of anti-PSA antibody PSA36 (0.05, 0.2, 1, and 5 μ g) were incubated with constant amounts of magnet beads (50 μ g). After incubation and washing, human serum containing 5 ng/mL PSA was added and incubated. Magnet beads were removed and the residual human serum sample was analyzed by ECLIA for PSA which was not bound to the antibody-bead-complex (= unbound PSA). The capture efficiency was inversely proportional to unbound PSA which was normalized to the initial PSA serum concentration. As shown in Figure 36a using 1 μ g anti-PSA antibody showed the best capture efficiency. Similar to that procedure, different amounts of magnet beads (10, 50, 100, and 250 μ g) were incubated with constant amounts of anti-PSA antibody (1 μ g) and unbound PSA was determined in residual human serum by ECLIA. It was shown that 100 μ g magnetic beads performed slightly better than 50 μ g whereas no significant difference was observed compared to

250 μg (Figure 36b). Based on standard conditions applied at the beginning of the method development, different parameters concerning incubation steps were varied and tested individually as follows. The incubation time was decreased from 30 to 10 min. The incubation temperature was decreased from 37 to 25 $^{\circ}\text{C}$. The stirring rate during incubation was decreased from 1000 to 500 rpm. The number of washing steps after antibody-bead incubation was increased from one to four. Results in Figure 36c obtained by measuring unbound PSA in residual human serum indicate that the capture efficiency is beneficially influenced by a lower incubation temperature whereas a slower stirring rate, a shorter incubation time and more wash steps did not show significant changes. In Figure 36d results of further approaches which are likely to impact immunoaffinity enrichment are illustrated. For example, resuspension of magnet beads could be achieved by vortexing and ultrasound mixing in which the latter led to extensive PSA loss after sample incubation. Pretreatment strategies such as previous sample dilution with 0.5 % tween in PBS buffer (1:5-dilution, v/v) and sample preincubation with antibody followed by magnet bead incubation clearly worsened analyte capturing. The simultaneous usage of two different anti-PSA antibodies PSA36 and PSA30 also showed diminished PSA enrichment capability compared to the initial workflow. All optimization approaches were performed in six replicates.

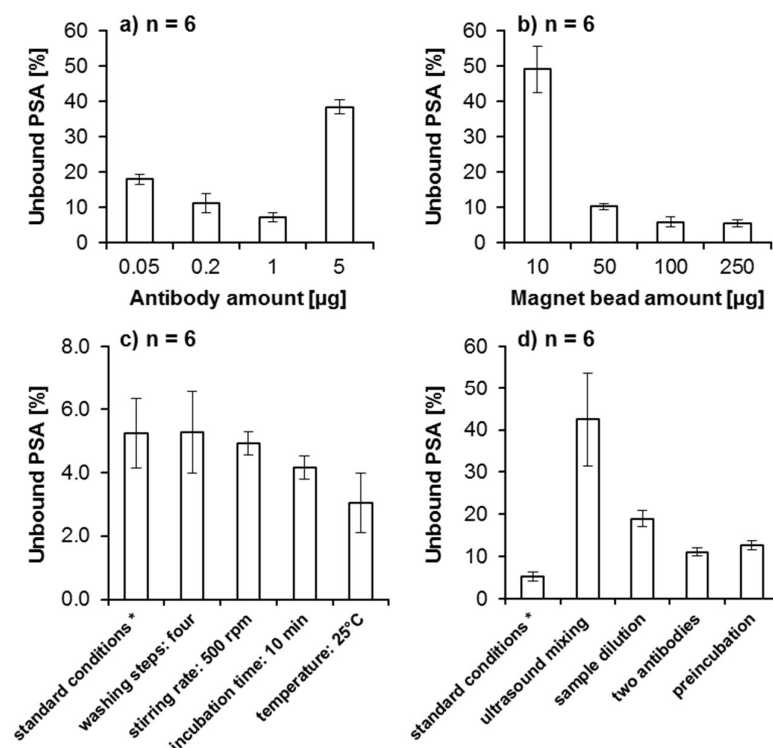


Figure 36: Optimization of immunoaffinity enrichment by testing of a) different amounts of anti-PSA antibody, b) different amounts of magnet beads, c) different incubation and washing conditions and d) different approaches such as ultrasound mixing, sample dilution, simultaneous usage of two antibodies and sample preincubation with antibody. Unbound PSA was normalized to the initial PSA serum concentration. Mean \pm standard deviation shown as error bars, n = 6.

*Standard incubation conditions: temperature = 37 $^{\circ}\text{C}$, stirring rate = 1000 rpm, time = 30 min, number of washing steps after antibody-bead incubation = 1, samples mixed by vortexing.

In summary, subsequent conditions were used for immunoaffinity enrichment of PSA: (1) the anti-PSA antibody PSA36 amount was 1 µg, (2) the streptavidin-coated magnet bead amount was 100 µg, (3) the incubation temperature was 25 °C, (4) the stirring rate during incubation was 1000 rpm, (5) the incubation time was 10 min, (6) a single wash step was used after antibody-bead incubation, and (7) magnet bead resuspension was achieved by moderate vortexing.

3.5.7.2. Optimization of partial deglycosylation and tryptic digestion

The most efficient endoglycosidase was selected in previous experiments (chapter III section 3.1). For the current workflow, conditions for partial deglycosylation were reinvestigated including Endo F3 amount, incubation time, and sample buffer (Figure 37). Each approach was performed in six replicates and core-fucosylated and total PSA were analyzed by LC-MS/MS as illustrated in Figure 35. Among different Endo F3 amounts (0.5, 2, 10 and 50 milliunits) the optimum for analysis of core-fucosylated PSA was 10 milliunits per 100 µL sample evaluated by using 5 ng/mL total PSA spiked-in human serum. Usage of higher Endo F3 amounts could not significantly improve signal intensity indicated by overlapping error bars. The average signal intensity of core-fucosylated PSA was increased after 6 h incubation time compared to 3 h and 25 h incubation time. Due to the large error bars obtained for 6 h, this result was not significant. From a practical perspective, an incubation time of 3 h was selected, hence shortening the overall workflow duration. The influence of four incubation buffers (20 mM and 100 mM sodium acetate pH 4.5, 100 mM sodium acetate pH 6 and 100 mM ABC buffer pH 8) on partial deglycosylation activity was tested. No significant differences could be observed for core-fucosylated PSA. Analysis of total PSA was not affected by variations of any of the described parameters indicated by constant total PSA peak areas.

LC-MS/MS analysis of 5 ng/mL PSA spiked-in serum samples prepared as illustrated in Figure 35 using various trypsin amounts (0.05, 0.2, 1, 5 and 20 µg) revealed that both core-fucosylated and total PSA had maximal intensities between 1 and 20 µg trypsin indicated by the highest signal at 5 µg trypsin (Figure 38). Investigation of different 100 mM sample buffers such as ABC (ammonium bicarbonate, pH 8), TEAB (triethylammonium bicarbonate, pH 8), HEPES (2-[4-(2-hydroxyethyl)piperazin-1-yl]ethanesulfonic acid, pH 8.4), TRIS (2-Amino-2-(hydroxymethyl)propane-1,3-diol, pH 8) buffer clearly showed the predominance of ABC as a buffer substance in mass spectrometric applications. TEAB buffer showed decreased signal intensities for core-fucosylated and total PSA compared to ABC, while no signals were observed using HEPES and TRIS buffer. This was most likely due to ion suppression of the ESI signal and/or extensive adduct formation caused by non-volatile electrolytes.

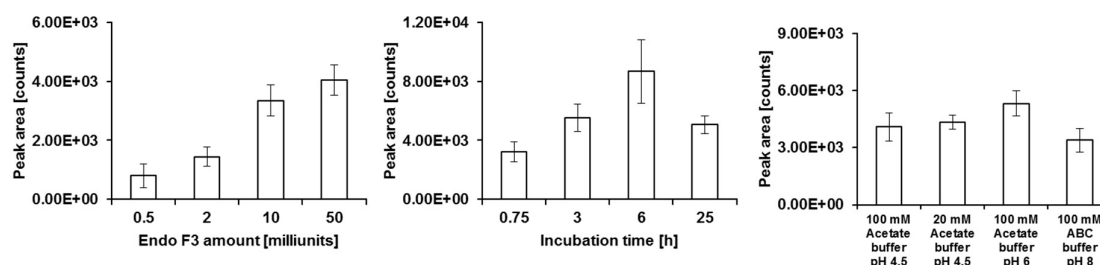
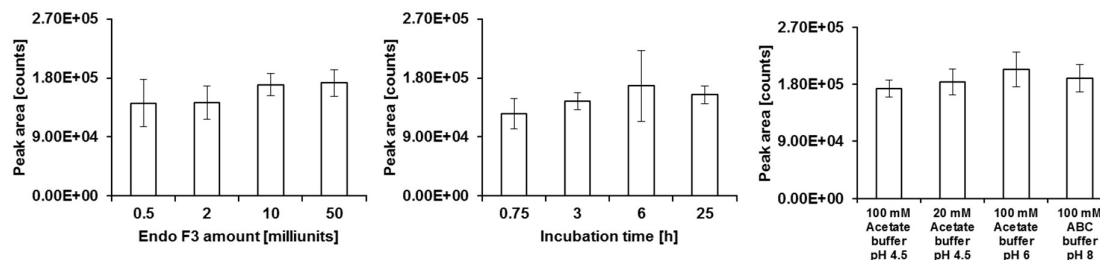
a) core-fucosylated PSA, [N(GlcNAc+Fuc)K, m/z 464.2/261.1], $n = 6$:**b) total PSA, [LSEPAELTDAVK, m/z 636.9/943.4], $n = 6$:**

Figure 37: Optimization of partial deglycosylation by testing of different Endo F3 amounts, incubation times and sample buffers. a) core-fucosylated PSA (N(GlcNAc+Fuc)K, m/z 464.2/261.1) and b) total PSA (LSEPAELTDAVK, m/z 636.9/943.4) were analyzed by LC-MS/MS using 5 ng/mL total PSA spiked-in serum samples. Mean \pm standard deviation shown as error bars, $n = 6$.

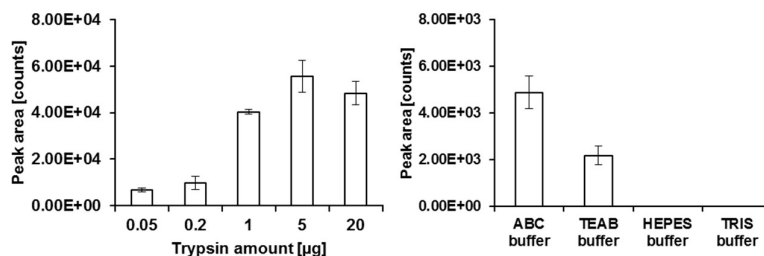
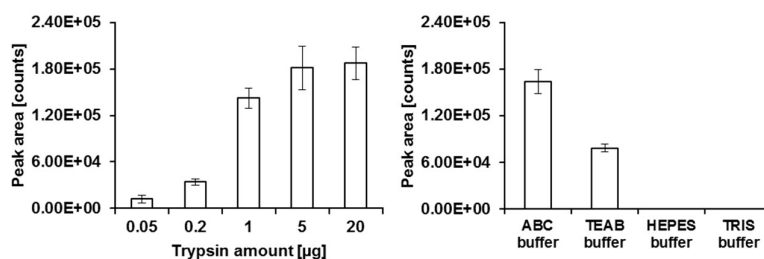
a) core-fucosylated PSA, [N(GlcNAc+Fuc)K, m/z 464.2/261.1], $n = 6$:**b) total PSA, [LSEPAELTDAVK, m/z 636.9/943.4], $n = 6$:**

Figure 38: Optimization of tryptic digestion by testing of different trypsin amounts and sample buffers. a) core-fucosylated PSA (N(GlcNAc+Fuc)K, m/z 464.2/261.1) and b) total PSA (LSEPAELTDAVK, m/z 636.9/943.4) were analyzed by LC-MS/MS using 5 ng/mL total PSA spiked-in serum samples, $n = 6$. ABC = ammonium bicarbonate, TEAB = triethylammonium bicarbonate, HEPES = 2-[4-(2-hydroxyethyl)piperazin-1-yl]ethanesulfonic acid, TRIS = 2-Amino-2-(hydroxymethyl)propane-1,3-diol.

3.5.8. Comparison of streptavidin-coated solid support materials for immunoaffinity enrichment

Two optimized workflows using different streptavidin-coated solid support materials, MSIA tips and magnetic particles were evaluated. The MSIA tip-based and the magnet bead-based workflow were executed as shown in Figure 25 and Figure 35, respectively. Comparison of the two solid support materials was based on the analysis of 0 and 5 ng/mL total PSA-spiked in serum aliquots. Each aliquot was prepared six times with both workflows followed by LC-MS/MS measurement. In average, the S/N ratio of core-fucosylated PSA obtained by the magnet bead-based workflow was 7 times higher than the S/N ratio obtained by the MSIA tip-based workflow. This was mainly due to high chromatographic interferences observed in PSA-free serum samples prepared by the MSIA tip-based workflow as seen in the representative chromatogram of core-fucosylated PSA (Figure 39). The magnet bead-based workflow was more sensitive by a factor of 3 regarding total PSA quantification. Moreover, the assay imprecision could be improved by using magnetic beads revealed by CV values of respective analyte peak areas obtained by analysis of six 5 ng/mL total PSA spiked-in serum samples. CV values of core-fucosylated PSA were 13.4 % using magnetic beads and 23.2 % using MSIA tips. CV values of total PSA were 8.8 % using magnetic beads and 10.2 % using MSIA tips.

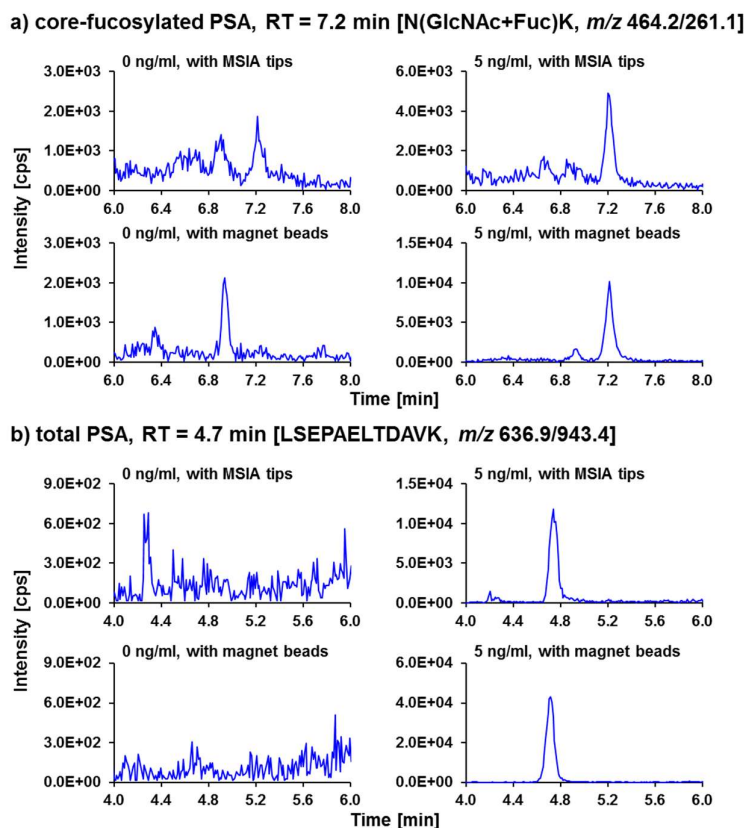


Figure 39: Extracted ion chromatograms of transitions monitored for a) core-fucosylated PSA (N(GlcNAc+Fuc)K, m/z 464.2/261.1) and b) total PSA (LSEPAELTDAVK, m/z 636.9/943.4) derived from 0 and 5 ng/mL PSA spiked-in serum samples prepared with MSIA tips or magnetic particles, respectively.

3.5.9. Characterization of the final workflow using magnet beads

3.5.9.1. Linearity, LLOD, LLOQ and imprecision of the magnet bead-based workflow

LC-MS/MS analysis of female serum samples containing different concentrations of core-fucosylated PSA (0, 0.4, 0.8, 1.6, 3.9, 7.8, 23.4 and 46.8 ng/mL) and total PSA (0, 0.5, 1, 2, 5, 10, 30 and 60 ng/mL) was performed using analyte-specific MS parameters as shown in Table 13. The most sensitive transition of each of the two peptides was selected for quantification, which means Q1/Q3 ion pairs were m/z 464.2/261.2 and m/z 636.9/943.4 for core-fucosylated and total PSA, respectively. Each concentration was prepared in triplicate on two different days followed by analysis as illustrated in Figure 35. Calibration curves were obtained by plotting peak areas of peptides N(GlcNAc+Fuc)K or LSEPAELTDAVK against respective concentrations (Figure 40). Based on these results the linear range, lower limit of detection (LLOD), lower limit of quantification (LLOQ) and precision over the working range expressed as CV were evaluated. Both peptides showed good linearity within 0.4-46.8 ng/mL for core-fucosylated PSA and 0.5-60 ng/mL for total PSA, respectively. Calibration curves were obtained at two different days ($n = 3$ at each day) with average correlation coefficient $R^2 > 0.99$ for the core-fucosylated PSA peptide N(GlcNAc+Fuc)K and $R^2 > 0.98$ for the total PSA peptide LSEPAELTDAVK at both days (Figure 40) [108].

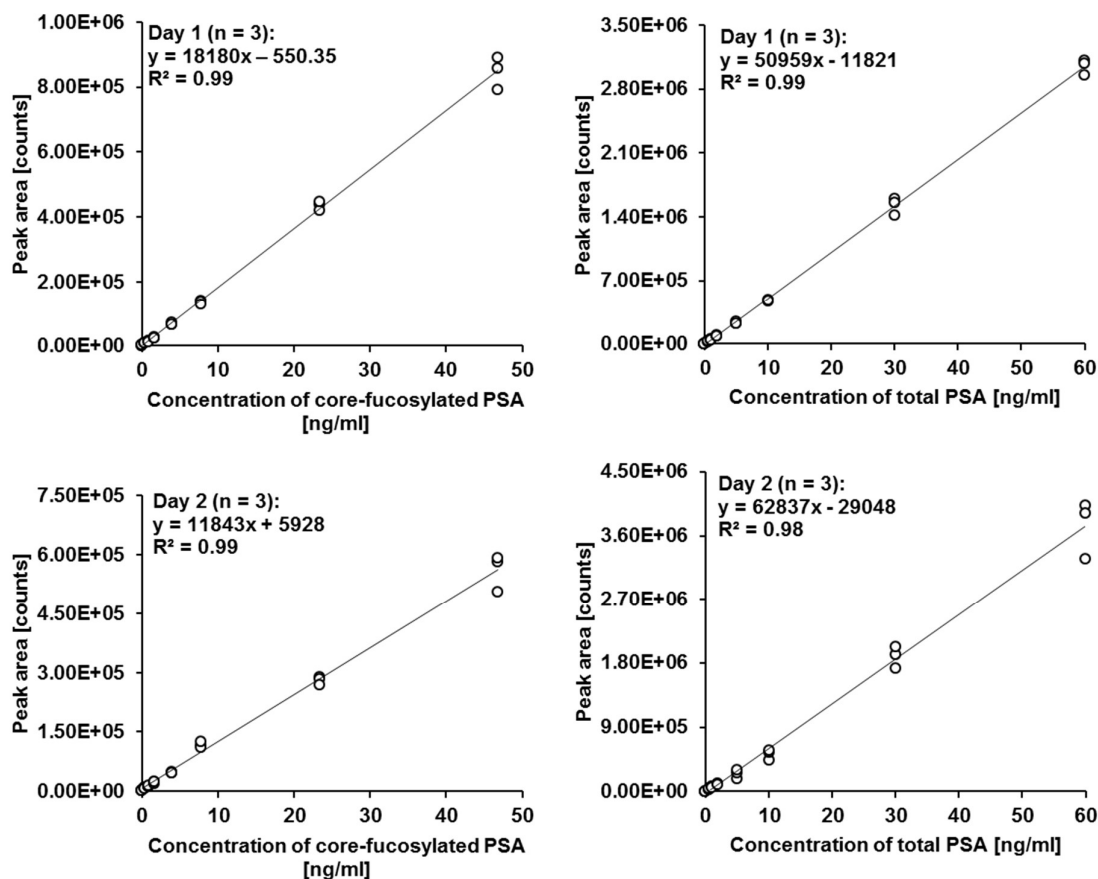
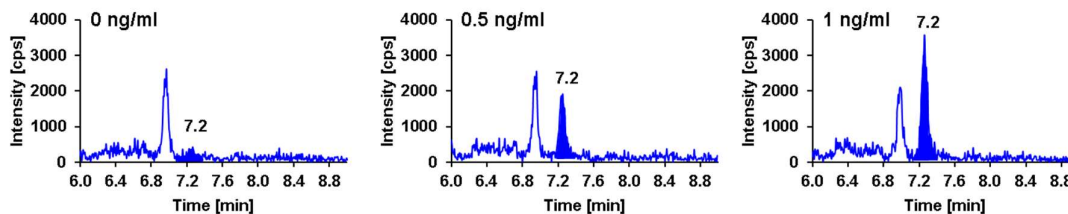


Figure 40: Calibration curves and correlation coefficients R^2 of core-fucosylated (left) and total PSA (right) obtained by plotting peak areas of N(GlcNAc+Fuc)K and LSEPAELTDAVK against respective concentrations at day one (top) and day two (bottom), $n = 3$ at each day. Reproduced from [108].

Combining results of day one and two ($n = 6$) gave calibration curves with average correlation coefficient $R^2 > 0.94$ for the core-fucosylated PSA peptide N(GlcNAc+Fuc)K and $R^2 > 0.98$ for the total PSA peptide LSEPAELTDAVK. In this work, peak intensities with a signal-to-noise ratio of 3 and 10 were considered acceptable for determining the LLOD and LLOQ, respectively. The LLOD value of core-fucosylated PSA was 0.4 ng/mL and the LLOQ value was 1 ng/mL whereas the LLOD and LLOQ of total PSA were lower than 0.5 ng/mL. Compared to intact glycopeptide analysis, a major advantage of the method is the increased ionization efficiency of partially deglycosylated peptides. In addition, the sensitivity of the assay was improved due to stacking effects of identical glycopeptides and data analysis was greatly simplified. Even though the method was not optimized for total PSA quantification, total PSA concentrations lower than 0.5 ng/mL could be quantified, which is more sensitive than similar approaches described in the current literature using immunoaffinity enrichment coupled to mass spectrometry [113, 119, 120]. However, as this method emphasizes the quantification of core-fucosylated PSA, it cannot compete with high-sensitive methods focusing on total PSA quantification only such as the PRISM-SRM workflow introduced by Shi *et al* [121]. Without addition of PSA, no peaks were detected at the respective retention times of core-fucosylated PSA (RT = 7.2 min) and total PSA (RT = 4.7 min) indicating the high specificity of the workflow. Representative chromatograms for 0, 0.5 and 1 ng/mL total PSA spiked-in serum sample are shown in Figure 41 [108].

a) core-fucosylated PSA [N(GlcNAc+Fuc)K, m/z 464.2/261.1]



b) total PSA [LSEPAELTDAVK, m/z 636.9/943.4]

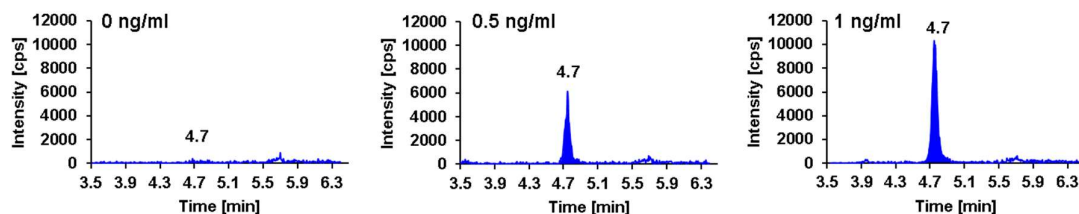


Figure 41: Extracted ion chromatograms of transitions monitored for a) core-fucosylated PSA (N(GlcNAc+Fuc)K, m/z 464.2/261.1) and b) total PSA (LSEPAELTDAVK, m/z 636.9/943.4) derived from 0, 0.5 and 1 ng/mL total PSA spiked-in female serum samples. Reproduced from [108].

Intra-day precision calculated by using three replicates of each concentration expressed as the CV ranged from 3.1 % to 10.5 % for core-fucosylated PSA and from 2.1 % to 9.8 % for total PSA at day one and from 2.1 % to 17.0 % for core-fucosylated PSA and from 4.1 % to 26.9 % for total PSA at day two depending on the relative concentration. Inter-day precision combining results of day one and two

ranged from 9.7 % to 23.2 % for core-fucosylated PSA and from 10.3 % to 18.3 % for total PSA. The average peak area ratio of core-fucosylated PSA to total PSA in the interesting concentration range of 1-10 ng/mL was 0.26 with a CV value of 20.8 % over two days ($n = 6$). Approaches for protein quantification often benefit from the usage of stable-isotope labeled (SIL) proteins, peptides or analogues thereof as internal standards, thereby positively impacting the imprecision of the method [122]. Thus, it should be possible to improve CV values of the described method by using SIL PSA, which is not commercially available yet. As an alternative, the usage of more easily accessible SIL peptides of PSA could improve the assay imprecision, although this strategy cannot reflect the whole sample preparation workflow. Still the imprecision of the method is acceptable, regarding the intended use e.g. as support for biomarker refinement studies, and data could be strengthened by measuring of larger patient cohorts or performing repetitive sample analysis [108].

3.5.9.2. Analysis of serum samples containing different amounts of fucosylated PSA

Applying LCA lectin chromatography, PSA from Scripps Laboratories was separated into two fractions consisting of non-fucosylated or fucosylated PSA. The fucosylation degree of these two fractions was determined by N-glycan analysis demonstrating the effectiveness of the LCA separation step because almost no fucosylated glycans could be detected in the non-fucosylated fraction whereas Fuc was bound to nearly all glycan structures in the fucosylated fraction. Finally, serum samples were prepared containing five different ratios of non-fucosylated to fucosylated PSA (100:0, 75:25, 50:50, 25:75 and 0:100) at total PSA concentrations of 10 ng/mL as determined by ECLIA. Each of the five ratio samples was processed six times as illustrated in Figure 35 ($n = 6$) resulting in six calibration curves with an average correlation coefficient $R^2 > 0.97$ (Figure 42). CV values of the peak area ratio of core-fucosylated PSA to total PSA ranged from 4.1 % to 8.6 %. This proof-of-concept experiment revealed the method's feasibility to distinguish between different relative core-fucosylation degrees [108].

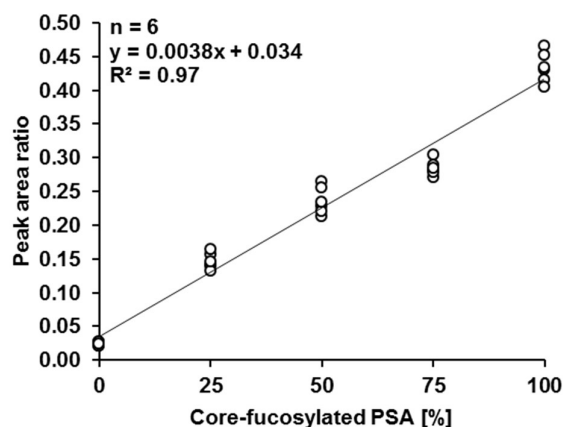


Figure 42: Calibration curve of serum samples containing different ratios of non-fucosylated to fucosylated PSA by plotting the peak area ratio of N(GlcNAc+Fuc)K to LSEPAELTDAVK against the relative amount of fucosylated PSA ranging from 0 to 100 % ($n = 6$, $R^2 > 0.97$). Reproduced from [108].

3.5.9.3. Analysis of human specimens

The described method was applied to quantify core-fucosylated and total PSA in native serum samples. For this purpose, three human serum specimens with total PSA levels of 2.03 ng/mL (subject A), 6.06 ng/mL (subject B) and 9.95 ng/mL (subject C) were prepared in triplicate at different days as illustrated in Figure 35 and quantitated by external calibration using five calibrators with different concentrations of core-fucosylated PSA (0.78, 2.34, 4.68, 7.02 and 9.36 ng/mL) and total PSA (1, 3, 6, 9 and 12 ng/mL). Representative chromatograms in Figure 43 demonstrate that the method is able to detect core-fucosylated and total PSA in native human specimens covering the critical grey area in PCa diagnosis. CV values of subject A, B and C were 22.4 %, 17.0 % and 27.3 % for core-fucosylated PSA, 16.6 %, 5.6 % and 13.1 % for total PSA, and 10.4, 12.8 and 21.5 for the ratio of core-fucosylated to total PSA (Table 16). These CVs were comparable to CVs obtained under artificial conditions of PSA spiked-in serum samples [108].

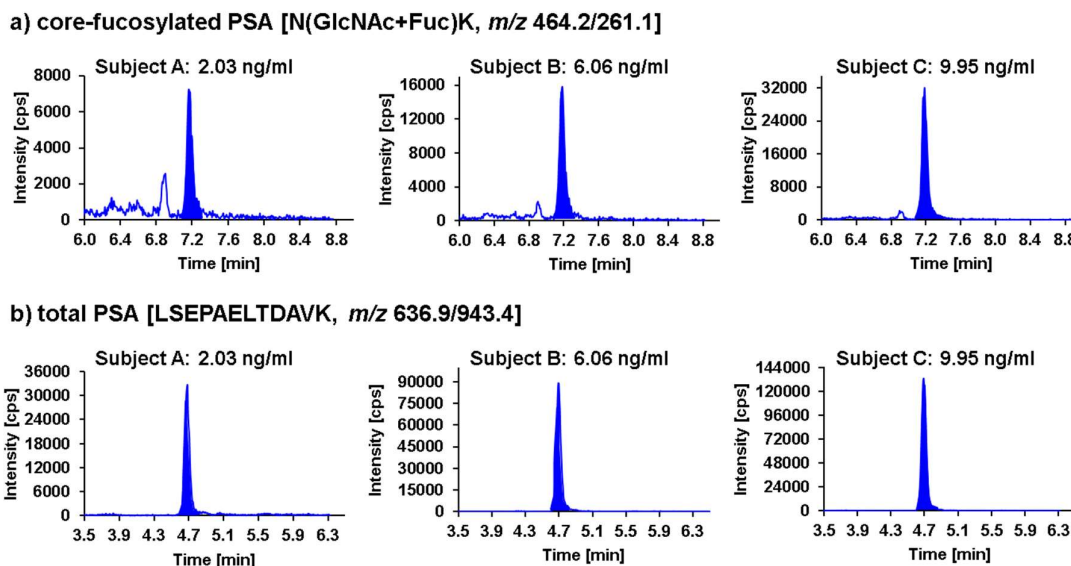


Figure 43: Extracted ion chromatograms of transitions monitored for a) core-fucosylated PSA (N(GlcNAc+Fuc)K, m/z 464.2/261.1) and b) total PSA (LSEPAELTDAVK, m/z 636.9/943.4) derived from three human specimen with total PSA levels of 2.03, 6.06 and 9.95 ng/mL. Reproduced from [108].

Table 16: Results of the analysis of three anonymized human specimens by ECLIA ($n = 1$) and LC-MS/MS ($n = 3$) expressed as mean \pm standard deviation.

Human Specimen	total PSA determined by LC-MS/MS [ng/mL]	core-fucosylated PSA determined by LC-MS/MS [ng/mL]	ratio of core-fucosylated PSA to total PSA determined by LC-MS/MS [%]	total PSA determined by ECLIA [ng/mL]
Patient A	1.93 \pm 0.32	1.90 \pm 0.43	100.7 \pm 10.5	2.03
Patient B	6.43 \pm 0.36	4.75 \pm 0.81	73.6 \pm 9.4	6.06
Patient C	10.95 \pm 1.43	9.73 \pm 2.66	88.4 \pm 19.0	9.95

4. Conclusions

In this chapter, a sensitive endoglycosidase-assisted LC-MS/MS assay based on immunoaffinity enrichment using magnet beads, consecutive two-step on bead partial deglycosylation and tryptic digestion followed by LC-MS/MS analysis was developed allowing for the multiplex quantification of core-fucosylated PSA down to 1 ng/mL and total PSA lower than 0.5 ng/mL in human serum. The method was shown to be linear from 0.5 to 60 ng/mL total PSA, clearly covering the critical grey area in PCa diagnosis. The imprecision of the method ranged from 9.7 % to 23.2 % for core-fucosylated PSA and 10.3 % to 18.3 % for total PSA depending on the PSA level, which is acceptable for the intended use in a biomarker refinement study. To meet the critical requirements as mass spectrometric application in the clinical routine, the imprecision of the method would have to be optimized as CV values are still too high. This could be achieved by internal standardization. As stable-isotope labeled (SIL) forms of PSA are at present commercially not available, the preparation of such standards could be a future task for the scientific community [108].

The feasibility of the method to detect core-fucosylated and total PSA in native samples was shown using three human specimens with low ng/mL total PSA concentrations. As there is little information about how large serum levels of core-fucosylated PSA differ in prostate cancer compared to benign conditions, the described method could be used in comprehensive patient cohorts to study the potential value of core-fucosylated PSA as a biomarker for discrimination between BPH and PCa or for identification of high aggressive PCa in the critical grey area ranging from 4 to 10 ng/mL. Moreover, by exchanging the total PSA antibody employed in this study, core-fucosylation analysis of free PSA is also feasible using a specific antibody against free PSA. As specific and sensitive methods for the simultaneous quantification of low-concentrated glycoproteins and its core-fucosylated subpopulations are rare, the described strategy could also be used for the analysis of other low-concentrated glycoproteins in human serum to monitor their potential changes in site-specific core-fucosylation in different diseases [108].

Chapter IV

A case study: Is core-fucosylated prostate-specific antigen (PSA) a refined biomarker for differentiation of benign prostate hyperplasia (BPH) and prostate cancer of different aggressiveness?

Chapter IV: A case study: Is core-fucosylated prostate-specific antigen (PSA) a refined biomarker for differentiation of benign prostate hyperplasia (BPH) and prostate cancer of different aggressiveness?

1. Introduction

Prostate cancer (PCa) is the second most frequently diagnosed cancer and the fifth leading cause of cancer death in men, representing a major public health concern worldwide. In 2012, globally 1.1 million estimated new cases were reported and approximately 307,500 men died from PCa [123]. These counts are expected to increase to nearly 1.7 million new PCa cases and 500,000 deaths until 2030 [124]. Incidence rates of PCa vary by more than 25-fold worldwide, in which approximately 75 % of the registered cases occur in developed countries, largely due to the broad use of prostate-specific antigen (PSA) testing and subsequent biopsy in those regions. [125] The risk to develop PCa increases with advanced age, black race, familial predisposition and certain genetic changes [125].

First indications of PCa can be obtained by digital rectal examination (DRE) and screening of PSA serum levels. The increase of total PSA representing abnormalities in prostate gland structure and vascularization has been associated with PCa since the mid-1980s [126]. Today, PSA serum levels are known to be elevated as well in situations including benign prostate hyperplasia (BPH), prostatitis or extrinsic manipulations of the prostate e.g. by bicycling or catheterization [127]. As a consequence, PSA testing lacks in specificity and results in an alarming number of false positive readings, especially when PSA values fall within the critical “grey area” ranging from 4 – 10 ng/mL leading to the risk of overdiagnosis and overtreatment with adverse side effects [4]. On the other hand, low non-diagnostic PSA serum concentrations were detected in men with aggressive PCa [128]. Several authors actually proposed to lower the PSA cut-offs to 1.5 or 2.6 – 4 ng/mL to enhance the likelihood for early detection of curable PCa (Early Warning PSA-zone, EWP Zone) [129-131]. Still, there is no clear PSA cut-off with simultaneous high sensitivity and high specificity for differentiation of benign from cancerous conditions nor non-aggressive from aggressive PCa forms [132]. Only aggressive PCa need immediate treatment, while observation might be sufficient for patients with non-aggressive PCa. Thus, new or refined biomarkers detecting clinically significant and aggressive PCa are highly demanded.

In the past, numerous approaches have been proposed in order to tackle the limitations of PSA testing such as using of age-specific PSA cut-offs, normalizing PSA to the prostate volume (PSA density), and monitoring PSA kinetics in serum including PSA velocity (PSAV) and PSA doubling time (PSA-DT) [133-135]. However, only small improvements in predictive value have been found among these efforts. Improvements in the analysis of various molecular forms of PSA in serum have allowed the measurement of free PSA and its distinct cleavage isoforms pro-PSA and BPH-associated PSA

(BPSA) [120, 136, 137]. Other forms include complexed PSA which is bound to serum proteins, mainly to α 1-antichymotrypsin and α 2-macroglobulin [93]. The ratio of free PSA to total PSA (%-free PSA), which was shown by Catalona *et al.* to be decreased in PCa compared to BPH, has been approved by the FDA as an adjunct to total PSA in men with total PSA serum concentrations between 4 and 10 ng/mL [138]. Although, %-free PSA slightly improved the ability to distinguish between PCa and BPH the most appropriate %-free PSA cut-off value remains debatable and the identification of non-aggressive and aggressive PCa is still not feasible. From a medical point of view it means that the final decision in PCa diagnosis still necessitates histopathological verification of adenocarcinoma in prostate cores derived from transrectal ultrasound (TRUS)-guided biopsy or in specimens obtained from transurethral resection of the prostate (TURP) or prostatectomy for benign prostatic enlargement [139]. These techniques are invasive and cause embarrassment or discomfort to patients [124]. An important part of the decision-making process concerning the need for active treatment or surveillance alone is the Gleason score (GS) grading system in which $GS \leq 6$ are regarded as low risk cancer and $GS > 6$ as intermediate/high risk cancer [140]. However, early-stage PCa detection is challenging as the majority of prostatic cancers are slow growing and asymptomatic [141]. Besides GS, the reproducibility of which is not optimal, and PSA testing, a few new prognostic tests are now commercially available for PCa management [142, 143]. An urinary assay for Prostate Cancer Antigen 3 (PCA3), a prostate-specific, non-coding mRNA biomarker obtained after prostatic massage during DRE, appears to be useful for detection in men with elevated PSA but its usefulness for differentiation between non-aggressive and aggressive PCa is uncertain [144, 145]. The Prostate Health Index (PHI) test combines free, total and the (-2)pro-PSA into a single score. The 4Kscore test measures a panel of four kallikreins (free PSA, total PSA, intact PSA and kallikrein-like peptidase 2 [hK2]). Both tests are intended to reduce the number of unnecessary prostate biopsies in PSA tested men and demonstrated to outperform PCa detection by %-free PSA [146, 147]. These examples reveal that new markers in combination with conventional PSA are providing promise to aid in PCa diagnosis.

The focus in the research community has currently been on discovering non-invasive markers derived from proteins, tumor cells or nucleic acids in the blood or urine of patients with prostate cancer [141, 148-152]. Among these targets, glycosylated proteins play an emerging role as it was shown that altered glycosylation patterns can be linked to oncologic malignancies such as breast, liver, colon or prostate cancer [153-156]. PSA also known as human kallikrein 3 (KLK3) is a 28-32 kDa glycoprotein approximately containing 8 % (*m/m*) carbohydrates attached to a single N-glycosylation site at asparagine-69 [3, 157]. Changes in glycosylation of PSA associated with PCa development and progression have been analyzed in several foundational studies focusing on human samples of different origin including prostate tissue, cell lines, seminal fluid, urine and serum [2, 98, 158-160]. These studies span the breadth from whole glycoform profiling to targeted analysis of single glycan modifications such as terminal sialylation or site-specific core-fucosylation [4, 161]. With regard to the evaluation of glycosylation changes of PSA in human serum as prognostic and diagnostic marker for prostate cancer, some of these assays lack in

sensitivity for usage in the critical grey area or have not been tested using statistically significant sample numbers. In summary, currently there is no non-invasive diagnostic tool that can distinguish non-aggressive from aggressive tumors which would be of particular importance as recently shown by Wilt *et al.* after 20 years follow-up for PIVOT (Prostate Cancer Intervention versus Observation Trial) [158, 162]. Among men with localized PCa of different risk, surgery did not demonstrate significantly higher overall or PCa survival than observation, but was associated with higher frequency of adverse side-effects such as urinary incontinence and erectile dysfunction.

The aim of this case study is to assess the potential diagnostic value of core-fucosylated PSA (fuc-PSA) as biomarker for differentiation of BPH and PCa and for identification of aggressive PCa. For this purpose a comprehensive patient cohort was used comprising 150 samples categorized into three groups: (1) BPH, (2) non-aggressive PCa ($GS \leq 6$), and (3) aggressive PCa ($GS > 6$). In order to analyze the above specimens a previously developed endoglycosidase-assisted LC-MS/MS-based strategy was applied for the analysis of fuc-PSA in the low ng/mL range in human serum which is described in chapter III [108].

2. Experimental section

2.1. Reagents and materials

Streptavidin-coated magnetic particles (Ref. 11641786001), biotinylated monoclonal antibody PSA36 against total PSA (= free + complexed PSA) binding to epitope 6b [84], total PSA CalSet II (Ref. 04485220190) and PC TM1 control solution of the PreciControl Tumor Marker set (Ref. 11776452122) were obtained from Roche Diagnostics GmbH (Mannheim, Germany). Phosphate buffered saline (PBS), trypsin from porcine pancreas, tween 20 and ammonium bicarbonate (ABC) were purchased from Sigma-Aldrich (St. Louis, USA). Endoglycosidase F3 (Endo F3) from *Elizabethkingia meningosepticum* was obtained from Ludger Ltd (Oxfordshire, UK). Anhydrous sodium acetate and glacial acetic acid were from Merck (Darmstadt, Germany). Acetonitrile (ACN) and formic acid (FA) both ULC/MS grade were purchased from Biosolve (Dieuze, France).

2.2. Preparation of calibrators and control samples

Calibrator solutions were prepared by using total PSA CalSet II, which contains calibrator 1 and 2 consisting of human PSA in female serum matrix at 0 ng/mL and 60 ng/mL total PSA, respectively. The fucosylation degree of PSA spiked in calibrator 2 was determined to be 78 % by in-house LC-MS N-glycan analysis at Roche Diagnostics GmbH (Penzberg, Germany). Based on the two stock calibrators 1 and 2, five calibrator solutions Cal A, B, C, D and E were prepared at total PSA concentrations of 1, 3, 6, 9 and 12 ng/mL. Taking the fucosylation degree of 78 % into account, the fuc-PSA concentrations of Cal A-E were calculated to 0.78, 2.34, 4.67, 7.02 and 9.36 ng/mL. The PC TM1 control solution of the PreciControl Tumor Marker set served as a control sample during the entire study. Both calibrator solutions and the control sample were aliquoted and stored at -20 °C until analysis.

2.3. Patient samples

Serum samples were obtained from 50 BPH patients and 100 PCa patients provided by the HELIOS Klinikum Berlin-Buch, Charité Berlin, Urologische Klinik and Klinikum Ludwigshafen (all located in Germany), following the standard operating procedures of their Ethics Committee. Informed written consent was obtained from all subjects participating in the study. Total PSA serum levels of all samples were between 2 and 10 ng/mL. Serum samples were collected before any diagnostic procedure was started and stored at -80 °C until analysis. Repeated freezing and thawing was avoided. PCa diagnosis was verified using transrectal ultrasound-guided biopsy and/or adenomectomy/radical prostatectomy followed by histopathological analysis.

BPH patients (age range 47-80 years) had total PSA serum levels ranging from 2.03-9.13 ng/mL (average of 5.12 ng/mL) and free PSA serum levels ranging from 0.18-2.52 ng/mL (average of 1.03 ng/mL) (Table 17). PCa patients were classified according to the Gleason score (GS) grading system following the general guidelines of the European Association of Urology. GS were used from pathological examination or if not available from biopsy. Patients with $GS \leq 6$ were assigned to the

non-aggressive PCa group and patients with GS > 6 were assigned to the aggressive PCa group as reported previously [163]. Hence, out of the 100 PCa patients, 50 patients (age range 49-78) were classified as non-aggressive PCa with total PSA serum levels ranging from 2.49-9.95 ng/mL (average of 5.82 ng/mL) and free PSA serum levels ranging from 0.28-1.86 ng/mL (average of 0.80 ng/mL) and 50 patients (age range 52-75) were classified as aggressive PCa with total PSA serum levels ranging from 2.90-9.92 ng/mL (average of 5.86 ng/mL) and free PSA serum levels ranging from 0.21-1.95 ng/mL (average of 0.76 ng/mL). In 9 patients of the non-aggressive PCa group (n = 50) and in 6 patients of the aggressive PCa group (n = 50) cell patterns associated with both BPH and PCa were observed in tissue samples derived from different regions of the prostate.

2.4. Quantification of total and free PSA by ECLIA

Total and free PSA levels of patient samples, calibrator solutions and the control sample were measured using commercially available Elecsys® total PSA electrochemiluminescence immunoassay (ECLIA) on the **cobas e 601** analyzer at Roche Diagnostics GmbH (Penzberg, Germany) as described previously [59].

2.5. LC-MS/MS-based analysis of total PSA and core-fucosylated PSA

The method used for quantification of total PSA and its core-fucosylated subpopulation applying immunoaffinity enrichment, two enzymatic steps and LC-MS/MS analysis is described in detail in the previous chapter and a related manuscript [108]. Briefly, biotinylated anti-PSA antibody PSA36 was bound to streptavidin-coated magnetic particles. Afterwards, 100 µL serum sample were added to the antibody-bound magnetic particles to enrich total PSA from the complex serum matrix. By means of a magnet separator (DynaMag™-2 Magnet), the supernatant was removed and magnetic particles were washed to remove unspecific bound serum contaminants. Enriched PSA, still captured by the immunoaffinity complex, was partially deglycosylated using Endo F3 in order to simplify glycosylation complexity followed by tryptic digestion to generate surrogate peptides. The supernatant was transferred to a new vial, dried in a vacuum concentrator (Eppendorf concentrator 5301) and re-dissolved for LC-MS/MS analysis. Finally, total PSA and fuc-PSA were analyzed by measuring peptide LSEPAELTDAVK and glycopeptide N(GlcNAc+Fuc)K, respectively, using an Infinity 1290 UHPLC from Agilent Technologies (Santa Clara, USA) connected to a QTRAP 6500 MS instrument equipped with TurboV™ Ion Source from AB Sciex (Darmstadt, Germany).

Table 1: Clinical and pathological characteristics of 150 patient samples.

Pathology	Cases	N (all GS)	GS	N	Age average	±SD	Range	tPSA [ng/ml]	±SD	Range	fPSA [ng/ml]	±SD	Range
BPH		50		50	66.6	7.88	47-80	5.12	1.88	2.03-9.13	1.03	0.56	0.18-2.52
PCa	non-aggressive	41	5	4	66.8	5.38	60-72	5.98	2.60	3.87-9.53	1.02	0.56	0.53-1.66
			6	37	63.0	7.71	49-78	5.54	1.67	2.49-9.95	0.73	0.34	0.28-1.86
			7	15	64.1	7.91	52-75	6.00	1.70	3.44-9.65	0.84	0.40	0.40-1.95
	aggressive	44	8	14	64.8	5.31	53-72	6.13	2.37	3.17-9.92	0.77	0.35	0.21-1.38
			9	13	66.3	5.42	55-73	5.90	1.73	3.83-9.00	0.71	0.28	0.42-1.33
PCa+BPH	non-aggressive	9	10	2	70.0	5.66	66-74	6.21	3.90	3.45-8.97	0.50	0.12	0.42-0.59
			6	9	65.4	6.84	55-75	6.25	2.19	3.46-9.34	0.92	0.23	0.48-1.22
			7	2	58.0	5.66	54-62	3.78	1.25	2.90-4.66	0.58	0.08	0.52-0.64
	aggressive	6	8	2	67.5	6.36	63-72	5.59	0.78	5.03-6.14	0.84	0.77	0.29-1.38
			9	2	68.5	6.36	64-73	4.70	1.85	3.39-6.01	0.78	0.42	0.48-1.07

BPH: Benign prostate hyperplasia

PCa: Prostate cancer

GS: Gleason score (used from pathology, if not available from biopsy)

SD: Standard deviation

tPSA: total PSA serum level

fPSA: free PSA serum level

2.6. Study design

In this study, up to 36 samples were analyzed per day, including calibrator solutions, control samples and patient samples. On each of the 19 study days samples were measured in the following sequence order: two blanks (acetonitrile containing 0.1 % FA), sample for system suitability pre-test (neat PSA-derived peptide solution), blank, calibrator solutions Cal A-D, control sample, patient samples, calibrator solutions Cal A-D, control sample, blank, sample for system suitability post-test, two blanks. Three replicates of each patient sample were randomly distributed on the 19 study days and individually analyzed. In total, 678 single measurements consisting of 190 calibrator solutions, 38 control samples and 450 patient samples were performed.

2.7. Data analysis and statistics

Total PSA and fuc-PSA were analyzed by peak integration of their respective surrogate peptides LSEPAELTDAVK and N(GlcNAc+Fuc)K using Analyst software (Version 1.6.2, AB Sciex). Automatic peak integration was performed by the IntelliQuant integration algorithm. Peaks were integrated manually, if peak assignment was incorrect or peak integration was inadequate. Using calibrator solutions Cal A-E, calibration curves for total PSA and fuc-PSA were generated by plotting peak areas of their respective surrogate peptides LSEPAELTDAVK and N(GlcNAc+Fuc)K (y) against respective analyte concentrations (x). As described before, on each study day one set of calibrator solutions Cal A-E was analyzed at the beginning and one set at the end of a LC-MS/MS sequence (calibrator bracketing) giving two calibration curves for total PSA and two for fuc-PSA. Both calibrator sets were taken together, resulting in average calibration curves for total and fuc-PSA, which were used for calculation of total and fuc-PSA concentrations of patient samples and control samples. Method comparison using total PSA serum levels measured by LC-MS/MS and ECLIA was performed by Deming Regression using software JMP 12.1.0. The %-core-fucosylated PSA of each patient was calculated as the median of fuc-PSA serum levels divided by the median of total PSA serum levels obtained from three LC-MS/MS replicates (%-fuc-PSA-MS). The median of fuc-PSA serum levels obtained by LC-MS/MS analysis was also standardized to total PSA serum levels measured by ECLIA (%-fuc-PSA-ECLIA). Patients were divided into three groups: (1) BPH, (2) non-aggressive PCa, and (3) aggressive PCa. Receiver operating characteristic (ROC) curves and box plot diagrams were prepared using the free software R 3.2.2 available at <https://www.R-project.org> in order to evaluate the diagnostic value of fuc-PSA for differentiation of PCa patients from participants with BPH. ROC curves were also used to investigate the diagnostic value of fuc-PSA with regards to the aggressiveness of PCa according to the GS which were used as the boundary between non-aggressive ($GS \leq 6$) and aggressive PCa ($GS > 6$). Standardized (%-fuc- PSA) and non-standardized core-fucosylated PSA (fuc-PSA) were compared to free PSA, total PSA and %-free PSA (= free PSA standardized to total PSA). Differences in clinical groups were tested using the Wilcoxon rank sum test. Confidence levels for the area under the ROC curve were calculated by the DeLong method [164].

3. Results

A previously described LC-MS/MS-based method was applied on a patient cohort consisting of 150 specimens in order to evaluate the potential value of core-fucosylated PSA (fuc-PSA) as biomarker for discrimination between BPH and PCa or for identification of aggressive PCa in the low ng/mL concentration range. Total PSA serum levels of patient samples ranged from 2-10 ng/mL clearly covering the critical grey area in PCa diagnosis. Each patient sample was measured in triplicate resulting in average coefficients of variation (CV) of 13.9 % for fuc-PSA and 8.7 % for total PSA. CV values > 20 % were observed in 21 out of 150 patient samples for fuc-PSA and in 7 out of 150 patient samples for total PSA. The median of fuc-PSA and total PSA were used for data analysis which showed good robustness to outliers.

As mentioned before, all LC-MS/MS measurements were monitored by a control sample which was analyzed in duplicate on each of the 19 study days. The average fuc-PSA concentration over all study days was 3.41 ng/mL with a CV value of 11.4 % and the average total PSA concentration was 4.77 ng/mL with a CV value of 7.0 %. The measured total PSA concentration was in excellent accordance with results previously determined by ECLIA giving a total PSA concentration of 4.72 ng/mL. The average %-fuc-PSA-MS was 71.4 % with a CV value of 9.8 %. Comparison of total PSA concentrations of 150 patient samples measured by LC-MS/MS and ECLIA performing a Bland-Altman analysis showed a good agreement between the two methods with a mean bias of 1.9 % and a 2S agreement range of ± 16.1 % (Figure 44). Method comparison using the Deming Regression procedure assuming equal error variances resulted in a regression equation of $y = 0.88x + 0.52$. The Spearman's rank correlation coefficient ρ was 0.98 (Figure 45). As shown in control charts of fuc-PSA, total PSA and %-fuc-PSA-MS, no specific trends could be observed within the 19 study days (Figure 46).

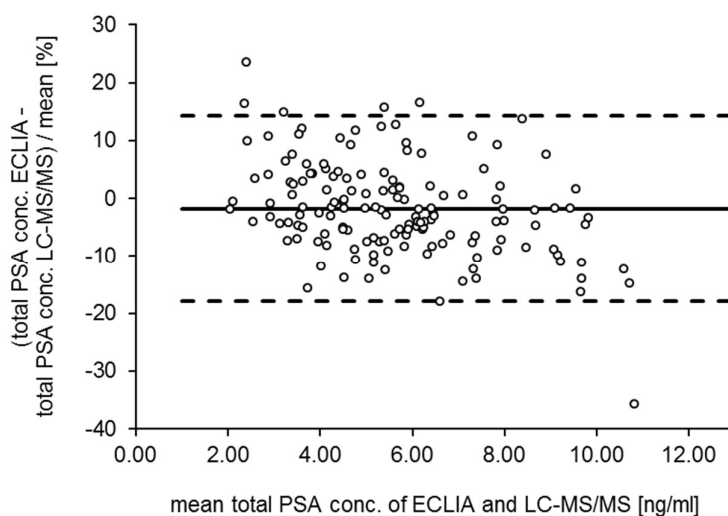


Figure 44: Relative Bland Altman plot for the comparison of total PSA serum concentrations of 150 patients measured by ECLIA and LC-MS/MS. The comparison of results showed a good agreement between the two methods with a mean bias of - 1.9 % and a 2S agreement range of ± 16.1 %.

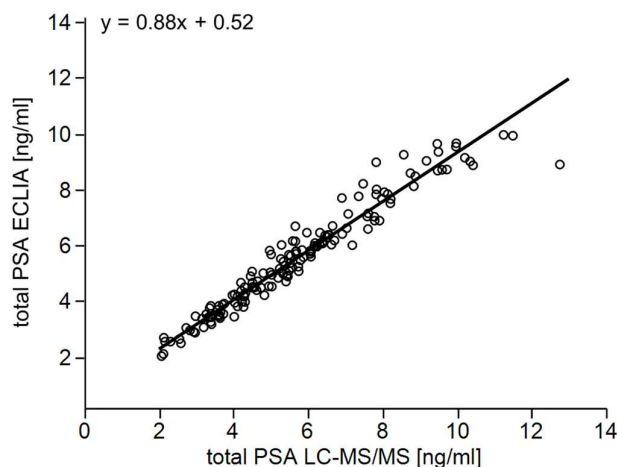


Figure 45: Method comparison using Deming Regression assuming equal error variances obtained by quantitative ECLIA and LC-MS/MS analysis of total PSA serum concentrations of 150 patient samples. The Spearman's rank correlation coefficient ρ was 0.98.

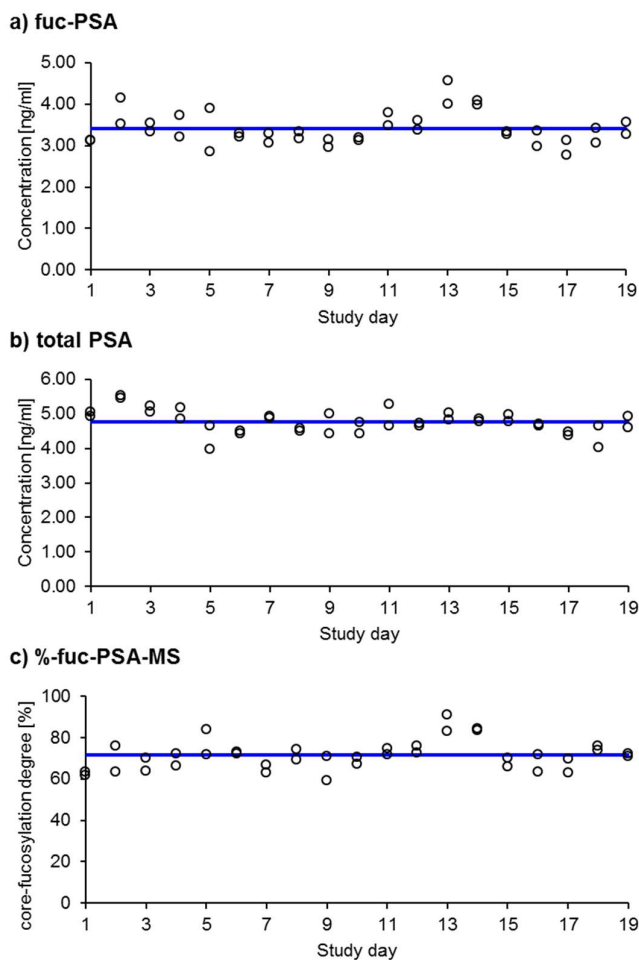


Figure 46: Control charts of serum levels of a) core-fucosylated PSA (fuc-PSA), b) total PSA and c) %core-fucosylated PSA standardized by total PSA from LC-MS/MS (%fuc-PSA-MS) obtained by repetitive analysis of a control sample at 19 study days. Blue line = mean.

ROC curve analysis was performed using all 150 patient samples in order to investigate the diagnostic value of fuc-PSA for differentiation of BPH ($n = 50$) from PCa ($n = 100$) (Figure 47, Table 18). Initially, ROC curve analysis was performed using several serum parameters including non-standardized fuc-PSA (AUC = 0.58) and standardized %-fuc-PSA-MS (AUC = 0.54) or %-fuc-PSA-ECLIA (AUC = 0.51). These results were compared to the AUC values of free PSA (AUC = 0.63), total PSA (AUC = 0.60) and %-free PSA (AUC = 0.74) measured by ECLIA and revealed that both non-standardized and standardized fuc-PSA had no diagnostic value for differentiation of BPH from PCa compared to conventional diagnostic PCa markers. ROC curves were also used to investigate the predictive power of fuc-PSA in the identification of aggressive PCa (Table 19). The GS was used as a cut-off point between non-aggressive PCa ($GS \leq 6$) and aggressive PCa ($GS > 6$). Results from serum samples of 100 patients diagnosed with PCa showed a slight diagnostic value for %-fuc-PSA-MS (AUC = 0.57) and a more meaningful value for %-fuc-PSA-ECLIA (AUC = 0.60). The AUC values of non-standardized fuc-PSA (AUC = 0.53), free PSA (AUC = 0.52), total PSA (AUC = 0.52) and %-free PSA (AUC = 0.55) were slightly inferior to AUC values obtained by using %-fuc-PSA (Figure 47). As shown in Figure 48, the aggressive PCa group showed decreased %-fuc-PSA values (Q1-Q3: 71-84 %) than non-aggressive PCa patients (Q1-Q3: 74-90 %). The PSA core-fucosylation ratio did not correlate with their total PSA levels and was therefore independent of the total PSA level in each of the patient groups (Figure 49).

Table 18: AUC values obtained by ROC curve analysis of 50 BPH and 100 PCa patients.

Acronym	Biomarker (platform)	Standard (platform)	AUC (95%-CI)
fuc-PSA	core-fucosylated PSA (MS)	none	0.58 (0.48-0.68)
%-fuc-PSA-MS	core-fucosylated PSA (MS)	total PSA (MS)	0.54 (0.43-0.64)
%-fuc-PSA-ECLIA	core-fucosylated PSA (MS)	total PSA (ECLIA)	0.51 (0.41-0.62)
free PSA	free PSA (ECLIA)	none	0.63 (0.53-0.73)
total PSA	total PSA (ECLIA)	none	0.60 (0.50-0.70)
%-free PSA	free PSA (ECLIA)	total PSA (ECLIA)	0.74 (0.65-0.83)

CI: Confidence intervals

Table 19: AUC values obtained by ROC curve analysis of 50 non-aggressive PCa ($GS \leq 6$) and 50 aggressive PCa ($GS > 6$) patients.

Acronym	Biomarker (platform)	Standard (platform)	AUC (95%-CI)
fuc-PSA	core-fucosylated PSA (MS)	none	0.53 (0.42-0.65)
%-fuc-PSA-MS	core-fucosylated PSA (MS)	total PSA (MS)	0.57 (0.45-0.68)
%-fuc-PSA-ECLIA	core-fucosylated PSA (MS)	total PSA (ECLIA)	0.60 (0.49-0.71)
free PSA	free PSA (ECLIA)	none	0.52 (0.41-0.64)
total PSA	total PSA (ECLIA)	none	0.52 (0.40-0.63)
%-free PSA	free PSA (ECLIA)	total PSA (ECLIA)	0.55 (0.43-0.66)

CI: Confidence intervals

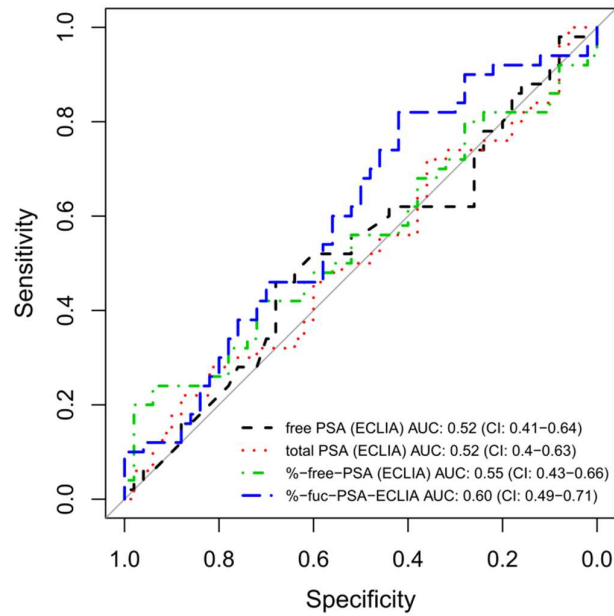


Figure 47: Comparison of ROC curves for free PSA, total PSA, %free-PSA, %core-fucosylated PSA standardized to total PSA determined by ECLIA (%fuc-PSA-ECLIA). The %fuc-PSA-ECLIA gave the highest AUC value (AUC = 0.60) for differentiation of non-aggressive (GS ≤ 6) and aggressive PCa (GS > 6).

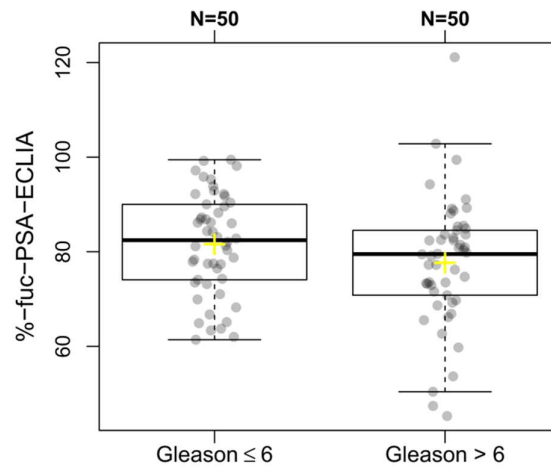


Figure 48: Box-plot of %core-fucosylated PSA standardized by total PSA from ECLIA (%fuc-PSA-ECLIA) used for differentiation of non-aggressive (GS ≤ 6) and aggressive PCa (GS > 6). The center line represents the median. The bottom (Q1) and the top (Q3) of the box represent the 25th and 75th percentiles, respectively.

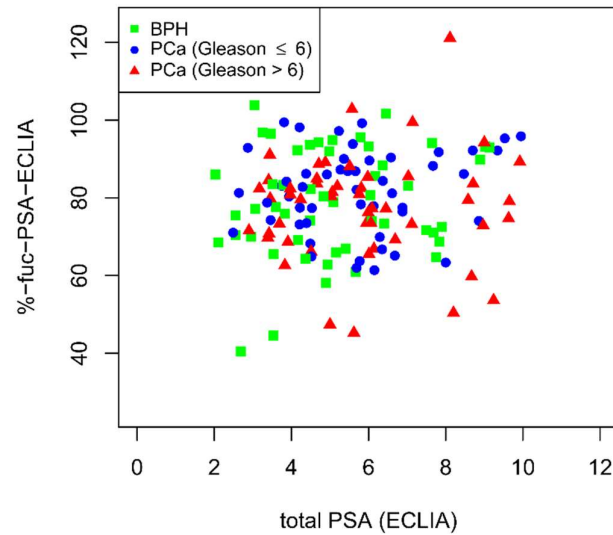


Figure 49: Scatter plot of %-core-fucosylated PSA standardized by total PSA from ECLIA (%-fuc-PSA-ECLIA) against total PSA serum levels measured by ECLIA (n = 150). The PSA core-fucosylation ratio did not correlate with their total PSA levels in none of the patient groups (BPH, non-aggressive PCa and aggressive PCa).

4. Discussion

In a cohort of 150 patient samples, measurement of fuc-PSA showed a slightly improved diagnostic differentiation between aggressive and non-aggressive PCa in comparison to standard free- and total PSA tests. Several studies, mostly based on enzyme-linked lectin assays (ELLA), have been applied to assess whether differences in terminal or core-fucosylation of PSA either in urine, seminal fluid, blood or tissue enable discrimination of BPH from PCa or identification of aggressive PCa [93, 99, 160, 165]. These lectin immunoassays have the same basic format as a standard enzyme-linked immunosorbent assay (ELISA), in which one antibody is replaced by a lectin recognizing carbohydrate moieties. However, reports with contradictory results have been described which might be due to the use of different sample matrices or different lectins (Table 20). For example, a significant decrease of core-fucosylated PSA with an AUC = 0.94 was recently reported by Llop *et al.* in GS > 6 PCa serum samples using *Pholiota squarrosa lectin* (PhoSL), while Li *et al.* found an increase in PSA core-fucosylation in serum of high-risk PCa patients with an AUC = 0.86 using *Aleuria aurantia lectin* (AAL) [4, 163].

In order to expand the field, the present work describes an LC-MS/MS-based study for evaluation of site-specific core-fucosylation changes of PSA in human sera derived from patients diagnosed with BPH and PCa of different degrees of aggressiveness. Total PSA serum concentrations of patient samples ranged from 2-10 ng/mL and thus, did not exceed the critical grey area of PCa diagnosis. In former lectin-based studies, patient samples with higher serum concentrations (up to 110 ng/mL) or urine samples with very high total PSA levels by nature ($\mu\text{g/mL}$ range) were analyzed [4, 160, 165]. This is largely because of the lack in sensitivity of these assays as lectins possess 100-10,000-fold lower binding affinities than antibodies [166]. In addition, low specificity of lectins towards glycan structures and their unspecific binding to glycoproteins from human matrix is an inherent problem of lectins resulting in high background signals obscuring the analyte signal of interest and worsening the limit of detection. Considering the low amount of core-fucosylated PSA in the critical grey area compared to the immense amount of other glycoproteins in blood, analysis of serum or plasma samples by lectin-based assays is challenging. In this study, these limitations could be tackled by combining the sensitivity of immunoassays with the specificity of mass spectrometric detection [108]. Patient samples ($n = 150$) used in this study were equally distributed into three groups (1) BPH, (2) non-aggressive PCa ($\text{GS} \leq 6$), and (3) aggressive PCa ($\text{GS} > 6$) in which classification was performed according to the GS as reported previously [163]. Method comparison showed a good agreement between total PSA levels obtained by LC-MS/MS and ECLIA with approximately 10 % bias which seems to be correctable by proper calibration. The %-core-fucosylated PSA variation (%-fuc-PSA-MS) in a control sample monitored over all 19 study days was lower than 10 % indicating the feasibility of the applied method for measuring fuc-PSA in the critical grey area.

Table 20: Overview of previous case studies on terminal and core-fucosylated PSA in different sample matrices using ELLA-type approaches.

First author [Reference]	Target	Sample matrix	Lectin used in ELLA	Number of cases (total serum PSA in ng/mL)	Fucosylation degree of PSA in PCa
Llop <i>et al.</i> [4]	core- fucosylated PSA	serum	PhoSL	BPH: 20 (7.8-18.2) PCa (GS 7-10): 20 (8.7-109.7)	decreased (AUC=0.94, Sens. 90 %, Spec. 95 %)
Barrabés <i>et al.</i> [160]	core- fucosylated PSA	urine	PhoSL	benign: 18 (1.4-9.2) PCa: 35 (2.3-1400)	no significant differences
Kekki <i>et al.</i> [165]	core- fucosylated PSA	urine	AAL	BPH: 15 (n/a) PCa: 16 (n/a)	increased (p=0.030)
Li <i>et al.</i> [163]	core- fucosylated PSA	serum	AAL	PCa (GS 6-9): 47 (1.9-54.5)	increased in GS > 7 (AUC=0.86) GS > 6 (AUC=0.77)
Dwek <i>et al.</i> [93]	terminal fucosylated PSA	serum	UEA-1	BPH: 13 (1.9-9.1) PCa: 13 (3.4-10.7)	increased (Sens. 92 %, Spec. 69 %)
Fukushima <i>et al.</i> [99]	terminal fucosylated PSA	serum	TJA-II	BPH: 20 (n/a) PCa: 20 (n/a)	increased (p<0.05)

PhoSL: *Pholiota squarossa* lectin (recognizes core $\alpha(1,6)$ -linked fucoses)
 UEA-1: *Ulex europaeus* agglutinin (recognizes terminal $\alpha(1,2)$ -linked fucoses)
 AAL: *Aleuria aurantia* lectin (recognizes core $\alpha(1,6)$ - and $\alpha(1,3)$ -linked fucoses)
 TJA-II: *Trichosanthes japonica* agglutinin-II (recognizes terminal $\alpha(1,2)$ -linked fucoses and β -N-acetylglucosamine residues)
 GS: Gleason score
 n/a: not applicable

The diagnostic power of fuc-PSA was assessed by ROC curve analysis and revealed two major findings. First, fuc-PSA (AUC = 0.58), %fuc-PSA-MS (AUC = 0.54), and %fuc-PSA-ECLIA (AUC = 0.51) had no diagnostic value for differentiation of BPH from PCa compared to conventional diagnostic PCa markers in which %free PSA gave the highest AUC value (AUC = 0.74). Decreased %free PSA serum levels in PCa compared to BPH patients have been also reported in a comprehensive study including 773 men [138]. Second, the highest AUC for differentiation of non-aggressive and aggressive PCa was obtained using %fuc-PSA standardized by total PSA determined by ECLIA (%fuc-PSA-ECLIA, AUC = 0.60) which was slightly better than standardization to total PSA obtained by LC-MS/MS (%fuc-PSA-MS, AUC = 0.57). This could probably be due to the higher imprecision of the LC-MS/MS method compared to the routinely used ECLIA workflow. Both

%-fuc-PSA values performed better than conventional markers such as free, total and %-free PSA (all $AUC \leq 0.55$). The %-fuc-PSA-ECLIA was found to be slightly decreased in the aggressive PCa group which is in agreement with reported results from serum, seminal fluid and urine [3, 4, 167, 168]. However, the obtained results were not as powerful as stated in previous studies which might be for different reasons. First, a subset of patient samples was used in this study which might possess only small differences in core-fucosylation degree of serum PSA. These changes would not be detectable by the method applied in this study. At present, there is little information about how pronounced differences in native serum samples actually are. Second, in previous studies patient samples with higher total PSA serum levels ranging from 8 to 110 ng/mL or 2 to 55 ng/mL were analyzed and total PSA values alone already identified high-risk PCa with AUC values of 0.89 or 0.81, respectively [4, 163]. Finally, selected patient panels in those studies were rather small (40 and 47 samples), which why larger scale studies might be necessary to further validate these findings. Although, it was the first time such a high number of patient samples ($n = 150$) was used for studying site-specific core-fucosylation changes of serum PSA, increasing number of patient samples could help to consolidate the obtained results as well. As shown in this and previous studies, a single biomarker (e.g. core-fucosylated PSA alone) might only unlikely possess diagnostic strength to indicate the likelihood of aggressive PCa. On the other hand, a combination of several complimentary biomarkers (e.g. ratio of core-fucosylated PSA to total PSA) may have potential for improvement of both clinical sensitivity and specificity.

5. Conclusions

In summary, a previously developed endoglycosidase-assisted LC-MS/MS-based approach was used to analyze serum core-fucosylated PSA from BPH and PCa patients of different degrees of aggressiveness ($n = 150$). The data revealed that %-fuc-PSA standardized to total PSA was slightly decreased in GS > 6 patient samples representing aggressive PCa and had better diagnostic power than conventional total PSA. However, on the basis of these findings it is still uncertain if %-fuc-PSA could be used clinically to improve and facilitate the differentiation of non-aggressive from aggressive tumors. Further validation in larger patient cohorts or the usage of improved methods regarding assay imprecision will be required to confirm obtained results of this study.

Chapter V

References

Chapter V: References

- [1] CR Bertozzi, LL Kiessling, Chemical glycobiology, Science 291 (2001) 2357-2364.
- [2] R Peracaula, G Tabares, L Royle, DJ Harvey, RA Dwek, PM Rudd, R de Llorens, Altered glycosylation pattern allows the distinction between prostate-specific antigen (PSA) from normal and tumor origins, Glycobiology 13 (2003) 457-470.
- [3] G Tabares, CM Radcliffe, S Barrabes, M Ramirez, RN Aleixandre, W Hoesel, RA Dwek, PM Rudd, R Peracaula, R de Llorens, Different glycan structures in prostate-specific antigen from prostate cancer sera in relation to seminal plasma PSA, Glycobiology 16 (2006) 132-145.
- [4] E Llop, M Ferrer-Batalle, S Barrabes, PE Guerrero, M Ramirez, R Saldo, PM Rudd, RN Aleixandre, J Comet, R de Llorens, R Peracaula, Improvement of prostate cancer diagnosis by detecting PSA glycosylation-specific changes, Theranostics 6 (2016) 1190-1204.
- [5] H Yu, J Reiser, U Besenfelder, E Razzazi-Fazeli, J Bergquist, G Brem, K Artemenko, C Mayrhofer, Exploring the oviductal fluid proteome by a lectin-based affinity approach, Proteomics 16 (2016) 2962-2966.
- [6] JB Vaught, MK Henderson, Biological sample collection, processing, storage and information management, IARC Sci Publ (2011) 23-42.
- [7] G Dimeski, RJ Barnett, Effects of total plasma protein concentration on plasma sodium, potassium and chloride measurements by an indirect ion selective electrode measuring system, Crit Care Resusc 7 (2005) 12-15.
- [8] NL Anderson, NG Anderson, The human plasma proteome: history, character, and diagnostic prospects, Mol Cell Proteomics 1 (2002) 845-867.
- [9] J Fandrey, B Walzog, Zusammensetzung und Volumen des Blutes. In: HC Pape, A Kurtz, S Silbernagl et al., Physiologie, 7. vollständig überarbeitete und erweiterte Auflage, Thieme, 2014.
- [10] RA Bowen, AT Remaley, Interferences from blood collection tube components on clinical chemistry assays, Biochem Med (Zagreb) 24 (2014) 31-44.
- [11] AJ Rai, CA Gelfand, BC Haywood, DJ Warunek, J Yi, MD Schuchard, RJ Mehig, SL Cockrill, GB Scott, H Tammen, P Schulz-Knappe, DW Speicher, F Vitzthum, BB Haab, G Siest, DW Chan, HUPO plasma proteome project specimen collection and handling: towards the standardization of parameters for plasma proteome samples, Proteomics 5 (2005) 3262-3277.
- [12] P Roepstorff, J Fohlman, Proposal for a common nomenclature for sequence ions in mass spectra of peptides, Biomed Mass Spectrom 11 (1984) 601.
- [13] No authors listed, IUPAC-IUB joint commission on biochemical nomenclature (JCBN). Nomenclature and symbolism for amino acids and peptides. Recommendations 1983, Eur J Biochem 138 (1984) 9-37.
- [14] JM Berg, JL Tymoczko, L Stryer, Stryer Biochemie, 7. Auflage, Springer-Verlag, 2013.
- [15] P Stanley, H Schachter, N Taniguchi, Chapter 8: N-Glycans. In: A Varki, RD Cummings, JD Esko et al., Essentials of Glycobiology, 2nd edition, Cold Spring Harbor (NY): Cold Spring Harbor Laboratory Press, 2009.
- [16] DD Pless, WJ Lennarz, Enzymatic conversion of proteins to glycoproteins, Proc Natl Acad Sci USA 74 (1977) 134-138.

- [17] H Geyer, R Geyer, Strategies for analysis of glycoprotein glycosylation, *Biochim Biophys Acta* 1764 (2006) 1853-1869.
- [18] RD Cummings, Use of lectins in analysis of glycoconjugates, *Methods Enzymol* 230 (1994) 66-86.
- [19] K Kakehi, M Kinoshita, D Kawakami, J Tanaka, K Sei, K Endo, Y Oda, M Iwaki, T Masuko, Capillary electrophoresis of sialic acid-containing glycoprotein. Effect of the heterogeneity of carbohydrate chains on glycoform separation using an alpha1-acid glycoprotein as a model, *Anal Chem* 73 (2001) 2640-2647.
- [20] SF Wheeler, PM Rudd, SJ Davis, RA Dwek, DJ Harvey, Comparison of the N-linked glycans from soluble and GPI-anchored CD59 expressed in CHO cells, *Glycobiology* 12 (2002) 261-271.
- [21] YC Lee, M Srajer Gajdosik, D Josic, SH Lin, Plasma membrane isolation using immobilized concanavalin A magnetic beads, *Methods Mol Biol* 909 (2012) 29-41.
- [22] BP Rempel, HC Winter, IJ Goldstein, O Hindsgaul, Characterization of the recognition of blood group B trisaccharide derivatives by the lectin from *Marasmius oreades* using frontal affinity chromatography-mass spectrometry, *Glycoconj J* 19 (2002) 175-180.
- [23] JM Burkhardt, C Schumbrutzki, S Wortelkamp, A Sickmann, RP Zahedi, Systematic and quantitative comparison of digest efficiency and specificity reveals the impact of trypsin quality on MS-based proteomics, *J Proteomics* 75 (2012) 1454-1462.
- [24] DL Crimmins, SM Mische, ND Denslow, Chemical cleavage of proteins in solution, *Curr Protoc Protein Sci* 41 (2005) 11.4.1-11.4.11.
- [25] E Song, S Pyreddy, Y Mechref, Quantification of glycopeptides by multiple reaction monitoring liquid chromatography/tandem mass spectrometry, *Rapid Commun Mass Spectrom* 26 (2012) 1941-1954.
- [26] L Xiong, FE Regnier, Use of a lectin affinity selector in the search for unusual glycosylation in proteomics, *J Chromatogr B Analyt Technol Biomed Life Sci* 782 (2002) 405-418.
- [27] H Kaji, H Saito, Y Yamauchi, T Shinkawa, M Taoka, J Hirabayashi, K Kasai, N Takahashi, T Isobe, Lectin affinity capture, isotope-coded tagging and mass spectrometry to identify N-linked glycoproteins, *Nat Biotechnol* 21 (2003) 667-672.
- [28] M Tajiri, S Yoshida, Y Wada, Differential analysis of site-specific glycans on plasma and cellular fibronectins: application of a hydrophilic affinity method for glycopeptide enrichment, *Glycobiology* 15 (2005) 1332-1340.
- [29] G Alvarez-Manilla, J Atwood, 3rd, Y Guo, NL Warren, R Orlando, M Pierce, Tools for glycoproteomic analysis: size exclusion chromatography facilitates identification of tryptic glycopeptides with N-linked glycosylation sites, *J Proteome Res* 5 (2006) 701-708.
- [30] H Zhang, XJ Li, DB Martin, R Aebersold, Identification and quantification of N-linked glycoproteins using hydrazide chemistry, stable isotope labeling and mass spectrometry, *Nat Biotechnol* 21 (2003) 660-666.
- [31] M Wuhrer, H Geyer, M von der Ohe, R Gerardy-Schahn, M Schachner, R Geyer, Localization of defined carbohydrate epitopes in bovine polysialylated NCAM, *Biochimie* 85 (2003) 207-218.
- [32] A Harazono, N Kawasaki, S Itoh, N Hashii, A Ishii-Watabe, T Kawanishi, T Hayakawa, Site-specific N-glycosylation analysis of human plasma ceruloplasmin using liquid chromatography with electrospray ionization tandem mass spectrometry, *Anal Biochem* 348 (2006) 259-268.

- [33] K Hakansson, HJ Cooper, MR Emmett, CE Costello, AG Marshall, CL Nilsson, Electron capture dissociation and infrared multiphoton dissociation MS/MS of an N-glycosylated tryptic peptic to yield complementary sequence information, *Anal Chem* 73 (2001) 4530-4536.
- [34] JM Hogan, SJ Pitteri, PA Chrisman, SA McLuckey, Complementary structural information from a tryptic N-linked glycopeptide via electron transfer ion/ion reactions and collision-induced dissociation, *J Proteome Res* 4 (2005) 628-632.
- [35] V Tretter, F Altmann, L Marz, Peptide-N4-(N-acetyl-beta-glucosaminyl)asparagine amidase F cannot release glycans with fucose attached alpha 1----3 to the asparagine-linked N-acetylglucosamine residue, *Eur J Biochem* 199 (1991) 647-652.
- [36] RA O'Neill, Enzymatic release of oligosaccharides from glycoproteins for chromatographic and electrophoretic analysis, *J Chromatogr A* 720 (1996) 201-215.
- [37] D Sagi, P Kienz, J Denecke, T Marquardt, J Peter-Katalinic, Glycoproteomics of N-glycosylation by in-gel deglycosylation and matrix-assisted laser desorption/ionisation-time of flight mass spectrometry mapping: application to congenital disorders of glycosylation, *Proteomics* 5 (2005) 2689-2701.
- [38] YJ Kim, A Freas, C Fenselau, Analysis of viral glycoproteins by MALDI-TOF mass spectrometry, *Anal Chem* 73 (2001) 1544-1548.
- [39] H Zhou, S Morley, S Kostel, MR Freeman, V Joshi, D Brewster, RS Lee, Universal solid-phase reversible sample-prep for concurrent proteome and n-glycome characterization, *J Proteome Res* 15 (2016) 891-899.
- [40] J Costa, DA Ashford, M Nimtz, I Bento, C Frazao, CL Esteves, CJ Faro, J Kervinen, E Pires, P Verissimo, A Wlodawer, MA Carrondo, The glycosylation of the aspartic proteinases from barley (*Hordeum vulgare* L.) and cardoon (*Cynara cardunculus* L.), *Eur J Biochem* 243 (1997) 695-700.
- [41] X Liu, DJ McNally, H Nothhaft, CM Szymanski, JR Brisson, J Li, Mass spectrometry-based glycomics strategy for exploring N-linked glycosylation in eukaryotes and bacteria, *Anal Chem* 78 (2006) 6081-6087.
- [42] W Guo, Y Zhang, L Huang, Z Wang, High performance liquid chromatography/electrospray ionization ion-trap mass spectrometry analysis of chitooligosaccharides by pre-column derivatization with 3-amino-9-ethylcarbazole, *Se Pu* 28 (2010) 776-781.
- [43] C Wang, W Fan, P Zhang, Z Wang, L Huang, One-pot nonreductive O-glycan release and labeling with 1-phenyl-3-methyl-5-pyrazolone followed by ESI-MS analysis, *Proteomics* 11 (2011) 4229-4242.
- [44] GC Gil, YG Kim, BG Kim, A relative and absolute quantification of neutral N-linked oligosaccharides using modification with carboxymethyl trimethylammonium hydrazide and matrix-assisted laser desorption/ionization time-of-flight mass spectrometry, *Anal Biochem* 379 (2008) 45-59.
- [45] G Zauner, CA Koeleman, AM Deelder, M Wuhrer, Mass spectrometric O-glycan analysis after combined O-glycan release by beta-elimination and 1-phenyl-3-methyl-5-pyrazolone labeling, *Biochim Biophys Acta* 1820 (2012) 1420-1428.
- [46] Y Lu, C Wang, R Liu, W Jin, Y Wen, L Huang, Z Wang, 3-Amino-1-phenyl-2-pyrazoline-5-ketone as a heterobifunctional chromogenic reagent to derivatize reducing glycans for subsequent online LC/MS analysis, *Anal Biochem* 549 (2018) 1-11.
- [47] SH Walker, AD Taylor, DC Muddiman, Individuality Normalization when Labeling with Isotopic Glycan Hydrazide Tags (INLIGHT): a novel glycan-relative quantification strategy, *J Am Soc Mass Spectrom* 24 (2013) 1376-1384.

- [48] K Songsrirote, Z Li, D Ashford, A Bateman, J Thomas-Oates, Development and application of mass spectrometric methods for the analysis of progranulin N-glycosylation, *J Proteomics* 73 (2010) 1479-1490.
- [49] F Higel, U Demelbauer, A Seidl, W Friess, F Sorgel, Reversed-phase liquid-chromatographic mass spectrometric N-glycan analysis of biopharmaceuticals, *Anal Bioanal Chem* 405 (2013) 2481-2493.
- [50] L Veillon, Y Huang, W Peng, X Dong, BG Cho, Y Mechref, Characterization of isomeric glycan structures by LC-MS/MS, *Electrophoresis* 38 (2017) 2100-2114.
- [51] M Raessler, B Wissuwa, A Breul, W Unger, T Grimm, Determination of water-extractable nonstructural carbohydrates, including inulin, in grass samples with high-performance anion exchange chromatography and pulsed amperometric detection, *J Agric Food Chem* 56 (2008) 7649-7654.
- [52] Z Szabo, JR Thayer, D Reusch, Y Agroskin, R Viner, J Rohrer, SP Patil, M Krawitzky, A Huhmer, N Avdalovic, SH Khan, Y Liu, C Pohl, High performance anion exchange and hydrophilic interaction liquid chromatography approaches for comprehensive mass spectrometry-based characterization of the n-glycome of a recombinant human erythropoietin, 17 (2018) 1559-1574.
- [53] S Kandzia, J Costa, N-glycosylation analysis by HPAEC-PAD and mass spectrometry, *Methods Mol Biol* 1049 (2013) 301-312.
- [54] M Wuhrer, AR de Boer, AM Deelder, Structural glycomics using hydrophilic interaction chromatography (HILIC) with mass spectrometry, *Mass Spectrom Rev* 28 (2009) 192-206.
- [55] C Ashwood, CH Lin, M Thaysen-Andersen, NH Packer, discrimination of isomers of released N- and O-glycans using diagnostic product ions in negative ion PGC-LC-ESI-MS/MS, *J Am Soc Mass Spectrom* (2018) (in press).
- [56] IA Darwish, Immunoassay methods and their applications in pharmaceutical analysis: Basic methodology and recent advances, *Int J Biomed Sci* 2 (2006) 217-235.
- [57] HC Graves, N Wehner, TA Stamey, Ultrasensitive radioimmunoassay of prostate-specific antigen, *Clin Chem* 38 (1992) 735-742.
- [58] S Gofflot, MB El, D Zorzi, L Melen, S Roels, D Quatpers, J Grassi, E Vanopdenbosch, E Heinen, W Zorzi, Immuno-quantitative polymerase chain reaction for detection and quantitation of prion protein, *J Immunoassay Immunochem* 25 (2004) 241-258.
- [59] AW Butch, D Crary, M Yee, Analytical performance of the Roche total and free PSA assays on the Elecsys 2010 immunoanalyzer, *Clin Biochem* 35 (2002) 143-145.
- [60] I Hemmila, Fluoroimmunoassays and immunofluorometric assays, *Clin Chem* 31 (1985) 359-370.
- [61] H Kimura, M Mukaida, G Wang, J Yuan, K Matsumoto, Dual-label time-resolved fluoroimmunoassay of psychopharmaceuticals and stimulants in serum, *Forensic Sci Int* 113 (2000) 345-351.
- [62] A Florentinus-Mefailoski, JG Marshall, Linear quantification of a streptavidin-alkaline phosphatase probe for enzyme-linked immuno mass spectrometric assay, *Anal Biochem* 503 (2016) 50-55.
- [63] S Ramagiri, I Moore, Hybridizing LBA with LC-MS/MS: the new norm for biologics quantification, *Bioanalysis* 8 (2016) 483-486.

- [64] JB Fenn, M Mann, CK Meng, SF Wong, CM Whitehouse, Electrospray ionization for mass spectrometry of large biomolecules, *Science* 246 (1989) 64-71.
- [65] L Dillen, W Cools, L Vereyken, W Lorreyne, T Huybrechts, R de Vries, H Ghobarah, F Cuyckens, Comparison of triple quadrupole and high-resolution TOF-MS for quantification of peptides, *Bioanalysis* 4 (2012) 565-579.
- [66] V Vidova, Z Spacil, A review on mass spectrometry-based quantitative proteomics: Targeted and data independent acquisition, *Anal Chim Acta* 964 (2017) 7-23.
- [67] G Mermelekas, A Vlahou, J Zoidakis, SRM/MRM targeted proteomics as a tool for biomarker validation and absolute quantification in human urine, *Expert Rev Mol Diagn* 15 (2015) 1441-1454.
- [68] AB Sciex website. <https://sciex.com/products/mass-spectrometers/triple-quad-systems/triple-quad-6500-system-x36184> (last accessed on 2nd June 2018).
- [69] P Hernandez, M Muller, RD Appel, Automated protein identification by tandem mass spectrometry: issues and strategies, *Mass Spectrom Rev* 25 (2006) 235-254.
- [70] JR Whiteaker, L Zhao, HY Zhang, LC Feng, BD Piening, L Anderson, AG Paulovich, Antibody-based enrichment of peptides on magnetic beads for mass-spectrometry-based quantification of serum biomarkers, *Anal Biochem* 362 (2007) 44-54.
- [71] H Li, R Popp, CH Borchers, Affinity-mass spectrometric technologies for quantitative proteomics in biological fluids, *Trends Analyt Chem* 90 (2017) 80-88.
- [72] A Florentinus-Mefailoski, JG Marshall, Pyridoxamine-5-phosphate enzyme-linked immune mass spectrometric assay substrate for linear absolute quantification of alkaline phosphatase to the yoctomole range applied to prostate specific antigen, *Anal Chem* 86 (2014) 10684-10691.
- [73] M Merchant, SR Weinberger, Recent advancements in surface-enhanced laser desorption/ionization-time of flight-mass spectrometry, *Electrophoresis* 21 (2000) 1164-1177.
- [74] DR Dufield, OV Nemirovskiy, MG Jennings, MD Tortorella, AM Malfait, WR Mathews, An immunoaffinity liquid chromatography-tandem mass spectrometry assay for detection of endogenous aggrecan fragments in biological fluids: Use as a biomarker for aggrecanase activity and cartilage degradation, *Anal Biochem* 406 (2010) 113-123.
- [75] C Lanshoeft, O Heudi, S Cianferani, AP Warren, F Picard, O Kretz, Quantitative analysis of hIgG1 in monkey serum by LC-MS/MS using mass spectrometric immunoassay, *Bioanalysis* 8 (2016) 1035-1049.
- [76] NG Welch, JA Scoble, BW Muir, PJ Pigram, Orientation and characterization of immobilized antibodies for improved immunoassays (Review), *Biointerphases* 12 (2017) 02d301.
- [77] A Drabik, J Ner-Kluza, A Bodzon-Kulakowska, P Suder, Protocol: MYTHBUSTERS: a universal procedure for sample preparation for mass spectrometry, *Eur J Mass Spectrom* (Chichester) 22 (2016) 269-273.
- [78] JR Whiteaker, L Zhao, L Anderson, AG Paulovich, An automated and multiplexed method for high throughput peptide immunoaffinity enrichment and multiple reaction monitoring mass spectrometry-based quantification of protein biomarkers, *Mol Cell Proteomics* 9 (2010) 184-196.
- [79] D Lin, WE Alborn, RJ Slebos, DC Liebler, Comparison of protein immunoprecipitation-multiple reaction monitoring with ELISA for assay of biomarker candidates in plasma, *J Proteome Res* 12 (2013) 5996-6003.

- [80] PJ Ippoliti, E Kuhn, DR Mani, L Fagbami, H Keshishian, MW Burgess, JD Jaffe, SA Carr, Automated microchromatography enables multiplexing of immunoaffinity enrichment of peptides to greater than 150 for targeted ms-based assays, *Anal Chem* 88 (2016) 7548-7555.
- [81] PR Crocker, T Feizi, Carbohydrate recognition systems: functional triads in cell-cell interactions, *Curr Opin Struct Biol* 6 (1996) 679-691.
- [82] T Feizi, Carbohydrate-mediated recognition systems in innate immunity, *Immunol Rev* 173 (2000) 79-88.
- [83] KW Moremen, M Tiemeyer, AV Nairn, Vertebrate protein glycosylation: diversity, synthesis and function, *Nat Rev Mol Cell Biol* 13 (2012) 448-462.
- [84] UH Stenman, E Paus, WJ Allard, I Andersson, C Andres, TR Barnett, C Becker, A Belenky, L Bellanger, CM Pellegrino, OP Bormer, G Davis, B Dowell, LS Grauer, DC Jette, B Karlsson, FT Kreutz, TM van der Kwast, L Lauren, M Leinimaa, J Leinonen, H Lilja, HJ Linton, M Nap, J Hilgers et al., Summary report of the TD-3 workshop: characterization of 83 antibodies against prostate-specific antigen, *Tumour Biol* 20 Suppl 1 (1999) 1-12.
- [85] R Apweiler, H Hermjakob, N Sharon, On the frequency of protein glycosylation, as deduced from analysis of the SWISS-PROT database, *Biochim Biophys Acta* 1473 (1999) 4-8.
- [86] DJ Gill, H Clausen, F Bard, Location, location, location: new insights into O-GalNAc protein glycosylation, *Trends Cell Biol* 21 (2011) 149-158.
- [87] JW Dennis, IR Nabi, M Demetriou, Metabolism, cell surface organization, and disease, *Cell* 139 (2009) 1229-1241.
- [88] U Kuzmanov, H Kosanam, EP Diamandis, The sweet and sour of serological glycoprotein tumor biomarker quantification, *BMC Med* 11 (2013) 31.
- [89] PM Drake, W Cho, B Li, A Prakobphol, E Johansen, NL Anderson, FE Regnier, BW Gibson, SJ Fisher, Sweetening the pot: adding glycosylation to the biomarker discovery equation, *Clin Chem* 56 (2010) 223-236.
- [90] Z Tan, H Yin, S Nie, Z Lin, J Zhu, MT Ruffin, MA Anderson, DM Simeone, DM Lubman, Large-scale identification of core-fucosylated glycopeptide sites in pancreatic cancer serum using mass spectrometry, *J Proteome Res* 14 (2015) 1968-1978.
- [91] H Yin, Z Lin, S Nie, J Wu, Z Tan, J Zhu, J Dai, Z Feng, J Marrero, DM Lubman, Mass-selected site-specific core-fucosylation of ceruloplasmin in alcohol-related hepatocellular carcinoma, *J Proteome Res* 13 (2014) 2887-2896.
- [92] Y Liang, T Ma, A Thakur, H Yu, L Gao, P Shi, X Li, H Ren, L Jia, S Zhang, Z Li, M Chen, Differentially expressed glycosylated patterns of alpha-1-antitrypsin as serum biomarkers for the diagnosis of lung cancer, *Glycobiology* 25 (2015) 331-340.
- [93] MV Dwek, A Jenks, AJ Leatham, A sensitive assay to measure biomarker glycosylation demonstrates increased fucosylation of prostate specific antigen (PSA) in patients with prostate cancer compared with benign prostatic hyperplasia, *Clin Chim Acta* 411 (2010) 1935-1939.
- [94] A Prcic, E Begic, M Hiros, Usefulness of total PSA value in prostate diseases diagnosis, *Acta Inform Med* 24 (2016) 156-161.
- [95] MJ Barry, Screening for prostate cancer--the controversy that refuses to die, *N Engl J Med* 360 (2009) 1351-1354.

- [96] PJ Lamy, Y Allory, AS Gauchez, B Asselain, P Beuzeboc, P de Cremoux, J Fontugne, A Georges, C Hennequin, J Lehmann-Che, C Massard, I Millet, T Murez, MH Schlageter, O Rouviere, D Kassab-Chahmi, F Rozet, JL Descotes, X Rebillard, Prognostic biomarkers used for localised prostate cancer management: a systematic review, *Eur Urol Focus* (2017).
- [97] P Sountoulides, G Moutzouris, Prostate-specific antigen screening, why have the guidelines changed?, *Expert Rev Anticancer Ther* 14 (2014) 1277-1281.
- [98] RR Drake, EE Jones, TW Powers, JO Nyalwidhe, Altered glycosylation in prostate cancer, *Adv Cancer Res* 126 (2015) 345-382.
- [99] K Fukushima, T Satoh, S Baba, K Yamashita, alpha1,2-Fucosylated and beta-N-acetylgalactosaminylated prostate-specific antigen as an efficient marker of prostatic cancer, *Glycobiology* 20 (2010) 452-460.
- [100] DF Zielinska, F Gnad, JR Wisniewski, M Mann, Precision mapping of an in vivo N-glycoproteome reveals rigid topological and sequence constraints, *Cell* 141 (2010) 897-907.
- [101] Z Lin, H Yin, A Lo, MT Ruffin, MA Anderson, DM Simeone, DM Lubman, Label-free relative quantification of alpha-2-macroglobulin site-specific core-fucosylation in pancreatic cancer by LC-MS/MS, *Electrophoresis* 35 (2014) 2108-2115.
- [102] H Yin, Z Tan, J Wu, J Zhu, KA Shedden, J Marrero, DM Lubman, Mass-selected site-specific core-fucosylation of serum proteins in hepatocellular carcinoma, *J Proteome Res* 14 (2015) 4876-4884.
- [103] Z Lin, DM Simeone, MA Anderson, RE Brand, X Xie, KA Shedden, MT Ruffin, DM Lubman, Mass spectrometric assay for analysis of haptoglobin fucosylation in pancreatic cancer, *J Proteome Res* 10 (2011) 2602-2611.
- [104] M Mancera-Artu, E Gimenez, J Barbosa, V Sanz-Nebot, Identification and characterization of isomeric N-glycans of human alpha-acid-glycoprotein by stable isotope labelling and ZIC-HILIC-MS in combination with exoglycosidase digestion, *Anal Chim Acta* 940 (2016) 92-103.
- [105] P Hagglund, R Matthiesen, F Elortza, P Hojrup, P Roepstorff, ON Jensen, J Bunkenborg, An enzymatic deglycosylation scheme enabling identification of core fucosylated N-glycans and O-glycosylation site mapping of human plasma proteins, *J Proteome Res* 6 (2007) 3021-3031.
- [106] Y Zhao, W Jia, J Wang, W Ying, Y Zhang, X Qian, Fragmentation and site-specific of core fucosylated glycoprotein by multiple reaction monitoring-mass spectrometry, *Anal Chem* 83 (2011) 8802-8809.
- [107] H Tang, P Hsueh, D Kletter, M Bern, B Haab, The detection and discovery of glycan motifs in biological samples using lectins and antibodies: new methods and opportunities, *Adv Cancer Res* 126 (2015) 167-202.
- [108] R Lang, A Leinenbach, J Karl, M Swiatek-de Lange, U Kobold, M Vogeser, An endoglycosidase-assisted LC-MS/MS-based strategy for the analysis of site-specific core-fucosylation of low-concentrated glycoproteins in human serum using prostate-specific antigen (PSA) as example, *Clin Chim Acta* 480 (2018) 1-8.
- [109] MR Wilkins, I Lindskog, E Gasteiger, A Bairoch, JC Sanchez, DF Hochstrasser, RD Appel, Detailed peptide characterization using PEPTIDEMASS--a world-wide-web-accessible tool, *Electrophoresis* 18 (1997) 403-408.
- [110] HH Freeze, C Kranz, Endoglycosidase and glycoamidase release of N-linked glycans, *Curr Protoc Mol Biol Chapter* 17 (2010) Unit 17.13A.

- [111] TH Plummer, Jr., AW Phelan, AL Tarentino, Porcine fibrinogen glycopeptides: substrates for detecting endo-beta-N-acetylglucosaminidases F2 and F3(1), *Anal Biochem* 235 (1996) 98-101.
- [112] AN Hoofnagle, JR Whiteaker, SA Carr, E Kuhn, T Liu, SA Massoni, SN Thomas, RR Townsend, LJ Zimmerman, E Boja, J Chen, DL Crimmins, SR Davies, Y Gao, TR Hiltke, KA Ketchum, CR Kinsinger, M Mesri, MR Meyer, WJ Qian, RM Schoenherr, MG Scott, T Shi, GR Whiteley, JA Wrobel, C Wu, BL Ackermann, R Aebersold, DR Barnidge, DM Bunk, N Clarke, JB Fishman, RP Grant, U Kusebauch, MM Kushnir, MS Lowenthal, RL Moritz, H Neubert, SD Patterson, AL Rockwood, J Rogers, RJ Singh, JE Van Eyk, SH Wong, S Zhang, DW Chan, X Chen, MJ Ellis, DC Liebler, KD Rodland, H Rodriguez, RD Smith, Z Zhang, H Zhang, AG Paulovich, Recommendations for the generation, quantification, storage, and handling of peptides used for mass spectrometry-based assays, *Clin Chem* 62 (2016) 48-69.
- [113] EW Klee, OP Bondar, MK Goodmanson, SA Trushin, EJ Bergstralh, RJ Singh, NL Anderson, GG Klee, Serum concentrations of prostate-specific antigen measured using immune extraction, trypsin digestion, and tandem mass spectrometry quantification of LSEPAELTDAVK peptide, *Arch Pathol Lab Med* 138 (2014) 1381-1386.
- [114] A Vegvari, K Sjodin, M Rezeli, J Malm, H Lilja, T Laurell, G Marko-Varga, Identification of a novel proteoform of prostate specific antigen (SNP-L132I) in clinical samples by multiple reaction monitoring, *Mol Cell Proteomics* 12 (2013) 2761-2773.
- [115] H Yin, J Zhu, J Wu, Z Tan, M An, S Zhou, Y Mechref, DM Lubman, A procedure for the analysis of site-specific and structure-specific fucosylation in alpha-1-antitrypsin, *Electrophoresis* 37 (2016) 2624-2632.
- [116] MCS Levernaes, MN Broughton, L Reubsaet, TG Halvorsen, To elute or not to elute in immunocapture bottom-up LC-MS, *J Chromatogr B Analyt Technol Biomed Life Sci* 1055-1056 (2017) 51-60.
- [117] B Chauve, D Guilleme, P Cleon, JL Veuthey, Evaluation of various HILIC materials for the fast separation of polar compounds, *J Sep Sci* 33 (2010) 752-764.
- [118] T Fortin, A Salvador, JP Charrier, C Lenz, F Bettsworth, X Lacoux, G Choquet-Kastylevsky, J Lemoine, Multiple reaction monitoring cubed for protein quantification at the low nanogram/milliliter level in nondepleted human serum, *Anal Chem* 81 (2009) 9343-9352.
- [119] EW Klee, OP Bondar, MK Goodmanson, SA Trushin, RJ Singh, NL Anderson, GG Klee, Mass spectrometry measurements of prostate-specific antigen (PSA) peptides derived from immune-extracted PSA provide a potential strategy for harmonizing immunoassay differences, *Am J Clin Pathol* 141 (2014) 527-533.
- [120] YT Chen, LP Tuan, HW Chen, IA Wei, MY Chou, HM Chen, YC Tyan, SF Chen, Quantitative analysis of prostate specific antigen isoforms using immunoprecipitation and stable isotope labeling mass spectrometry, *Anal Chem* 87 (2015) 545-553.
- [121] T Shi, TL Fillmore, X Sun, R Zhao, AA Schepmoes, M Hossain, F Xie, S Wu, JS Kim, N Jones, RJ Moore, L Pasa-Tolic, J Kagan, KD Rodland, T Liu, K Tang, DG Camp 2nd, RD Smith, WJ Qian, Antibody-free, targeted mass-spectrometric approach for quantification of proteins at low picogram per milliliter levels in human plasma/serum, *Proc Natl Acad Sci USA* 109 (2012) 15395-15400.
- [122] KJ Bronsema, R Bischoff, NC van de Merbel, Internal standards in the quantitative determination of protein biopharmaceuticals using liquid chromatography coupled to mass spectrometry, *J Chromatogr B Analyt Technol Biomed Life Sci* 893-894 (2012) 1-14.
- [123] LA Torre, F Bray, RL Siegel, J Ferlay, J Lortet-Tieulent, A Jemal, Global cancer statistics, 2012, *CA Cancer J Clin* 65 (2015) 87-108.

- [124] S Sharma, J Zapatero-Rodriguez, R O'Kennedy, Prostate cancer diagnostics: Clinical challenges and the ongoing need for disruptive and effective diagnostic tools, *Biotechnol Adv* 35 (2017) 135-149.
- [125] MC Wong, WB Goggins, HH Wang, FD Fung, C Leung, SY Wong, CF Ng, JJ Sung, Global incidence and mortality for prostate cancer: Analysis of temporal patterns and trends in 36 countries, *Eur Urol* 70 (2016) 862-874.
- [126] JR Prensner, MA Rubin, JT Wei, AM Chinnaiyan, Beyond PSA: the next generation of prostate cancer biomarkers, *Sci Transl Med* 4 (2012) 127rv123.
- [127] MB Tchetgen, JE Oesterling, The effect of prostatitis, urinary retention, ejaculation, and ambulation on the serum prostate-specific antigen concentration, *Urol Clin North Am* 24 (1997) 283-291.
- [128] SF Shariat, A Semjonow, H Lilja, C Savage, AJ Vickers, A Bjartell, Tumor markers in prostate cancer I: blood-based markers, *Acta Oncol* 50 Suppl 1 (2011) 61-75.
- [129] AP Berger, H Volgger, H Rogatsch, D Strohmeier, H Steiner, H Klocker, G Bartsch, W Horninger, Screening with low PSA cutoff values results in low rates of positive surgical margins in radical prostatectomy specimens, *Prostate* 53 (2002) 241-245.
- [130] WJ Catalona, CG Ramos, GF Carvalhal, Y Yan, Lowering PSA cutoffs to enhance detection of curable prostate cancer, *Urology* 55 (2000) 791-795.
- [131] ED Crawford, JW Moul, KO Rove, CA Pettaway, LE Lamerato, A Hughes, Prostate-specific antigen 1.5-4.0 ng/mL: a diagnostic challenge and danger zone, *BJU Int* 108 (2011) 1743-1749.
- [132] IM Thompson, DP Ankerst, C Chi, MS Lucia, PJ Goodman, JJ Crowley, HL Parnes, CA Coltman, Jr., Operating characteristics of prostate-specific antigen in men with an initial PSA level of 3.0 ng/ml or lower, *Jama* 294 (2005) 66-70.
- [133] SF Shariat, PI Karakiewicz, V Margulis, MW Kattan, Inventory of prostate cancer predictive tools, *Curr Opin Urol* 18 (2008) 279-296.
- [134] TA Stamey, N Yang, AR Hay, JE McNeal, FS Freiha, E Redwine, Prostate-specific antigen as a serum marker for adenocarcinoma of the prostate, *N Engl J Med* 317 (1987) 909-916.
- [135] FH Schroder, HB Carter, T Wolters, RC van den Bergh, C Gosselaar, CH Bangma, MJ Roobol, Early detection of prostate cancer in 2007. Part 1: PSA and PSA kinetics, *Eur Urol* 53 (2008) 468-477.
- [136] J Peter, C Unverzagt, TN Krogh, O Vorm, W Hoesel, Identification of precursor forms of free prostate-specific antigen in serum of prostate cancer patients by immunosorption and mass spectrometry, *Cancer Res* 61 (2001) 957-962.
- [137] SD Mikolajczyk, LS Marks, AW Partin, HG Rittenhouse, Free prostate-specific antigen in serum is becoming more complex, *Urology* 59 (2002) 797-802.
- [138] WJ Catalona, AW Partin, KM Slawin, MK Brawer, RC Flanigan, A Patel, JP Richie, JB de Kernion, PC Walsh, PT Scardino, PH Lange, EN Subong, RE Parson, GH Gasior, KG Loveland, PC Southwick, Use of the percentage of free prostate-specific antigen to enhance differentiation of prostate cancer from benign prostatic disease: a prospective multicenter clinical trial, *Jama* 279 (1998) 1542-1547.

- [139] N Mottet, J Bellmunt, M Bolla, E Briers, MG Cumberbatch, M De Santis, N Fossati, T Gross, AM Henry, S Joniau, TB Lam, MD Mason, VB Matveev, PC Moldovan, RCN van den Bergh, T Van den Broeck, HG van der Poel, TH van der Kwast, O Rouviere, IG Schoots, T Wiegel, P Cornford, EAU-ESTRO-SIOG guidelines on prostate cancer. Part 1: Screening, diagnosis, and local treatment with curative intent, *Eur Urol* 71 (2017) 618-629.
- [140] R Kirby, Optimising the management of early prostate cancer, *Practitioner* 258 (2014) 15-18, 12.
- [141] G Sardana, EP Diamandis, Biomarkers for the diagnosis of new and recurrent prostate cancer, *Biomark Med* 6 (2012) 587-596.
- [142] JF Rodriguez, SE Eggner, Prostate cancer and the evolving role of biomarkers in screening and diagnosis, *Radiol Clin North Am* 56 (2018) 187-196.
- [143] C Sanhueza, M Kohli, Clinical and novel biomarkers in the management of prostate cancer, *Curr Treat Options Oncol* 19 (2018) 8.
- [144] IL Deras, SM Aubin, A Blase, JR Day, S Koo, AW Partin, WJ Ellis, LS Marks, Y Fradet, H Rittenhouse, J Groskopf, PCA3: a molecular urine assay for predicting prostate biopsy outcome, *J Urol* 179 (2008) 1587-1592.
- [145] D Hessels, MP van Gils, O van Hooij, SA Jannink, JA Witjes, GW Verhaegh, JA Schalken, Predictive value of PCA3 in urinary sediments in determining clinico-pathological characteristics of prostate cancer, *Prostate* 70 (2010) 10-16.
- [146] S Loeb, MG Sanda, DL Broyles, SS Shin, CH Bangma, JT Wei, AW Partin, GG Klee, KM Slawin, LS Marks, RH van Schaik, DW Chan, LJ Sokoll, AB Cruz, IA Mizrahi, WJ Catalona, The prostate health index selectively identifies clinically significant prostate cancer, *J Urol* 193 (2015) 1163-1169.
- [147] A Gupta, MJ Roobol, CJ Savage, M Peltola, K Pettersson, PT Scardino, AJ Vickers, FH Schroder, H Lilja, A four-kallikrein panel for the prediction of repeat prostate biopsy: data from the European Randomized Study of Prostate Cancer screening in Rotterdam, Netherlands, *Br J Cancer* 103 (2010) 708-714.
- [148] M Mincheff, S Zoubak, Y Makogonenko, Immune responses against PSMA after gene-based vaccination for immunotherapy-A: results from immunizations in animals, *Cancer Gene Ther* 13 (2006) 436-444.
- [149] SA Tomlins, SM Aubin, J Siddiqui, RJ Lonigro, L Sefton-Miller, S Miick, S Williamsen, P Hodge, J Meinke, A Blase, Y Penabella, JR Day, R Varambally, B Han, D Wood, L Wang, MG Sanda, MA Rubin, DR Rhodes, B Hollenbeck, K Sakamoto, JL Silberstein, Y Fradet, JB Amberson, S Meyers, N Palanisamy, H Rittenhouse, JT Wei, J Groskopf, AM Chinnaiyan, Urine TMPRSS2:ERG fusion transcript stratifies prostate cancer risk in men with elevated serum PSA, *Sci Transl Med* 3 (2011) 94ra72.
- [150] V Ivanovic, A Melman, B Davis-Joseph, M Valcic, J Geliebter, Elevated plasma levels of TGF-beta 1 in patients with invasive prostate cancer, *Nat Med* 1 (1995) 282-284.
- [151] B Ouyang, B Bracken, B Burke, E Chung, J Liang, SM Ho, A duplex quantitative polymerase chain reaction assay based on quantification of alpha-methylacyl-CoA racemase transcripts and prostate cancer antigen 3 in urine sediments improved diagnostic accuracy for prostate cancer, *J Urol* 181 (2009) 2508-2513; discussion 2513-2504.
- [152] T Okegawa, K Nutahara, E Higashihara, Prognostic significance of circulating tumor cells in patients with hormone refractory prostate cancer, *J Urol* 181 (2009) 1091-1097.
- [153] DL Meany, DW Chan, Aberrant glycosylation associated with enzymes as cancer biomarkers, *Clin Proteomics* 8 (2011) 7.

- [154] T Petretti, W Kemmner, B Schulze, PM Schlag, Altered mRNA expression of glycosyltransferases in human colorectal carcinomas and liver metastases, *Gut* 46 (2000) 359-366.
- [155] MM Jankovic, BS Milutinovic, Glycoforms of CA125 antigen as a possible cancer marker, *Cancer Biomark* 4 (2008) 35-42.
- [156] E Saeland, AI Belo, S Mongera, I van Die, GA Meijer, Y van Kooyk, Differential glycosylation of MUC1 and CEACAM5 between normal mucosa and tumour tissue of colon cancer patients, *Int J Cancer* 131 (2012) 117-128.
- [157] A Belanger, H van Halbeek, HC Graves, K Grandbois, TA Stamey, L Huang, I Poppe, F Labrie, Molecular mass and carbohydrate structure of prostate specific antigen: studies for establishment of an international PSA standard, *Prostate* 27 (1995) 187-197.
- [158] C Fredolini, LA Liotta, EF Petricoin, Application of proteomic technologies for prostate cancer detection, prognosis, and tailored therapy, *Crit Rev Clin Lab Sci* 47 (2010) 125-138.
- [159] X Yang, F Liu, Y Yan, T Zhou, Y Guo, G Sun, Z Zhou, W Zhang, X Guo, J Sha, Proteomic analysis of N-glycosylation of human seminal plasma, *Proteomics* 15 (2015) 1255-1258.
- [160] S Barrabes, E Llop, M Ferrer-Batalle, M Ramirez, RN Aleixandre, AS Perry, R de Llorens, R Peracaula, Analysis of urinary PSA glycosylation is not indicative of high-risk prostate cancer, *Clin Chim Acta* 470 (2017) 97-102.
- [161] E Song, A Mayampurath, CY Yu, H Tang, Y Mechref, Glycoproteomics: Identifying the glycosylation of prostate specific antigen at normal and high isoelectric points by LC-MS/MS, *J Proteome Res* 13 (2014) 5570-5580.
- [162] TJ Wilt, KM Jones, MJ Barry, GL Andriole, D Culkin, T Wheeler, WJ Aronson, MK Brawer, Follow-up of prostatectomy versus observation for early prostate cancer, *N Engl J Med* 377 (2017) 132-142.
- [163] QK Li, L Chen, MH Ao, JH Chiu, Z Zhang, H Zhang, DW Chan, Serum fucosylated prostate-specific antigen (PSA) improves the differentiation of aggressive from non-aggressive prostate cancers, *Theranostics* 5 (2015) 267-276.
- [164] ER DeLong, DM DeLong, DL Clarke-Pearson, Comparing the areas under two or more correlated receiver operating characteristic curves: a nonparametric approach, *Biometrics* 44 (1988) 837-845.
- [165] H Kekki, M Peltola, S van Vliet, C Bangma, Y van Kooyk, K Pettersson, Improved cancer specificity in PSA assay using Aleuria aurantia lectin coated Eu-nanoparticles for detection, *Clin Biochem* 50 (2017) 54-61.
- [166] DL Meany, Z Zhang, LJ Sokoll, H Zhang, DW Chan, Glycoproteomics for prostate cancer detection: changes in serum PSA glycosylation patterns, *J Proteome Res* 8 (2009) 613-619.
- [167] T Vermassen, C Van Praet, D Vanderschaeghe, T Maenhout, N Lumen, N Callewaert, P Hoebeke, S Van Belle, S Rottey, J Delanghe, Capillary electrophoresis of urinary prostate glycoproteins assists in the diagnosis of prostate cancer, *Electrophoresis* 35 (2014) 1017-1024.
- [168] KY White, L Rodemich, JO Nyalwidhe, MA Comunale, MA Clements, RS Lance, PF Schellhammer, AS Mehta, OJ Semmes, RR Drake, Glycomic characterization of prostate-specific antigen and prostatic acid phosphatase in prostate cancer and benign disease seminal plasma fluids, *J Proteome Res* 8 (2009) 620-630.

Appendix

List of identified PSA derived peptides using
different enzymes

Identified peptides of reduced and alkylated prostate-specific antigen (PSA, Uni-ProtKB P07288) after partial deglycosylation and subsequent proteolytic digestion are shown for the following enzymes:

Trypsin

Sequence	Modifications	z	[M+H] ⁺	MC
VVHYR		1	673.3781	0
DTIVANP		2	729.3774	0
SVILLGR		2	757.4927	0
FMLcAGR	C4(CAM)	2	854.4010	0
FmLcAGR	M2(OX); C4(CAM)	2	870.3959	0
IVGGWEcEK	C7(CAM)	2	1077.5034	0
WIKDTIVANP		2	1156.6361	1
LSEPAELTDAVK		2	1272.6679	0
KWIKDTIVANP		2	1284.7304	2
HSQPWQVLVASR		2	1407.7491	0
FLRPGDDSSHDLMLLR		3	1871.9447	0
FLRPGDDSSHDLMLLR	M13(OX)	3	1887.9394	0
NRFLRPGDDSSHDLMLLR		3	2142.0872	1
NRFLRPGDDSSHDLMLLR	M15(OX)	3	2158.0820	1
AVcGGVLVHPQWVLTAHcIR	C3(CAM); C19(CAM)	3	2344.2183	0
LQcVDLHVISNDVcAQVHPQK	C3(CAM); C14(CAM)	3	2460.2135	0
IVGGWEcEKHSQPWQVLVASR	C7(CAM)	3	2466.2346	1
KLQcVDLHVISNDVcAQVHPQK	C4(CAM); C15(CAM)	2	2588.3060	1
LQcVDLHVISNDVcAQVHPQKGTK	C3(CAM); C14(CAM)	3	2788.4243	1
KLQcVDLHVISNDVcAQVHPQKGTK	C4(CAM); C15(CAM)	3	2916.5225	2
HSLFHPEDTGQVFQVSHSFPHPPLYDMSLLK		4	3493.7055	0
HSLFHPEDTGQVFQVSHSFPHPPLYDmSLLK	M26(OX)	3	3509.6979	0
VmDLPTQEPALGTTcYASGWGSIEPEEFLTPK	M2(OX); C15(CAM)	3	3540.6566	0

Elastase

Sequence	Modifications	z	[M+H] ⁺	MC
DLHVI		1	596.3399	2
TKFML		2	639.3533	0
SEPAEL		1	645.3087	1
ELTDAV		1	647.3243	2
RLSEPA		1	672.3674	1
YDMSLL		1	741.3489	1
QVHPQKV		2	835.4779	1
cNGVLQGI	C1(CAM)	1	860.4292	2
QcVDLHV	C2(CAM)	2	870.4135	2
TKFMLcA	C6(CAM)	2	870.4211	1

TKFmLcA	M4(OX); C6(CAM)	2	886.4163	1
RLSEPAEL		1	914.4941	2
SHSFPHPHL		2	921.4573	0
MDLPTQEPA		2	1001.4605	0
mDLPTQEPA	M1(OX)	2	1017.4555	0
KVMDLPTQEPA		2	1228.6249	1
HYRKWIKDTI		2	1359.7535	1
VHYRKWIKDTI		2	1458.8218	2
GRHSLFHPEDTGQV		2	1579.7621	1
SHSFPHPPLYDMSLL		2	1643.7918	2
SHSFPHPPLYDmSLL	M11(OX)	2	1659.7882	2
SGWGSIEPEEFLLTPKKL		2	1917.9954	2
IVGGWEcEKHSQPWQV	C7(CAM)	2	1939.9130	2
VGGWEcEKHSQPWQVL	C6(CAM)	2	1939.9130	2
GGWEcEKHSQPWQVLV	C5(CAM)	2	1939.9130	2
GRHSLFHPEDTGQVFQV		2	1953.9589	2
TSWGSEPCALPERPSLYTKV	C8(CAM)	2	2278.1184	2

Proteinase K

Sequence	Modifications	z	[M+H] ⁺	MC
cGGVL	C1(CAM)	1	505.24385	1
FHPE		1	529.24042	1
IVGGW		1	531.29175	2
QEPAL		1	557.29305	2
GSIEPE		1	631.29304	2
DTGQVF		1	666.30908	2
RLSEPA		1	672.36708	2
cSGDSGGPL	C1(CAM)	1	849.34072	0
SHSFPHPHL		2	921.45754	1
PHPLYDmSL	M7(OX)	2	1088.51122	2
LRPGDDSSHDL		2	1211.56523	1
KNRFLRPGDDSSHDL		2	1756.87355	2

Thermolysin

Sequence	Modifications	z	[M+H] ⁺	MC
VLQG		1	416.2503	1
VTKF		1	494.2972	1
IVANP		1	513.3030	2
VISND		1	547.2722	1
VcGGVL	C2(CAM)	1	604.3123	1
LYTKV		2	623.3759	1

LYDMS		1	628.2647	1
LQcVD	C3(CAM)	1	634.2864	1
LSEPAE		1	645.3088	1
LTDVAK		2	646.3768	2
LLGRHS		2	682.3993	0
LGRHSL		2	682.3993	0
LGTTcY	C5(CAM)	1	714.3124	0
LYDMSL		1	741.3484	1
LYDmSL	M4(OX)	1	757.3436	1
IEPEEF		2	763.3509	1
VHPQWV		2	765.4043	0
ALPERPS		1	769.4202	1
LLKNRF		2	790.4931	1
LQcVDLH	C3(CAM)	2	884.4292	1
VSHSFPHP		2	907.4419	1
LRLSEPAE		2	914.4938	1
FHPEDTGQ		2	930.3946	0
MDLPTQEPA		2	1001.4611	2
mDLPTQEPA	M1(OX)	2	1017.4559	2
FHPEDTGQV		2	1029.4633	1
LFHPEDTGQ		2	1043.4784	1
LRPGDDSSHD		2	1098.4805	0
LFHPEDTGQV		2	1142.5478	2
LRPGDDSSHD		2	1211.5652	0
FLRPGDDSSHD		2	1245.5500	1
FHPEDTGQVFQ		2	1304.5896	1
IEPEEFLTPKK		2	1330.7257	2
LRPGDDSSHDLM		2	1342.6051	1
LRPGDDSSHDLM	M12(OX)	2	1358.6005	1
VLQGITSWGSEPC	C13(CAM)	2	1433.6699	2
ITSWGSEPCALPERPS	C9(CAM)	2	1786.8433	2
AGRWTGGKSTcSGDSGGPL	C11(CAM)	2	1850.8465	1
LcAGRWTGGKSTcSGDSGGPL	C2(CAM); C13(CAM)	2	2123.9599	1
AGRWTGGKSTcSGDSGGPLVcNG	C11(CAM); C21(CAM)	2	2281.0072	2

Protease Arg-C

Sequence	Modifications	z	[M+H] ⁺	MC
KWIKDTIVANP		2	1284.7314	0
nKSVILLGR	N1(HexNAc-dHex)	2	1348.7683	0
PSLYTKVVHYR		2	1362.7527	0
PGDDSSHDLMLLR		2	1455.6905	0
PGDDSSHDLMLLR	M10(OX)	2	1471.6857	0

FLRPGDDSSHDLMLLR		3	1871.9442	1
FLRPGDDSSHDLMLLR	M13(OX)	3	1887.9399	1
AVcGGVLVHPQWVLTAHcIR	C3(CAM); C19(CAM)	3	2344.2185	0
IVGGWEcEKHSQPWQVLVASR	C7(CAM)	3	2466.2340	0
WTGGKSTcSGDSGGPLVcNGVLQGITSWGSE	C8(CAM); C18(CAM);	3	3977.8152	0
PcALPER	C33(CAM)			

Pepsin (pH = 1.3)

Sequence	Modifications	z	[M+H] ⁺	MC
VcNGVL	C2(CAM)	1	661.3334	0
PERPSL		2	698.3830	0
GSEPCAL	C5(CAM)	1	733.3189	0
PTQEPAL		1	755.3937	0
LGRHSLF		2	829.4678	2
VHPQWVL		2	878.4886	1
GSIEPEEF		1	907.4048	0
RLSEPAEL		2	914.4939	1
TDAVKVMDL		2	991.5134	0
LRLSEPAEL		1	1027.5785	2
HPEDTGQVF		2	1029.4636	0
FHPEDTGQVF		2	1176.5314	1
VASRGRAVcGGVL	C9(CAM)	2	1301.7098	0
LTPKKLQcVDL	C8(CAM)	2	1314.7444	2
LRPGDDSSHDLM		2	1455.6906	2
RPGDDSSHDLM		2	1455.6906	2
LRPGDDSSHDLM	M12(OX)	2	1471.6848	2
RPGDDSSHDLM	M11(OX)	2	1471.6848	2
EcEKHSQPWQVL	C2(CAM)	2	1540.7221	1
TAAHcIRnKSVIL	C5(CAM); N8(HexNAc)	2	1685.9016	0
TDAVKVMDLPTQEPAL		2	1727.8901	1
TDAVKVmDLPTQEPAL	M7(OX)	2	1743.8865	1
TGGKSTcSGDSGGPLVcNGVL	C7(CAM); C17(CAM)	2	2022.9214	1
IVGGWEcEKHSQPWQVL	C7(CAM)	2	2052.9985	2
QGITSWGSEPCALPERPSL	C11(CAM)	2	2084.9873	2
HVISNDVcAQVHPQKVTKF	C8(CAM)	2	2207.1409	0

Chymotrypsin

Sequence	Modifications	z	[M+H] ⁺	MC
DmSLL	M2(OX)	1	594.2803	2
QcVDL	C2(CAM)	1	634.2862	0
VcNGVL	C2(CAM)	1	661.3333	0
KNRFL		1	677.4089	1
LKNRF		1	677.4089	1
LTPKKL		2	699.4763	1
GRHSLF		2	716.3837	1
TKVVHY		2	746.4192	0
TDAVKVM		2	763.4017	0
TDAVKVm	M7(OX)	1	779.3970	0
LGRHSLF		1	829.4679	2
VHPQWVL		2	878.4887	1
GSIEPEEF		2	907.4042	0
RLSEPAEL		2	914.4942	1
IKDTIVANP		2	970.5566	0
LRLSEPAEL		2	1027.5782	2
HPEDTGQVF		2	1029.4632	0
QVSHSFPHPL		2	1148.5843	0
FHPEDTGQVF		2	1176.5318	1
EcEKHSQPW	C2(CAM)	2	1200.5102	0
LRPGDDSSHD		2	1211.5656	1
RPGDDSSHDLM		2	1229.5215	1
RPGDDSSHDm	M11(OX)	2	1245.5170	1
VASRGRAVcGGVL	C9(CAM)	2	1301.7101	0
QVSHSFPHPY		2	1311.6471	1
RPGDDSSHDML		2	1342.6053	2
LRPGDDSSHDLM		2	1342.6054	2
LRPGDDSSHDm	M12(OX)	2	1358.6002	2
RPGDDSSHDmL	M11(OX)	2	1358.6011	2
TGGKSTcSGDSGGPL	C7(CAM)	2	1380.6059	0
SEPAELTDAVKVm	M13(OX)	2	1405.6888	1
RKWIKDTIVANP		2	1440.8316	1
DLPTQEPALGTTcY	C13(CAM)	2	1565.7165	1
GSEPCALPERPSLY	C5(CAM)	2	1575.7484	1
RLSEPAELTDAVKVM		3	1658.8795	2
RLSEPAELTDAVKVm	M15(OX)	3	1674.8752	2
IVGGWEcEKHSQPW	C7(CAM)	2	1712.7871	1
GRHSLFHPEDTGQVF		3	1726.8292	2
TGGKSTcSGDSGGPLVcNGVL	C7(CAM); C17(CAM)	2	2022.9213	1
VASRGRAVcGGVLVHPQWVL	C9(CAM)	3	2161.1831	2

TDAVKVMDLPTQEPALGTTcY	C20(CAM)	2	2310.1043	2
QcVDLHVISNDVcAQVHPQKVTKF	C2(CAM); C13(CAM)	3	2822.4099	1
QcVDLHVISNDVcAQVHPQKVTKFM	C2(CAM); C13(CAM)	4	2953.4406	2

CAM = Carbamidomethylation (+57.021 Da)

OX = Oxidation (+15.995 Da)

HexNAc = N-glycosylation with GlcNAc (+203.079 Da)

HexNAc-dHex = N-glycosylation with GlcNAc + Fuc (+349.137 Da)

z = Charge state

MC = Missed cleavage